Low x physics and parton saturation: theory review and new ideas

Anna Stasto
Penn State University,
and Institute of Nuclear Physics, Polish Academy of Sciences

ISVHECRI 2014, CERN, August 21st, 2014

Outline

- Relevance of low x for cosmic rays and ultrahigh energy neutrino interactions
- Low x theory: evolution equations
- Parton saturation
- More developments: higher order BFKL and BK, impact parameter dependence
- Selected phenomenological applications: neutrino cross sections, prompt neutrinos, diffractive production...

Relevance of low x region for CR and UHEnus

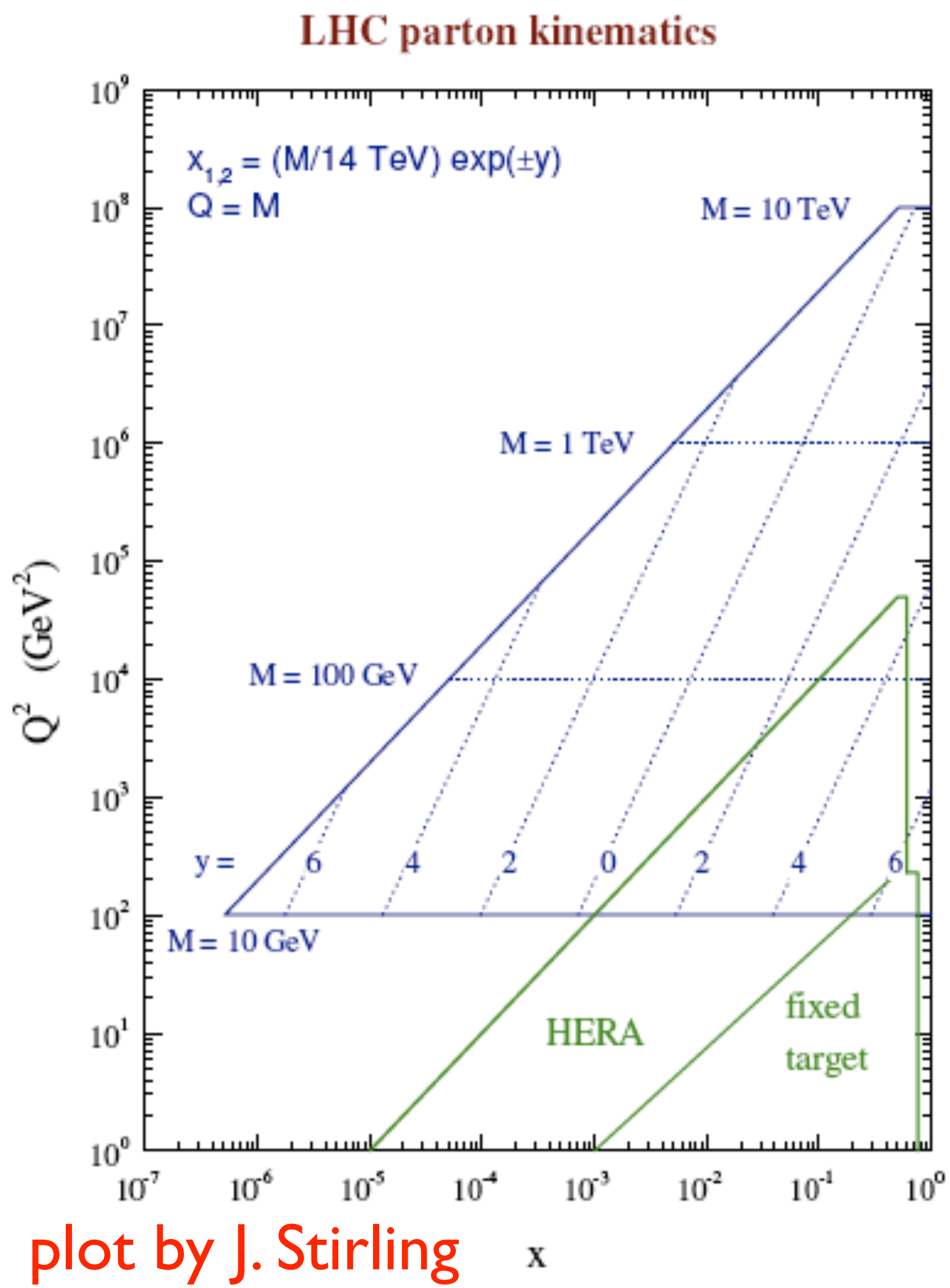

plot by J. Stirling

Relevance of low x region for CR and UHEnus

Kinematic boundary for LHC

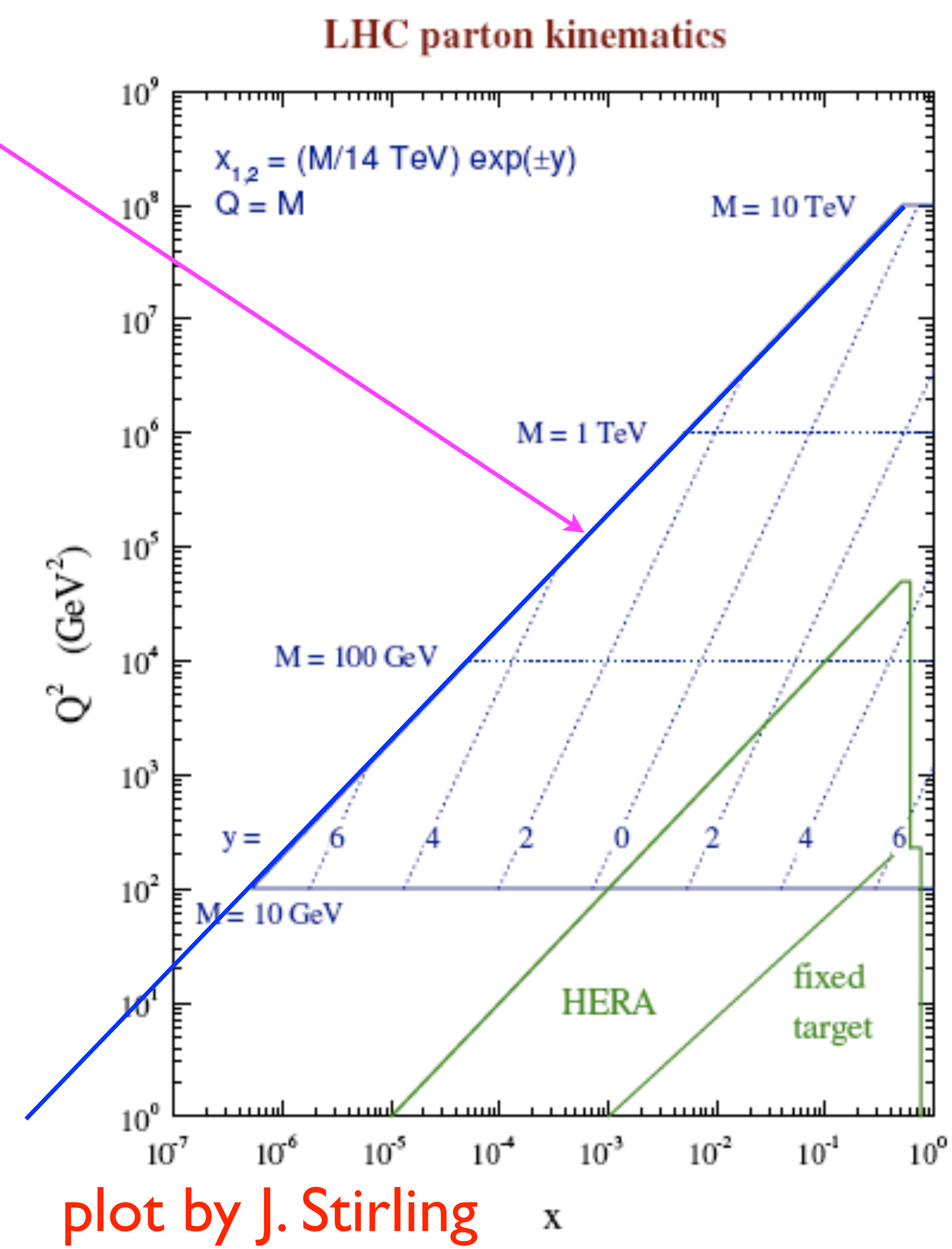

plot by J. Stirling

Relevance of low x region for CR and UHEnus

Kinematic boundary for LHC

Different scales

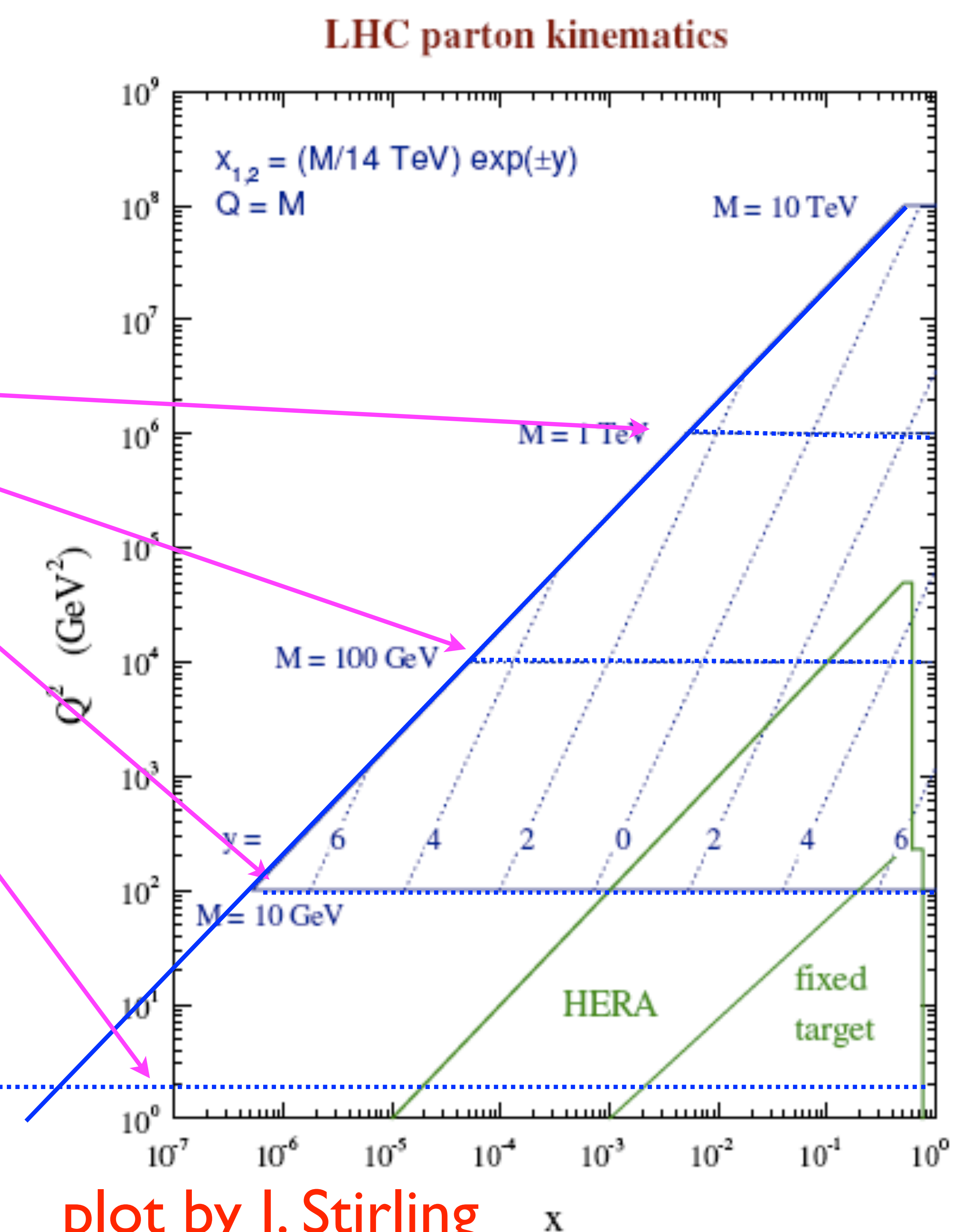

plot by J. Stirling

Relevance of low x region for CR and UHEnus

Kinematic boundary for LHC

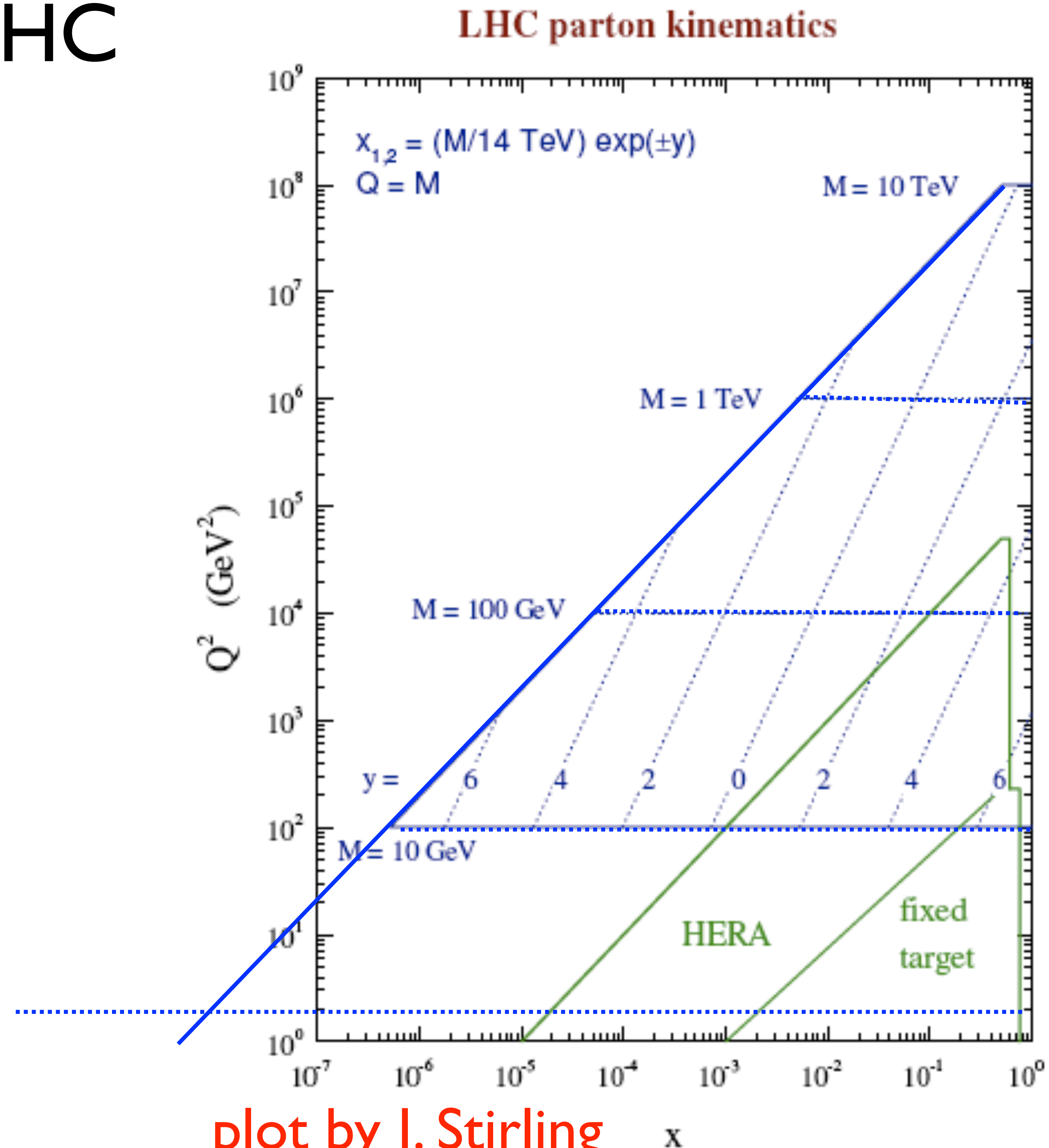

plot by J. Stirling

Relevance of low x region for CR and UHEnus

Kinematic boundary for LHC

Different rapidities

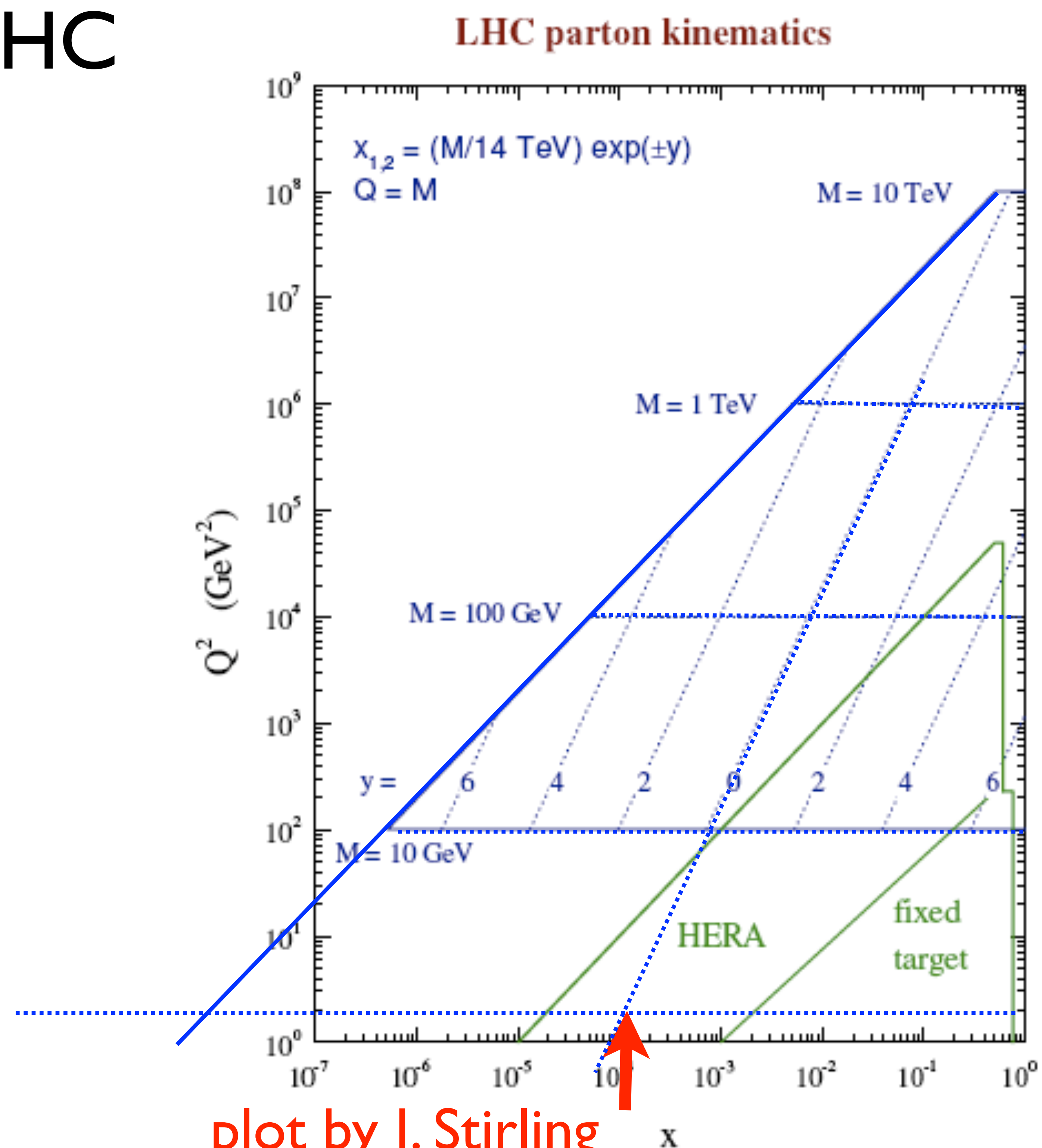

plot by J. Stirling

Relevance of low x region for CR and UHEnus

Kinematic boundary for LHC

Different rapidities

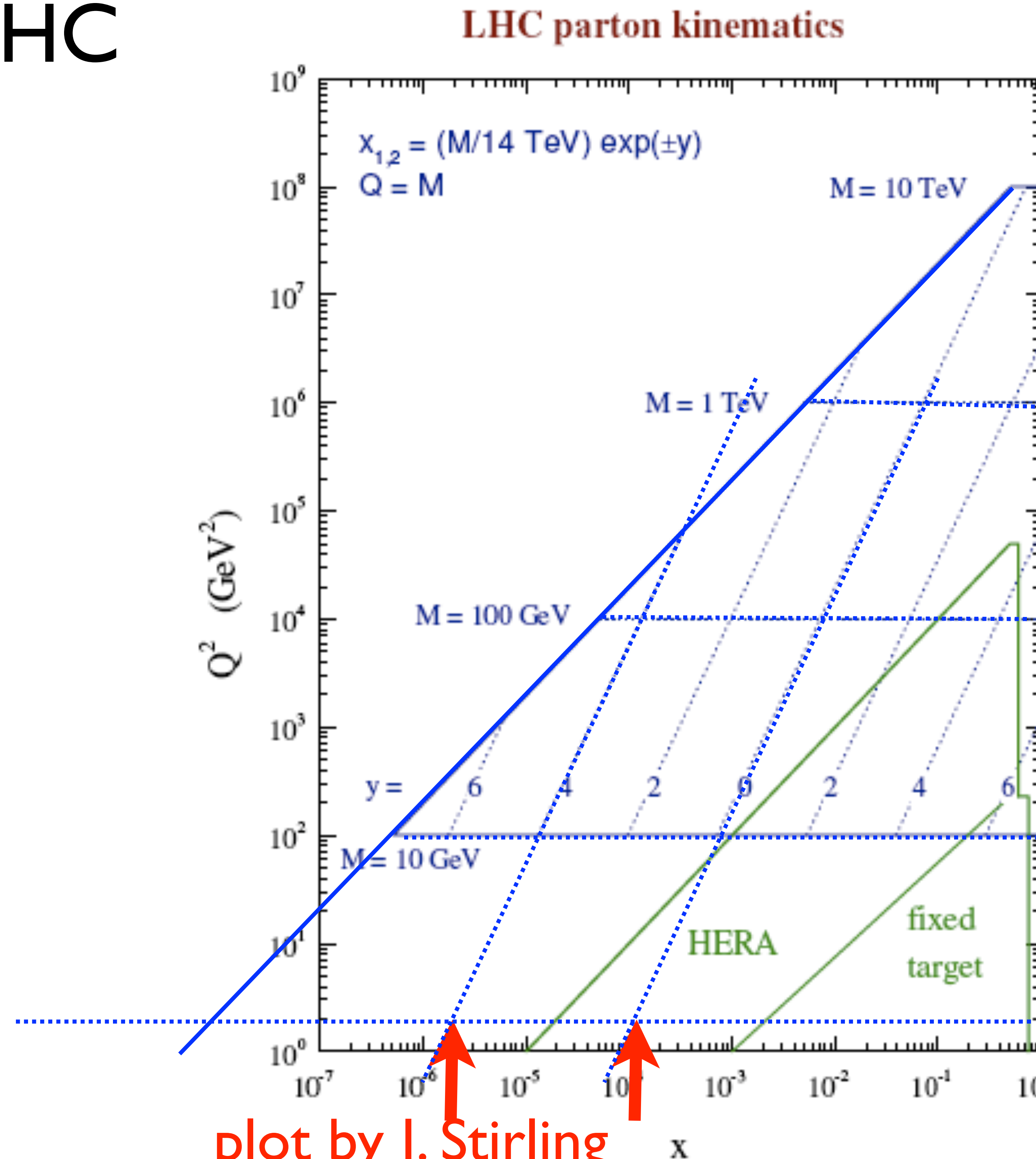

plot by J. Stirling

Relevance of low x region for CR and UHEnus

Kinematic boundary for CR: 100 TeV c.m.s.

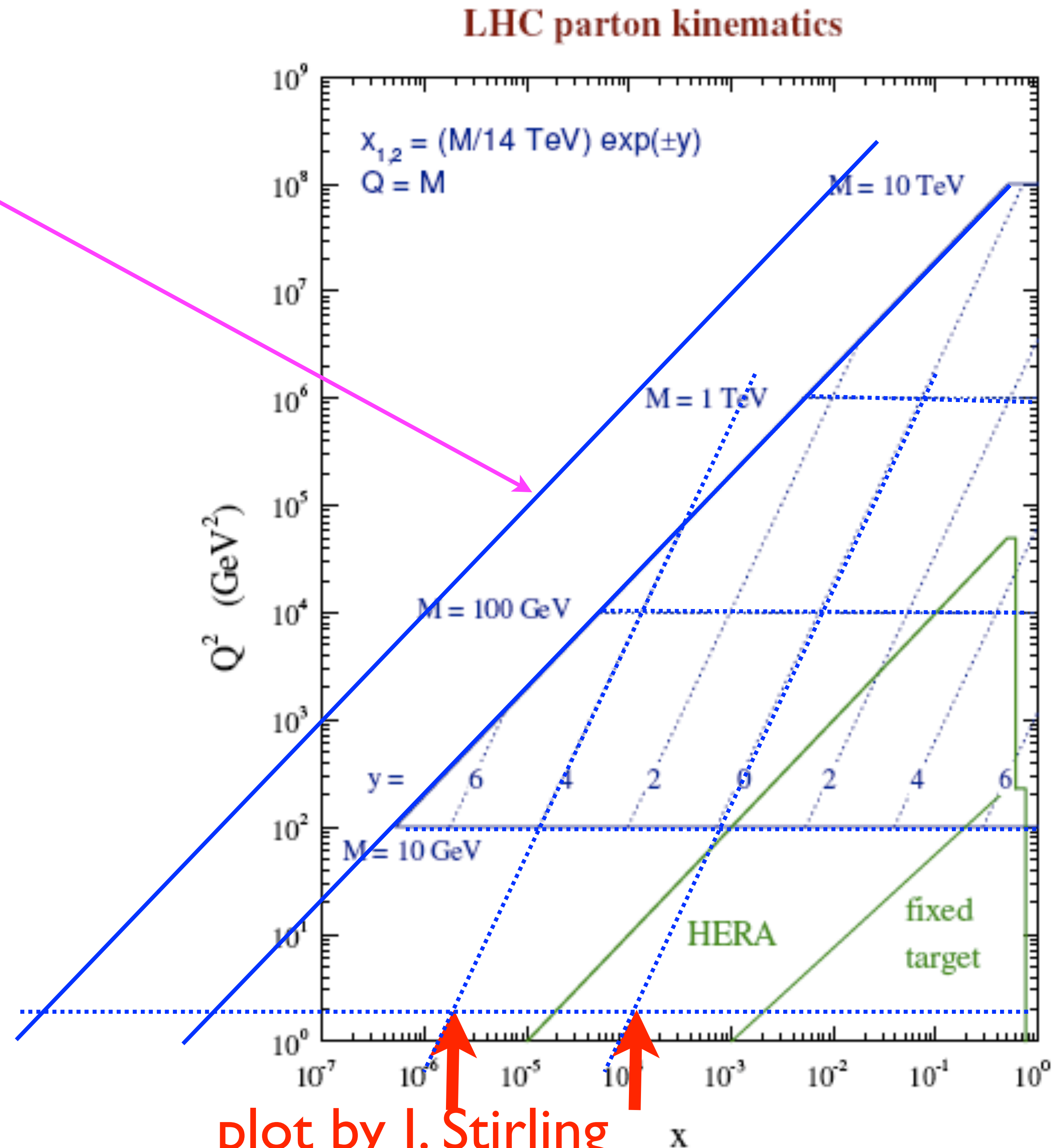

plot by J. Stirling

Relevance of low x region for CR and UHEnus

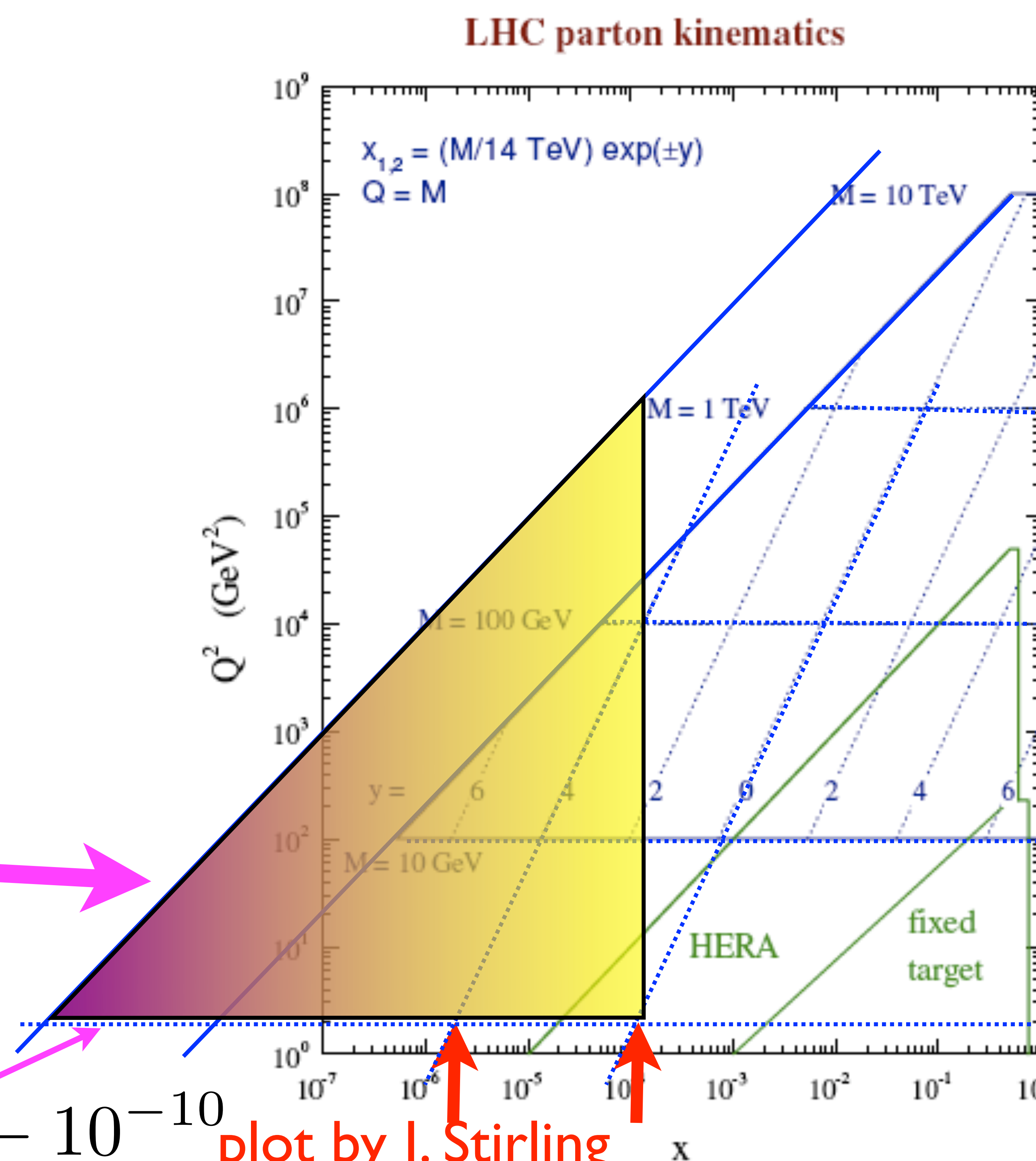

Very large region with very small x!

$x \sim 10^{-9} - 10^{-10}$

plot by J. Stirling

Relevance of low x region for CR and UHEnus

UHE neutrinos

Very large region with very small x!

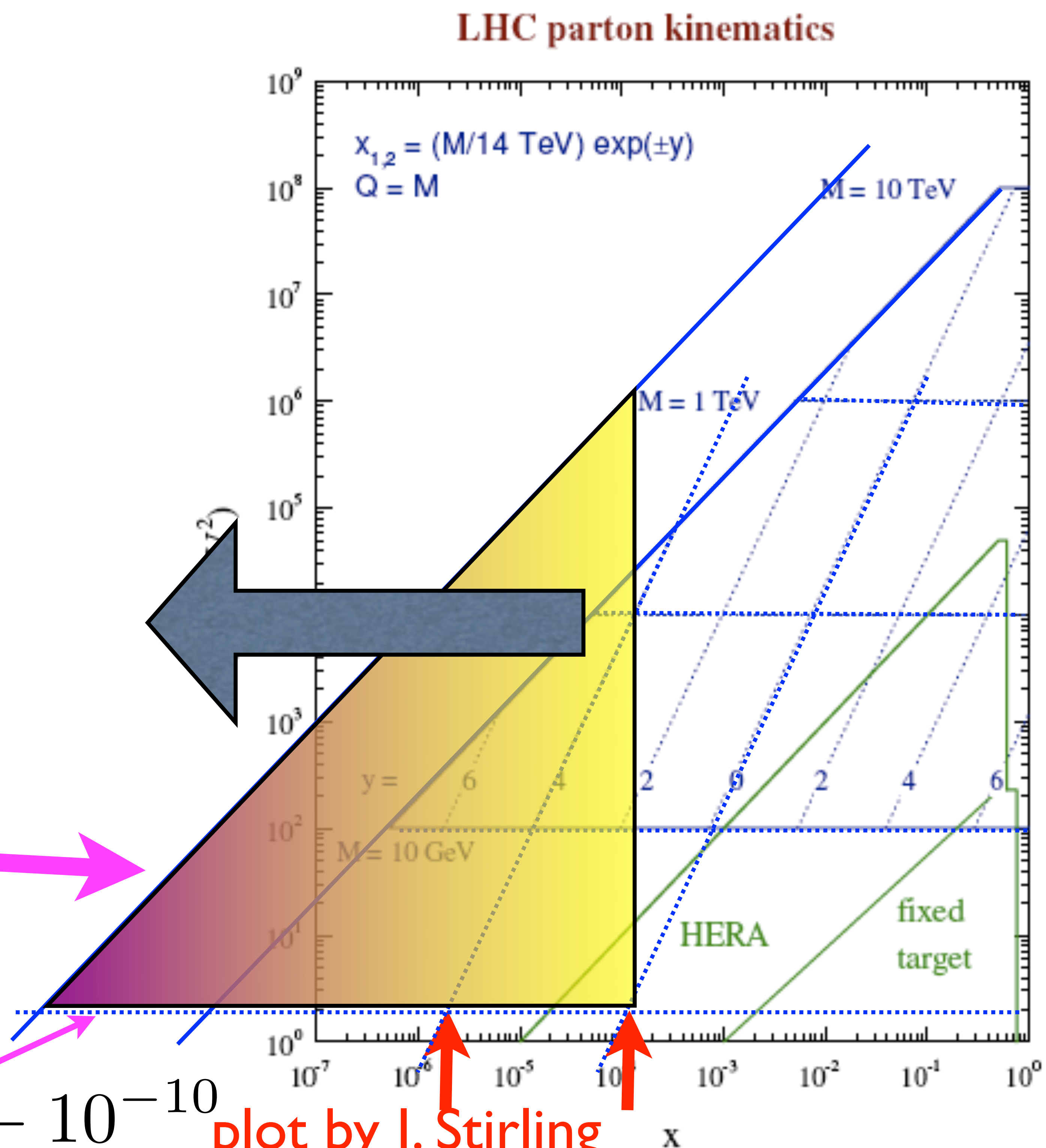

$x \sim 10^{-9} - 10^{-10}$

plot by J. Stirling

Standard Collinear framework (DIS example)

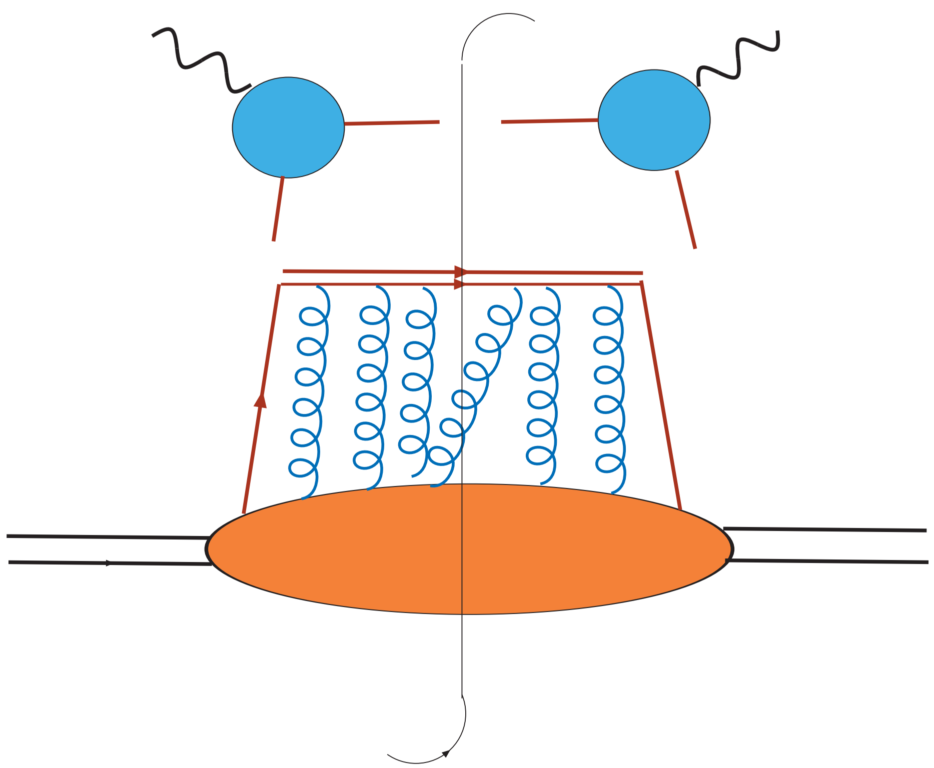

Standard Collinear framework (DIS example)

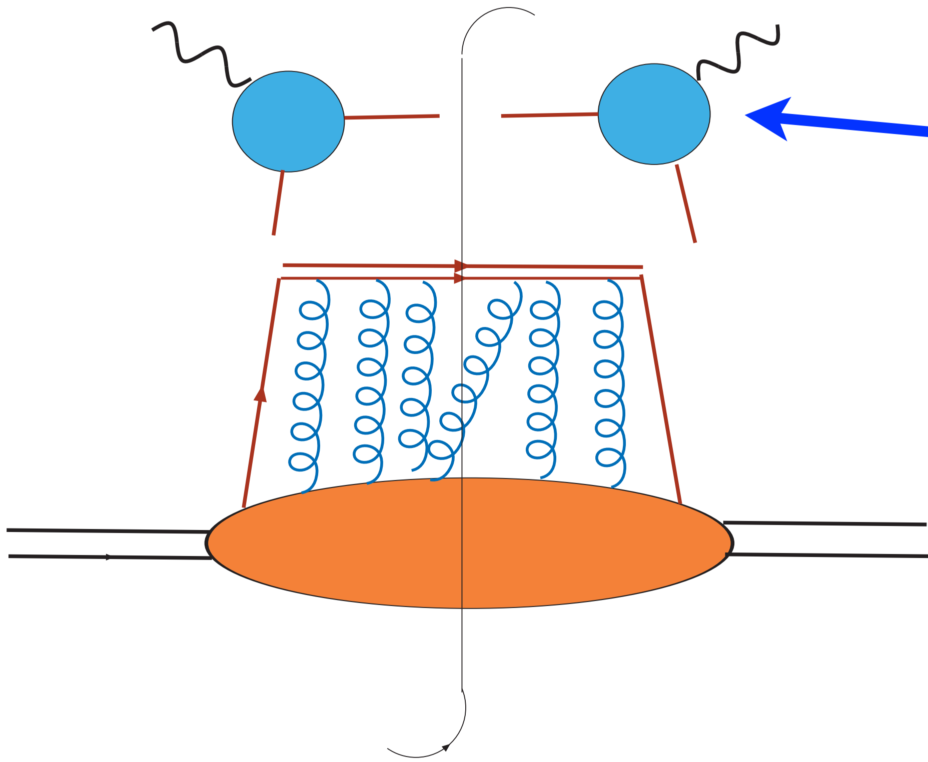

Hard scattering coefficient.
On-shell matrix element

$$H(Q/\mu, x/z, \alpha_s) = \sum_i \alpha_s^i \, H_i$$

Standard Collinear framework (DIS example)

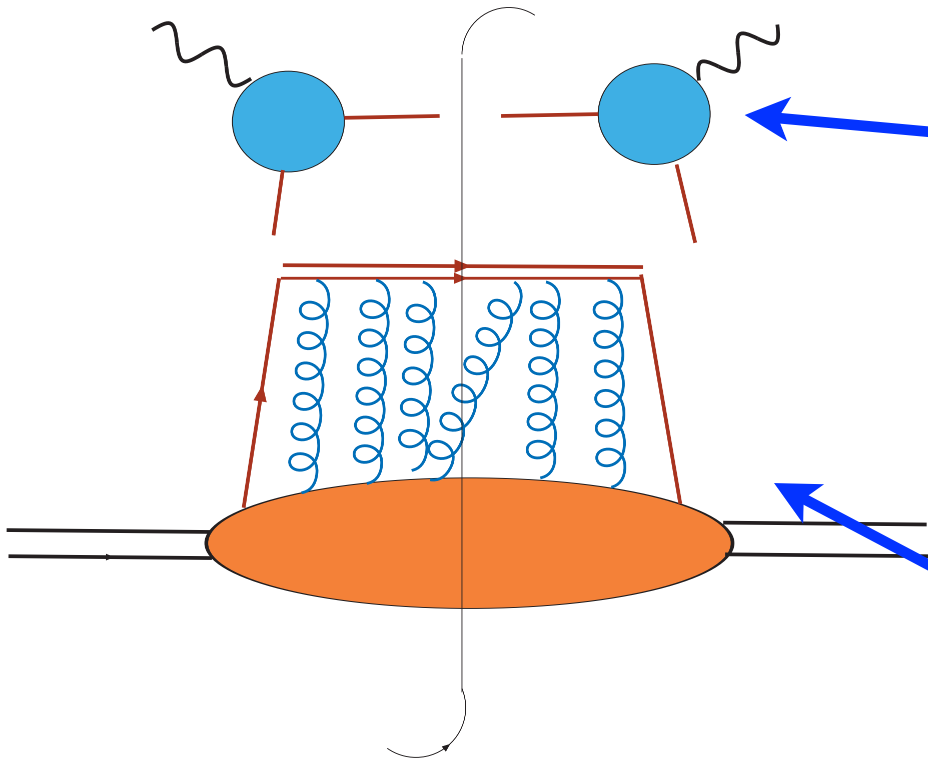

Hard scattering coefficient.
On-shell matrix element

$$H(Q/\mu, x/z, \alpha_s) = \sum_i \alpha_s^i \, H_i$$

Integrated parton distribution:

$$f(x, \mu)$$

Standard Collinear framework (DIS example)

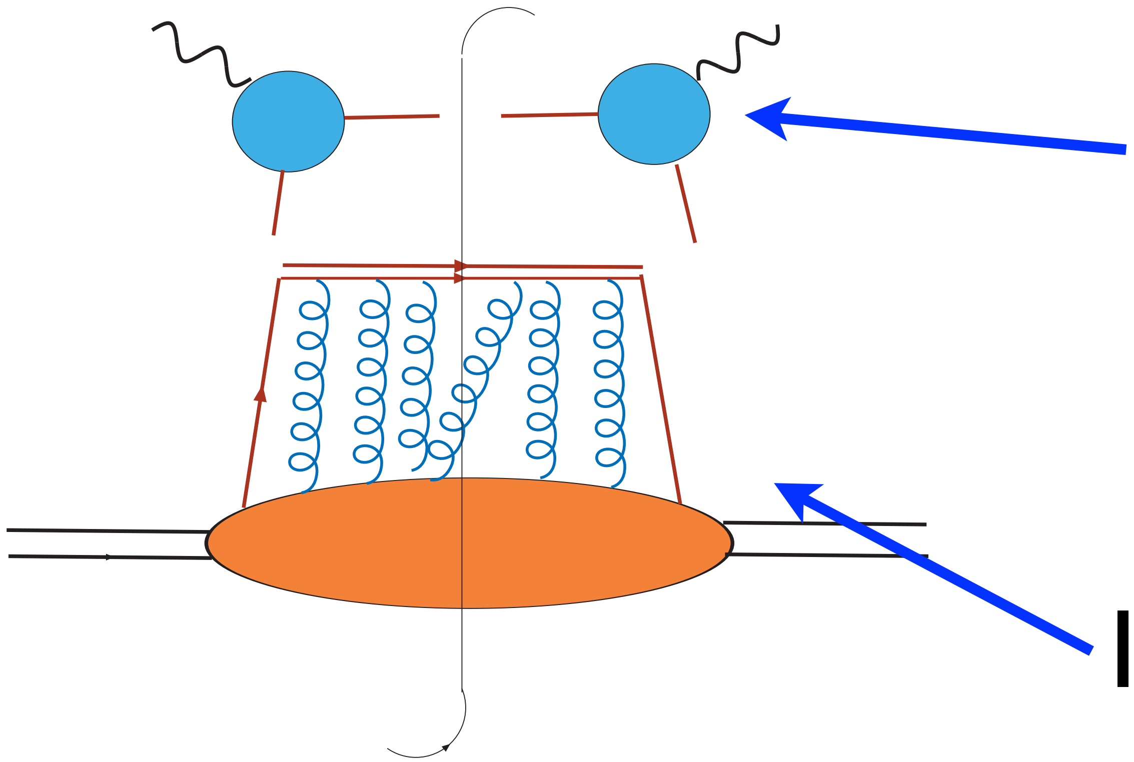

Hard scattering coefficient.
On-shell matrix element

$$H(Q/\mu, x/z, \alpha_s) = \sum_i \alpha_s^i \, H_i$$

Integrated parton distribution:

$$f(x, \mu)$$

Factorization for structure function:

$$F_{T,L}(x, Q^2) = \sum_j \int_x^1 \frac{dz}{z} f_{j/h}(z, \mu) H^j_{T,L}(x/z, Q/\mu, \alpha_s(\mu)) + \mathcal{O}(\Lambda/Q)$$

Standard Collinear framework (DIS example)

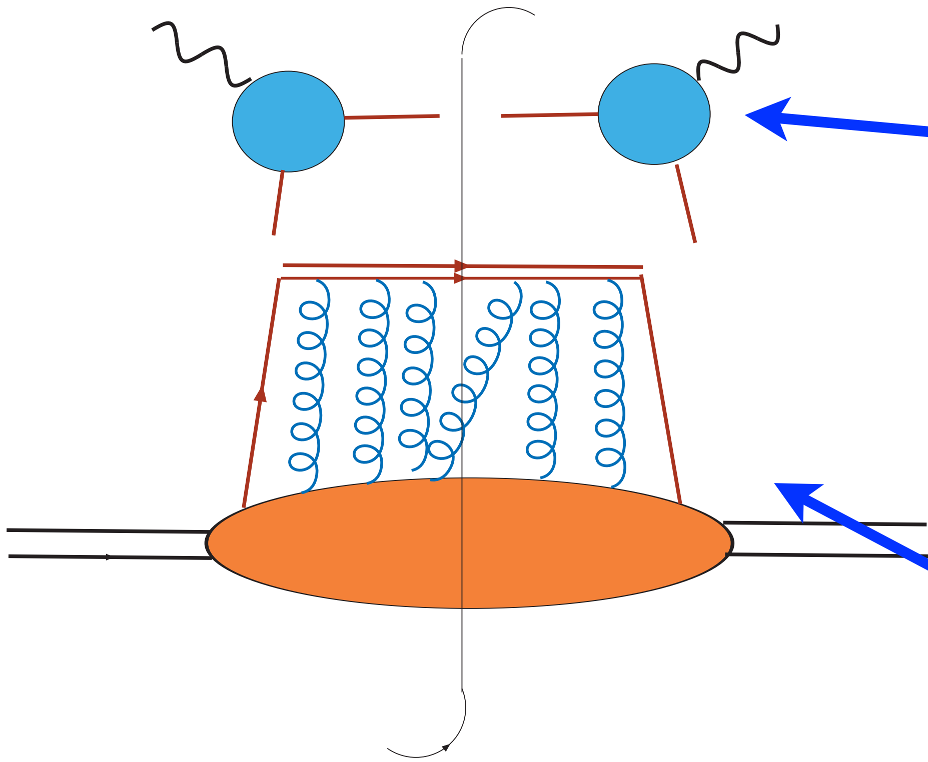

Hard scattering coefficient.
On-shell matrix element

$$H(Q/\mu, x/z, \alpha_s) = \sum_i \alpha_s^i \, H_i$$

Integrated parton distribution:

$$f(x, \mu)$$

Factorization for structure function:

$$F_{T,L}(x, Q^2) = \sum_j \int_x^1 \frac{dz}{z} f_{j/h}(z, \mu) H^j_{T,L}(x/z, Q/\mu, \alpha_s(\mu)) + \mathcal{O}(\Lambda/Q)$$

Renormalization group equations:

$$\mu \frac{d}{d\mu} f_{j/h}(x, \mu) = \sum_k \int_x^1 \frac{dz}{z} P_{jk}(z, \alpha_s(\mu)) f_{k/h}(x/z, \mu)$$

Standard Collinear framework (DIS example)

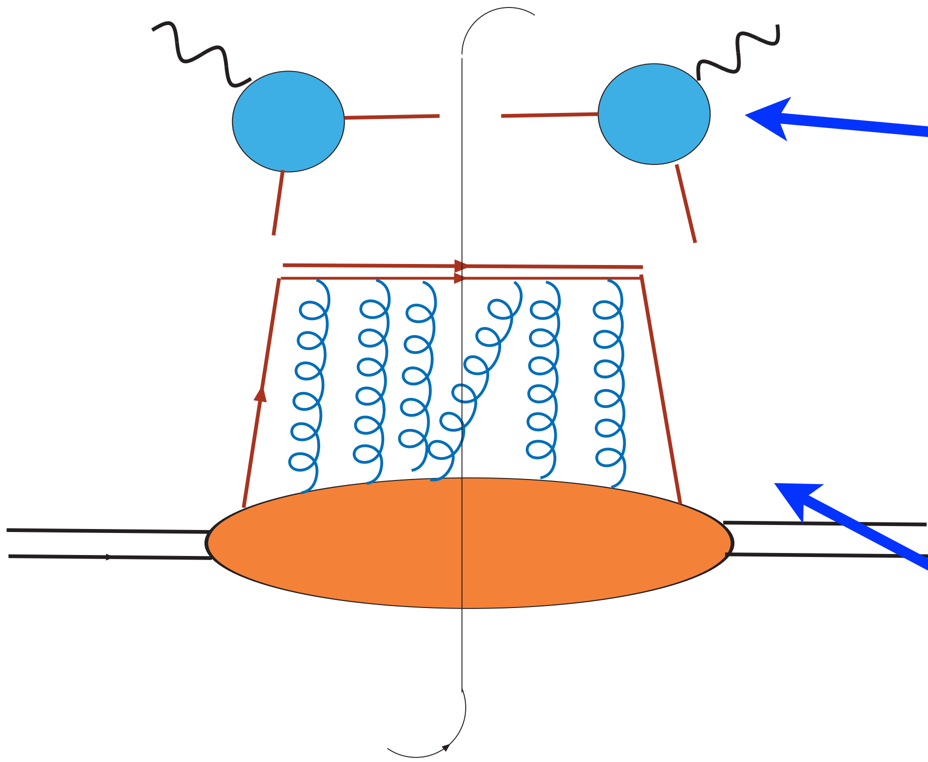

Hard scattering coefficient. On-shell matrix element

$$H(Q/\mu, x/z, \alpha_s) = \sum_i \alpha_s^i \, H_i$$

Integrated parton distribution:

$$f(x, \mu)$$

Factorization for structure function:

$$F_{T,L}(x, Q^2) = \sum_j \int_x^1 \frac{dz}{z} f_{j/h}(z, \mu) H^j_{T,L}(x/z, Q/\mu, \alpha_s(\mu)) + \mathcal{O}(\Lambda/Q)$$

Renormalization group equations:

$$\mu \frac{d}{d\mu} f_{j/h}(x, \mu) = \sum_k \int_x^1 \frac{dz}{z} P_{jk}(z, \alpha_s(\mu)) f_{k/h}(x/z, \mu)$$

Expansion for anomalous dimensions(splitting functions)

$$P_{jk}(z, \alpha_s(\mu)) = \sum_i (\alpha_s(\mu))^i P^{(i)}_{jk}(z)$$

Large corrections to fixed order at small x

$$x^{-1}F_L = C_{L,\mathrm{ns}} \otimes q_{\mathrm{ns}} + \langle e^2 \rangle \left(C_{L,\mathrm{q}} \otimes q_{\mathrm{s}} + C_{L,\mathrm{g}} \otimes g \right)$$

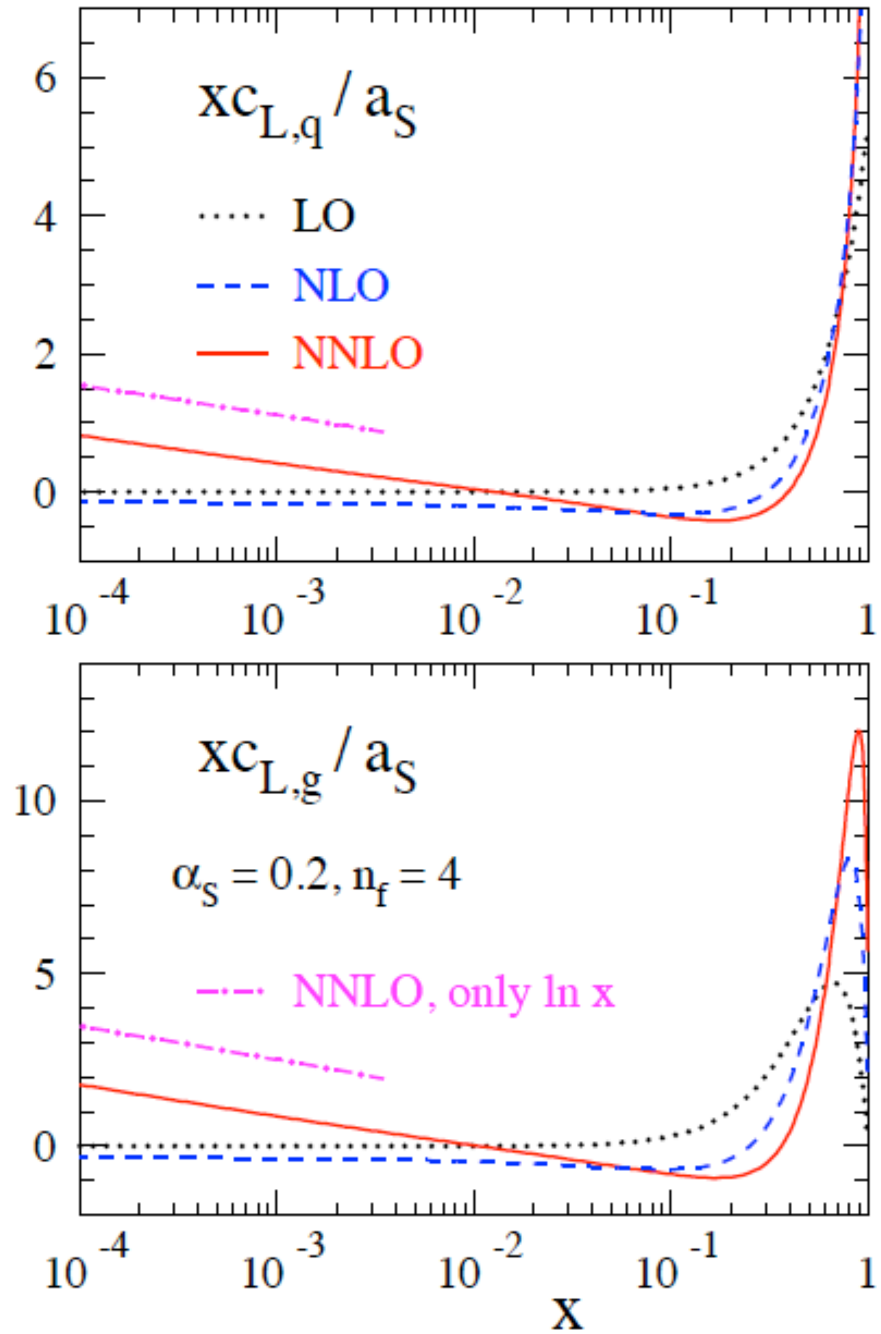

Moch, Vermaseren, Vogt

Singlet-quark and gluon coefficient of the longitudinal structure function up to NNLO order

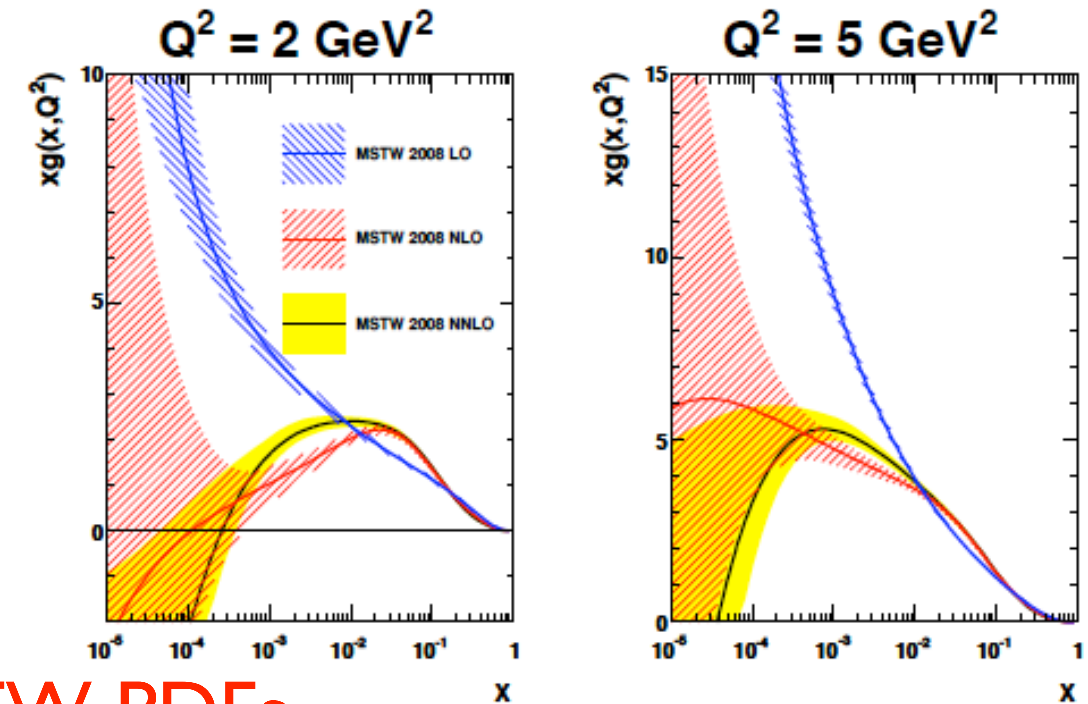

MSTW PDFs

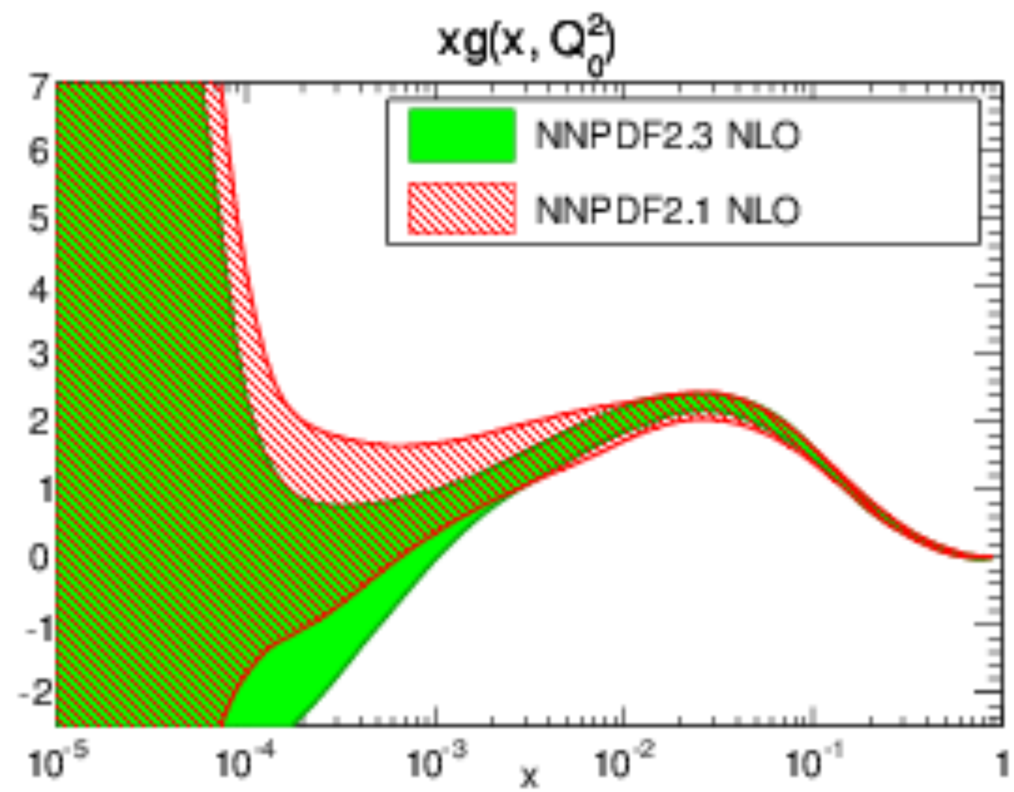

NNPDF2.3 PDFs

Large gluon uncertainties from fits to the data. Negative gluon...

High energy limit

$$\sqrt{s} \to \infty, x \to 0$$

Energy much larger than any other scale in the process

At small x there are potentially large logs:

$$xP_{gg}(x) \sim \alpha_S^n \ln^{n-1}(1/x), \quad xP_{qg}(x) \sim \alpha_S^n \ln^{n-2}(1/x) \quad \text{and} \quad xC_{L,g}(x) \sim \alpha_S^n \ln^{n-2}(1/x).$$

High energy limit

$$\boxed{\sqrt{s} \to \infty, x \to 0}$$

Energy much larger than any other scale in the process

At small x there are potentially large logs:

$$xP_{gg}(x) \sim \alpha_S^n \ln^{n-1}(1/x), \quad xP_{qg}(x) \sim \alpha_S^n \ln^{n-2}(1/x) \quad \text{and} \quad xC_{L,g}(x) \sim \alpha_S^n \ln^{n-2}(1/x).$$

At high energy, or small x we can have:

$$\boxed{\alpha_S \ln 1/x \sim 1}$$

High energy limit

$$\boxed{\sqrt{s} \to \infty, x \to 0}$$

Energy much larger than any other scale in the process

At small x there are potentially large logs:

$$xP_{gg}(x) \sim \alpha_S^n \ln^{n-1}(1/x), \quad xP_{qg}(x) \sim \alpha_S^n \ln^{n-2}(1/x) \quad \text{and} \quad xC_{L,g}(x) \sim \alpha_S^n \ln^{n-2}(1/x).$$

At high energy, or small x we can have:

$$\boxed{\alpha_S \ln 1/x \sim 1}$$

Need to resum them as well to all orders:

$$\boxed{(\alpha_S \ln 1/x)^n}$$

High energy limit

$$\boxed{\sqrt{s} \to \infty, x \to 0}$$

Energy much larger than any other scale in the process

At small x there are potentially large logs:

$$xP_{gg}(x) \sim \alpha_S^n \ln^{n-1}(1/x), \quad xP_{qg}(x) \sim \alpha_S^n \ln^{n-2}(1/x) \quad \text{and} \quad xC_{L,g}(x) \sim \alpha_S^n \ln^{n-2}(1/x).$$

At high energy, or small x we can have:

$$\boxed{\alpha_S \ln 1/x \sim 1}$$

Need to resum them as well to all orders:

$$\boxed{(\alpha_S \ln 1/x)^n}$$

Any fixed order here would not be sufficient, potentially very large corrections.

Many gluon emissions in small x limit

Cascade of the n soft gluons

Many gluon emissions in small x limit

Cascade of the n soft gluons

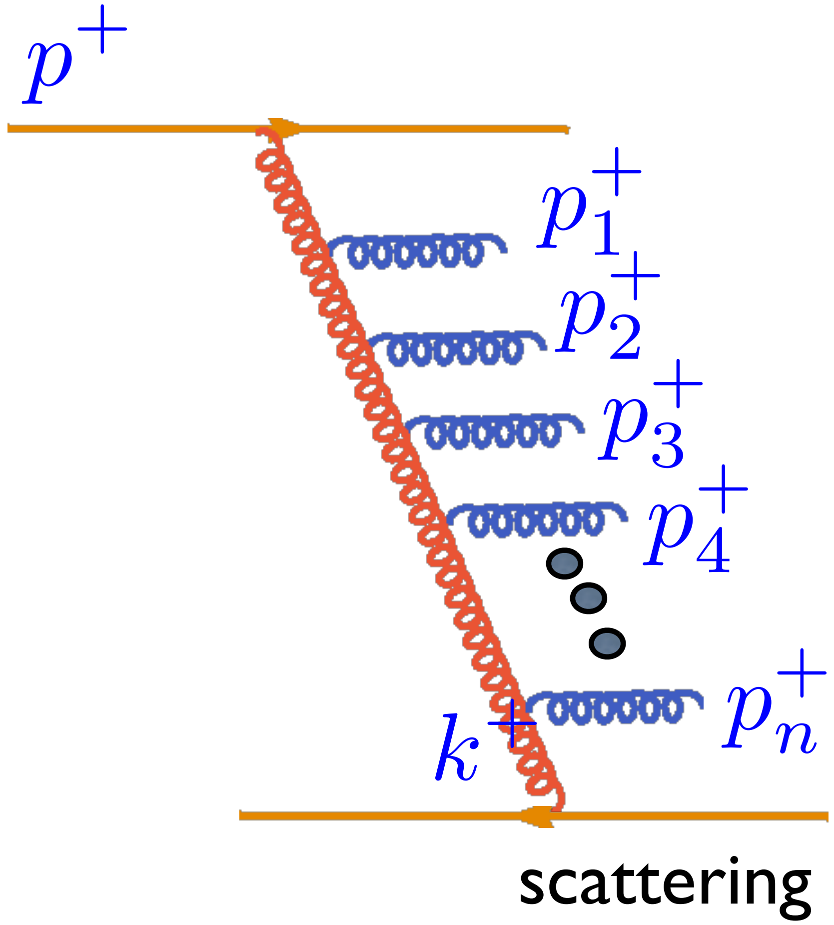

Many gluon emissions in small x limit

Cascade of the n soft gluons

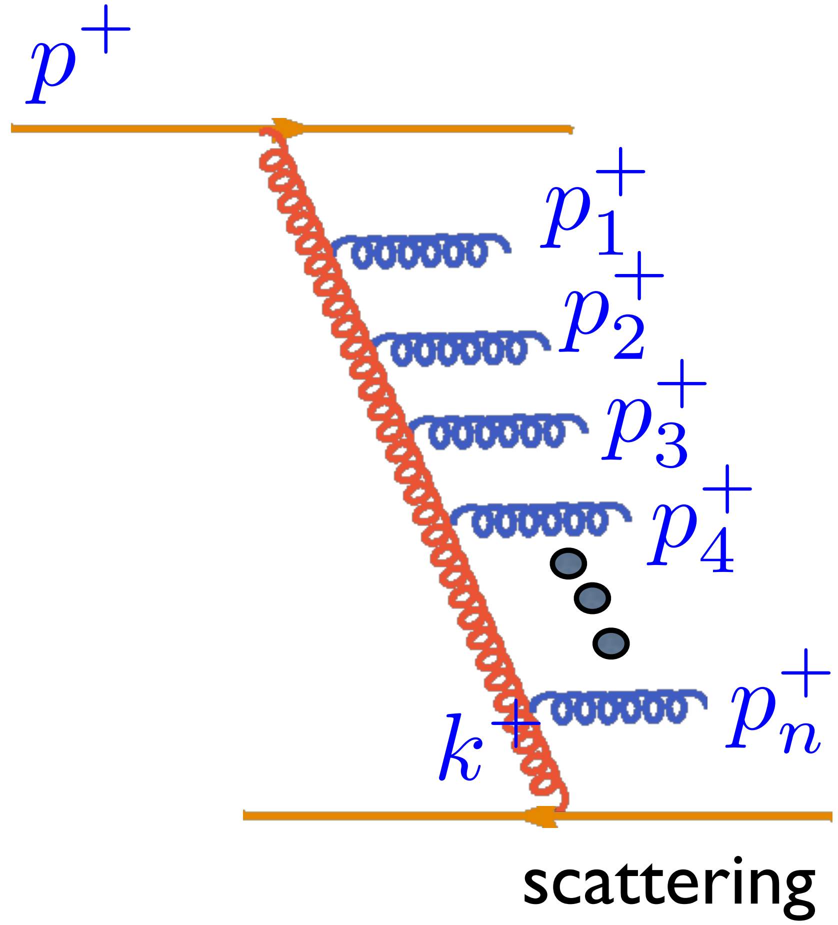

Strong ordering (in longitudinal momenta)

$$p^+ \gg p_1^+ \gg p_2^+ \gg \cdots \gg p_n^+ \gg k^+$$

Note: transverse momenta are not ordered

Many gluon emissions in small x limit

Cascade of the n soft gluons

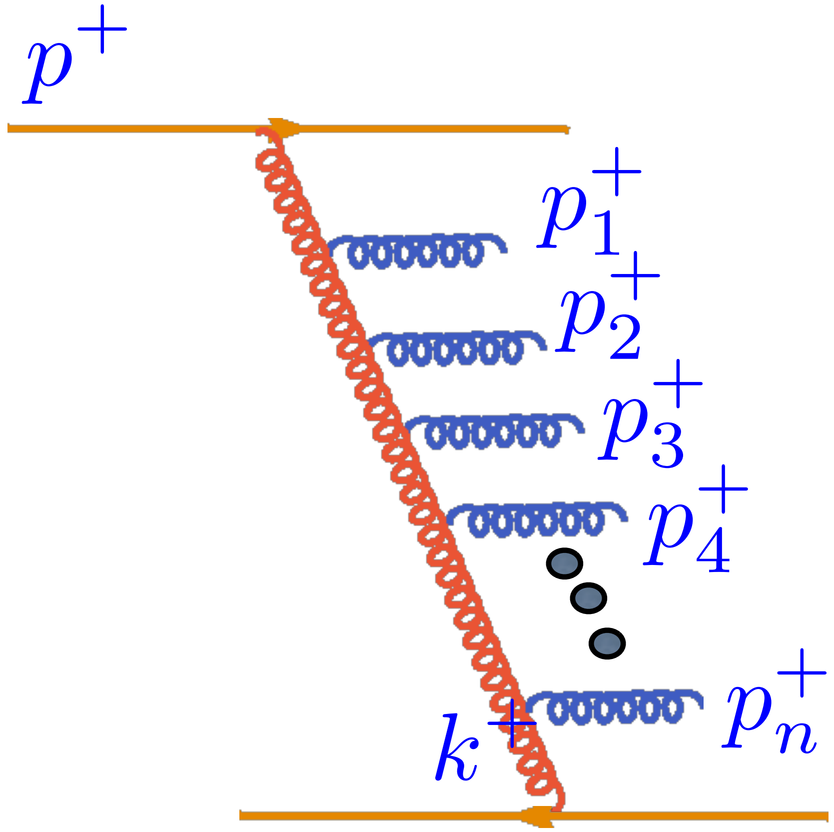

Strong ordering (in longitudinal momenta)

$$p^+ \gg p_1^+ \gg p_2^+ \gg \cdots \gg p_n^+ \gg k^+$$

Note: transverse momenta are not ordered

$$k^+ = xp^+$$

$$\frac{\alpha_s N_c}{\pi} \int_{k^+}^{p^+} \frac{dp_1^+}{p_1^+} = \frac{\alpha_s N_c}{\pi} \ln \frac{1}{x}$$

Large logarithm

Many gluon emissions in small x limit

Cascade of the n soft gluons

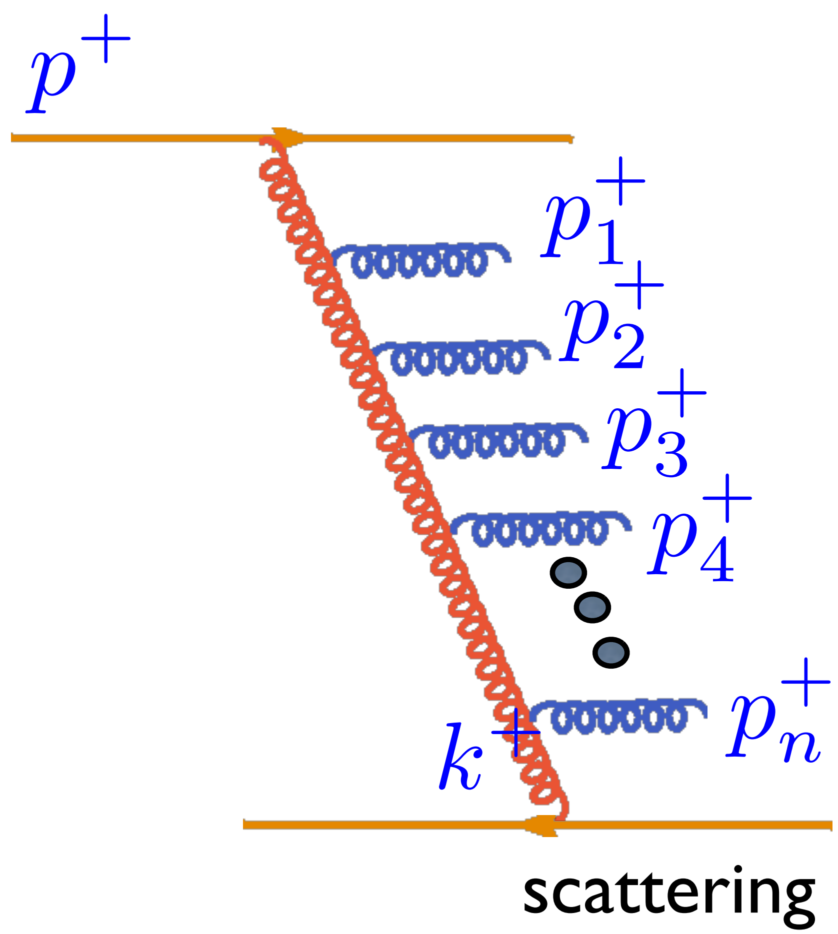

Strong ordering (in longitudinal momenta)

$$p^+ \gg p_1^+ \gg p_2^+ \gg \cdots \gg p_n^+ \gg k^+$$

Note: transverse momenta are not ordered

$$k^+ = xp^+$$

$$\frac{\alpha_s N_c}{\pi} \int_{k^+}^{p^+} \frac{dp_1^+}{p_1^+} = \frac{\alpha_s N_c}{\pi} \ln \frac{1}{x}$$

Large logarithm

Nested logarithmic integrals

$$\left(\frac{\alpha_s N_c}{\pi} \ln \frac{1}{x} \right)^n$$

Many gluon emissions in small x limit

Cascade of the n soft gluons

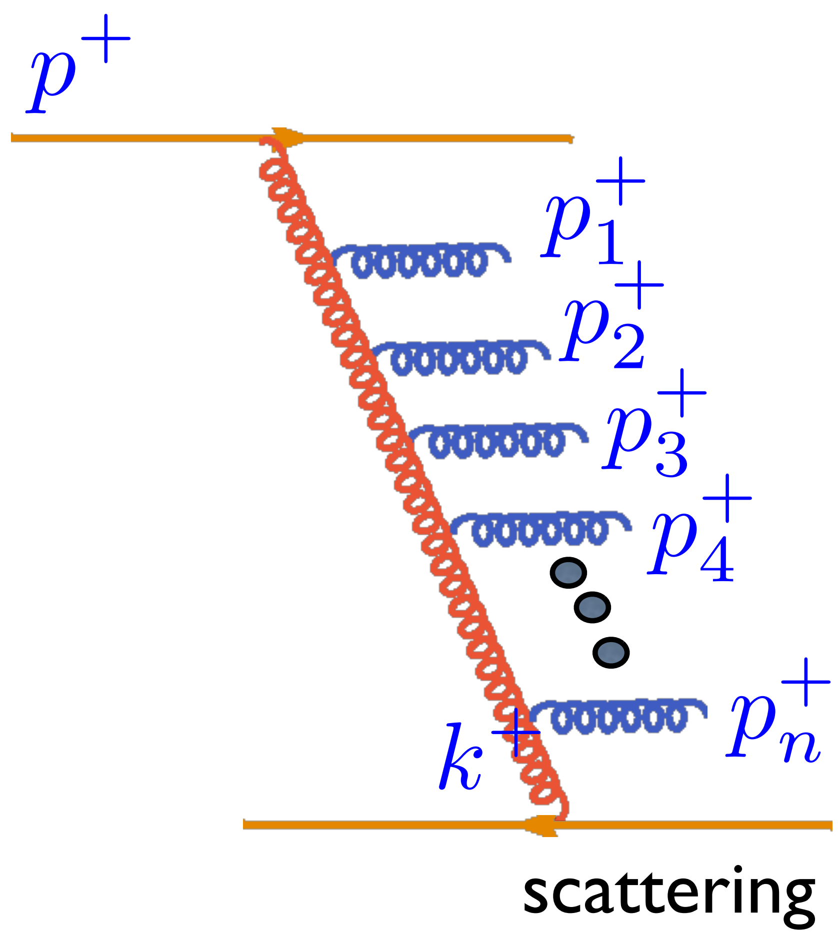

Strong ordering (in longitudinal momenta)

$$p^+ \gg p_1^+ \gg p_2^+ \gg \cdots \gg p_n^+ \gg k^+$$

Note: transverse momenta are not ordered

$$k^+ = xp^+$$

$$\frac{\alpha_s N_c}{\pi} \int_{k^+}^{p^+} \frac{dp_1^+}{p_1^+} = \frac{\alpha_s N_c}{\pi} \ln \frac{1}{x}$$

Large logarithm

Nested logarithmic integrals

$$\left(\frac{\alpha_s N_c}{\pi} \ln \frac{1}{x} \right)^n$$

Resummation of the gluon emissions performed by the equation

$$\frac{df_g(x,k_T)}{d\ln 1/x} = \frac{\alpha_s N_c}{\pi} \int d^2k'_T \mathcal{K}(k_T,k'_T)\; f_g(x,k'_T)$$

I.Balitsky,V.Fadin, E.Kuraev,L.Lipatov

integral over transverse momenta

kernel describing branching of gluons

unintegrated (transverse momentum dependent)gluon density

Small x evolution

$$\frac{df_g(x,k_T)}{d\ln 1/x} = \frac{\alpha_s N_c}{\pi}\int d^2k'_T \mathcal{K}(k_T,k'_T)\ f_g(x,k'_T)$$

Small x evolution

$$\frac{df_g(x,k_T)}{d\ln 1/x} = \frac{\alpha_s N_c}{\pi}\int d^2k'_T \mathcal{K}(k_T,k'_T)\; f_g(x,k'_T)$$

$$\omega_P = j-1 = \frac{\alpha_s N_c}{\pi} 4\ln 2$$

Solution: $f_g(x,k_T) \sim x^{-\omega_P}$

Leading exponent(spin)

Small x evolution

$$\frac{df_g(x,k_T)}{d\ln 1/x} = \frac{\alpha_s N_c}{\pi}\int d^2k'_T \mathcal{K}(k_T,k'_T)\; f_g(x,k'_T)$$

$$\omega_P = j-1 = \frac{\alpha_s N_c}{\pi}4\ln 2$$

Solution: $f_g(x,k_T) \sim x^{-\omega_P}$

Leading exponent(spin)

Rise too strong for the data!

$\sigma^{DIS}_{\gamma^* p} \sim s^{\omega_P}$ with $\omega_P \sim 0.5$

Small x evolution

$$\frac{df_g(x,k_T)}{d\ln 1/x} = \frac{\alpha_s N_c}{\pi}\int d^2k'_T \mathcal{K}(k_T,k'_T)\; f_g(x,k'_T)$$

$$\omega_P = j-1 = \frac{\alpha_s N_c}{\pi} 4\ln 2$$

Solution: $f_g(x,k_T) \sim x^{-\omega_P}$

Leading exponent(spin)

Rise too strong for the data!

$\sigma^{DIS}_{\gamma^* p} \sim s^{\omega_P}$ with $\omega_P \sim 0.5$

Take higher order corrections NLLx:

$$\alpha_s \mathcal{K}_0 + \alpha_s^2 \mathcal{K}_1 + \ldots$$

V.Fadin,L.Lipatov, G.Camici,M.Ciafaloni

$$\omega_P \simeq \bar{\alpha}_s 4\ln 2(1-6.5\bar{\alpha}_s)$$

Small x evolution

$$\frac{df_g(x,k_T)}{d\ln 1/x} = \frac{\alpha_s N_c}{\pi}\int d^2k'_T \mathcal{K}(k_T,k'_T)\, f_g(x,k'_T)$$

$$\omega_P = j-1 = \frac{\alpha_s N_c}{\pi} 4\ln 2$$

Solution: $f_g(x,k_T) \sim x^{-\omega_P}$

Leading exponent(spin)

Rise too strong for the data!

$\sigma^{DIS}_{\gamma^* p} \sim s^{\omega_P}$ with $\omega_P \sim 0.5$

Take higher order corrections NLLx:

$$\alpha_s \mathcal{K}_0 + \alpha_s^2 \mathcal{K}_1 + \ldots$$

V.Fadin,L.Lipatov, G.Camici,M.Ciafaloni

$$\omega_P \simeq \bar{\alpha}_s 4\ln 2(1-6.5\bar{\alpha}_s)$$

Very large next-to-leading correction!

BFKL at NLLx

LLx vs NLLx BFKL numerical solution for the gluon Green's function

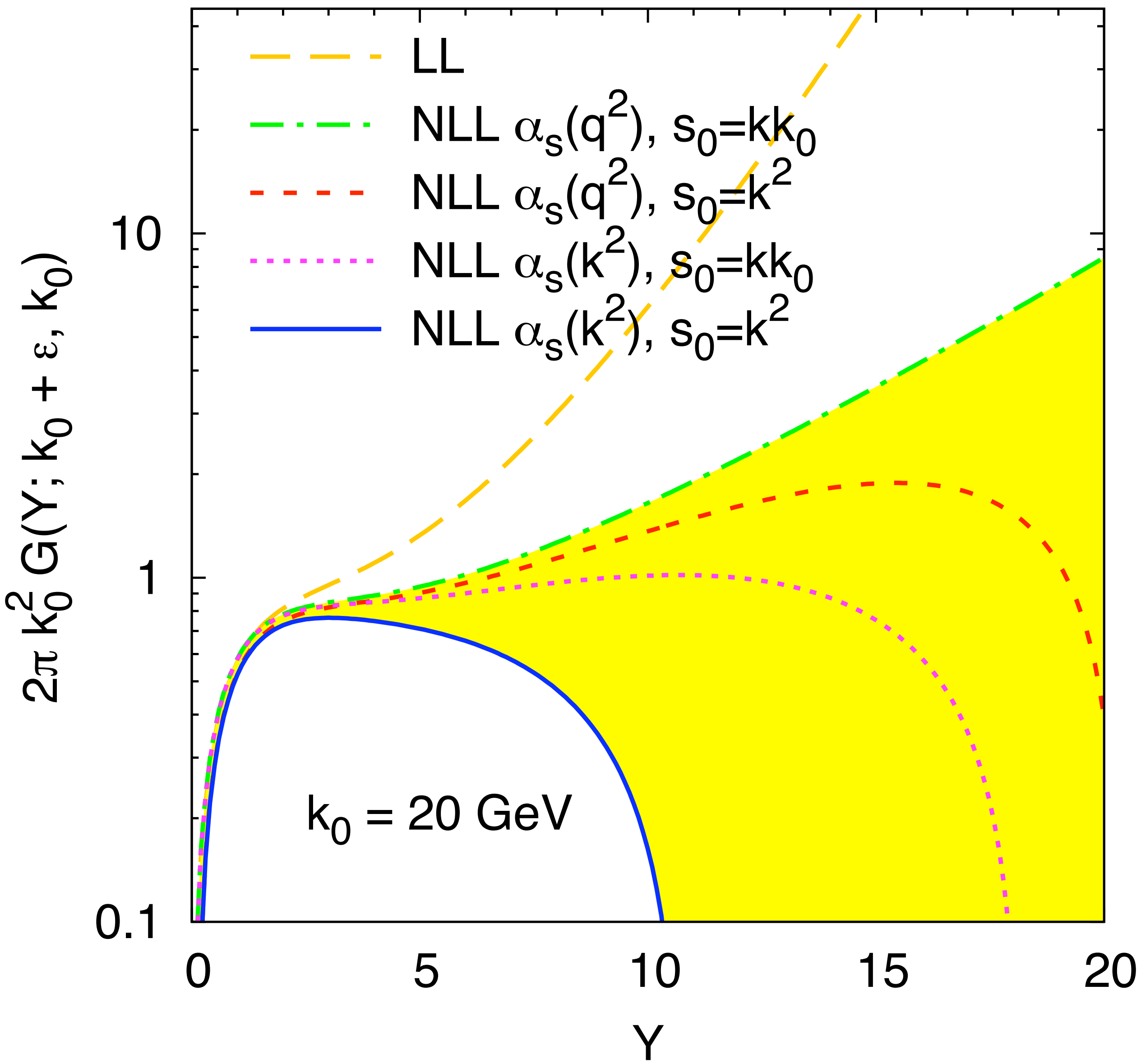

Note: Analytical solution at LLX in terms of properly defined eigenfunctions by Lipatov (1986) and at NLLx by Chirili and Kovchegov (2013)

- Scale of the coupling.
- Energy scale: $Y = \ln s/s_0$
- Differences large even though formally at NNLLx.

Very large correction at NLLx.
Need additional resummation at small x or stabilization of the result.

Why NLLx is so large in BFKL?

- Strong coupling constant is **<u>not</u>** a naturally small parameter in the Regge limit: $s \gg |t|, \Lambda^2_{QCD}$ but $\alpha_s(\mu^2),\ \mu^2 \neq s$

- Regge limit is inherently nonperturbative.

- Compare DGLAP (collinear approach): $Q^2 \gg \Lambda^2$ and $\alpha_s(Q^2) \ll 1$

- No momentum sum rule, since the evolution is local in x. In DGLAP: momentum sum rule satisfied at each order due to the initial assumption of the collinearity of the partons and the non-locality of the evolution in x.

- Approximations in the phase space (multi-Regge kinematics, quasi multi-Regge kinematics, etc..) cannot be recovered by the (fixed number of) the higher orders of expansion in the coupling constant.

Resummation

M. Ciafaloni, D. Colferai, G. Salam, AS ;G. Altarelli, R. Ball, S.Forte; R. Thorne;A. Sabio-Vera;Lipatov...

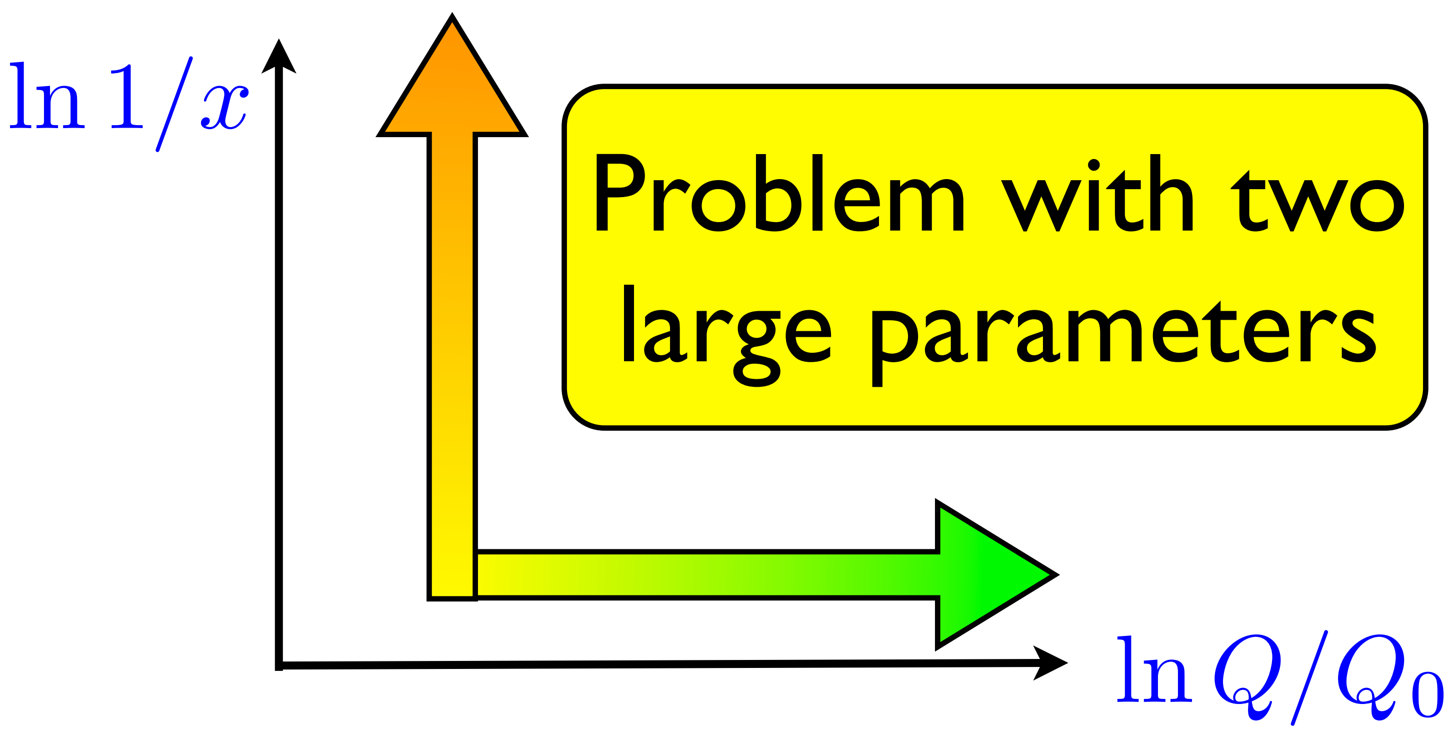

$$\left(\frac{\alpha_s N_c}{\pi} \ln \frac{1}{x}\right)^n$$

$$\left(\frac{\alpha_s N_c}{\pi} \ln \frac{Q}{Q_0}\right)^n$$

Resummed splitting function

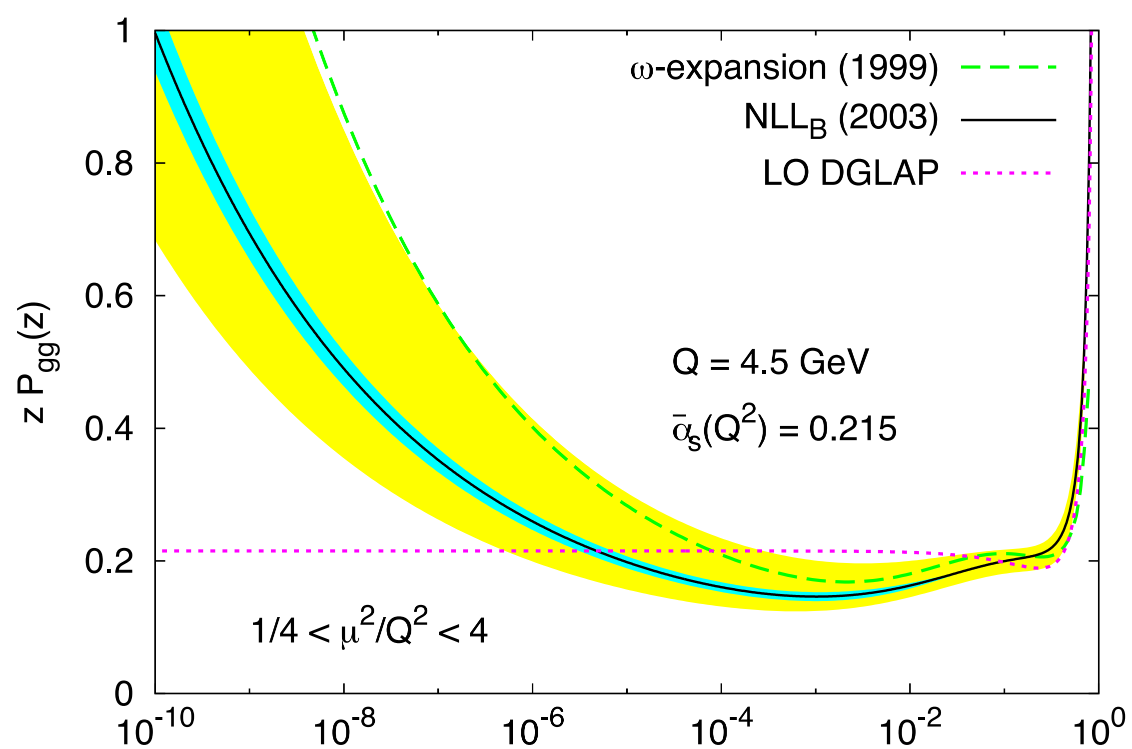

- Small x growth delayed to much smaller values of x and milder, $\omega_p \sim 0.3$
- Interesting feature: a dip seen at around $x \simeq 10^{-3}$
- The same feature seen in other schemes of resummation (Altarelli,Ball,Forte;Thorne).

Resummation

M. Ciafaloni, D. Colferai, G. Salam, AS ;G. Altarelli, R. Ball, S.Forte; R. Thorne;A.Sabio-Vera;Lipatov...

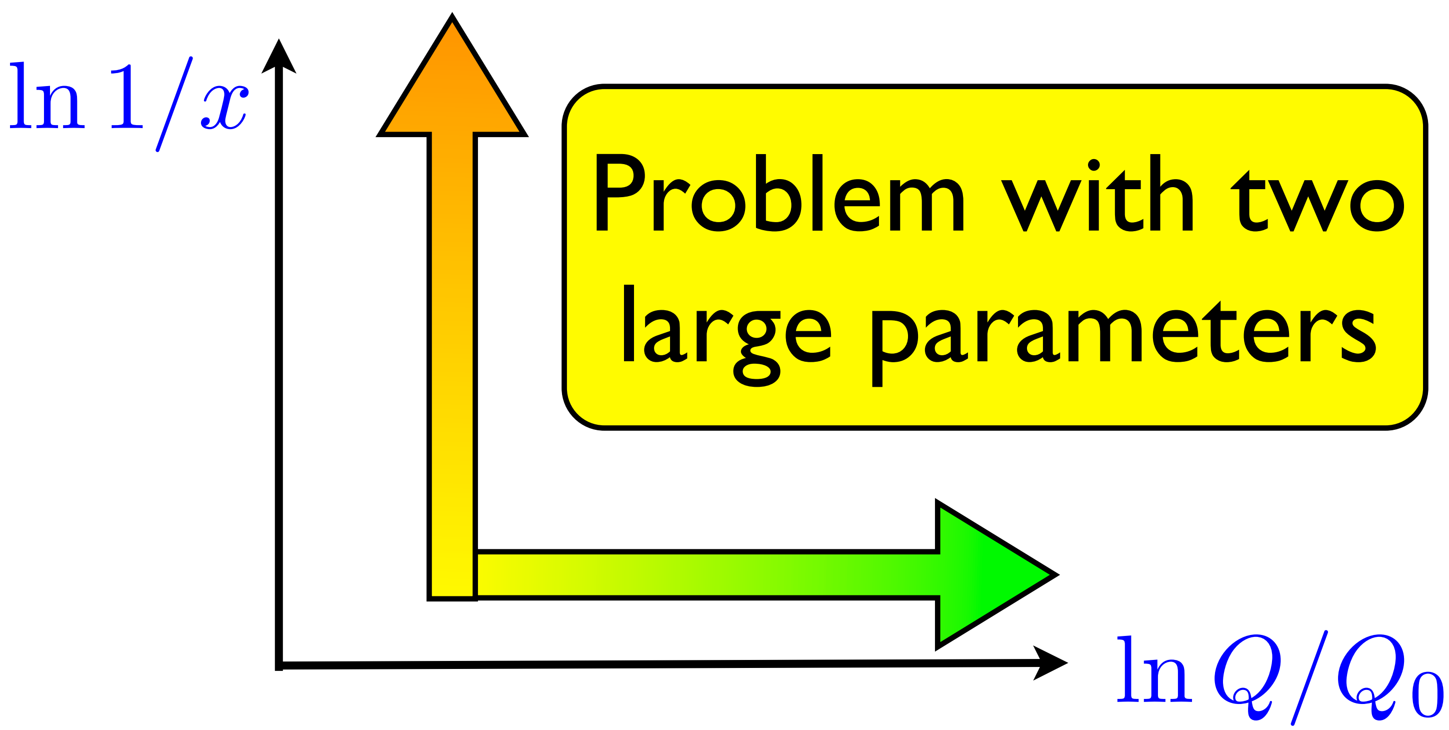

$$\left(\frac{\alpha_s N_c}{\pi}\ln\frac{1}{x}\right)^n$$ energy

$$\left(\frac{\alpha_s N_c}{\pi}\ln\frac{Q}{Q_0}\right)^n$$ scale (related to transverse momentum)

Resummed splitting function

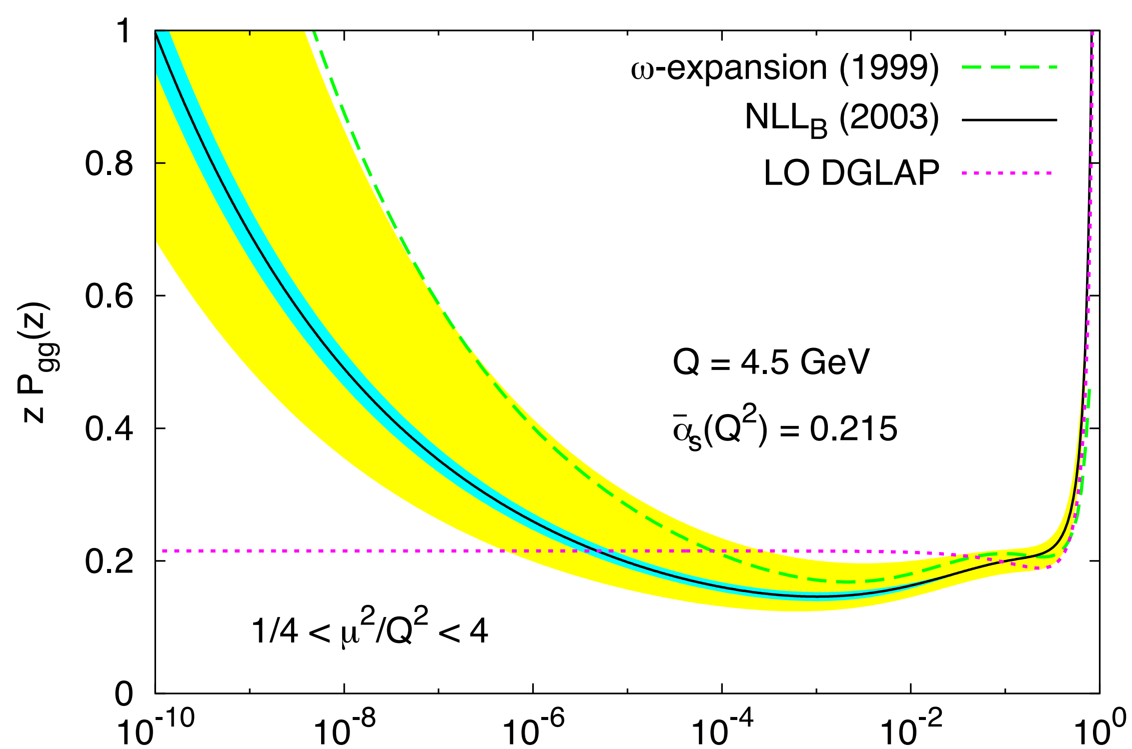

- Small x growth delayed to much smaller values of x and milder, $\omega_p \sim 0.3$
- Interesting feature: a dip seen at around $x \simeq 10^{-3}$
- The same feature seen in other schemes of resummation (Altarelli,Ball,Forte;Thorne).

Testing BFKL at colliders

Mueller-Navelet jets: two jets with similar transverse momenta and large rapidity separation

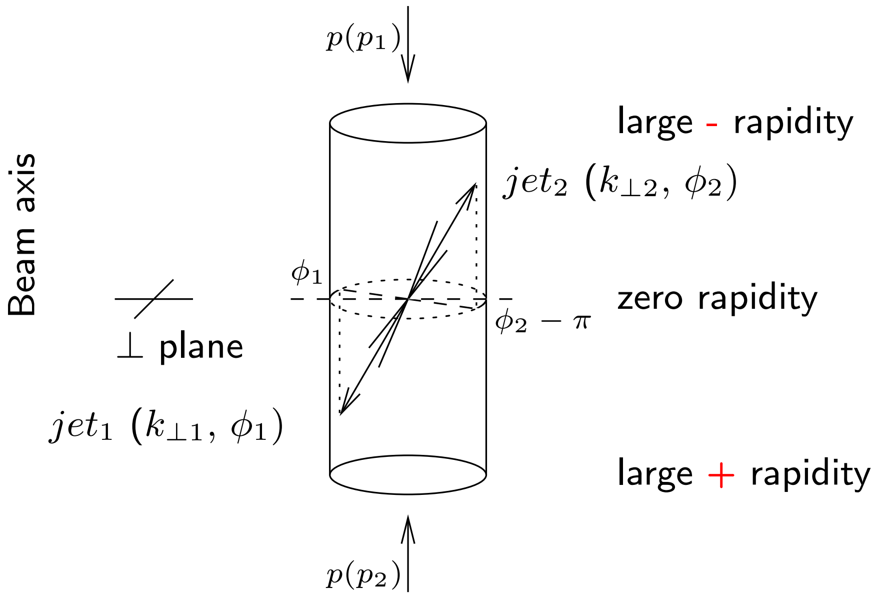

At LO collinear formalism such jets are emitted back to back.

Testing BFKL at colliders

Mueller-Navelet jets: two jets with similar transverse momenta and large rapidity separation

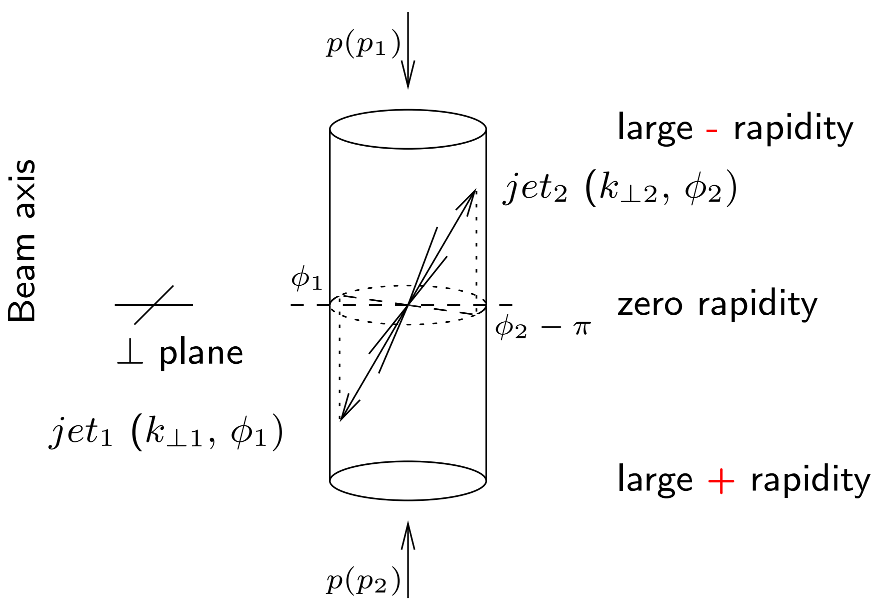

At LO collinear formalism such jets are emitted back to back.

Analysis of the azimuthal correlations using NLLx BFKL with Brodsky-Lepage-Mackenzie scale setting.

NLLx with BLM compares favorably with CMS data.

Ducloue, Szymanowski, Wallon

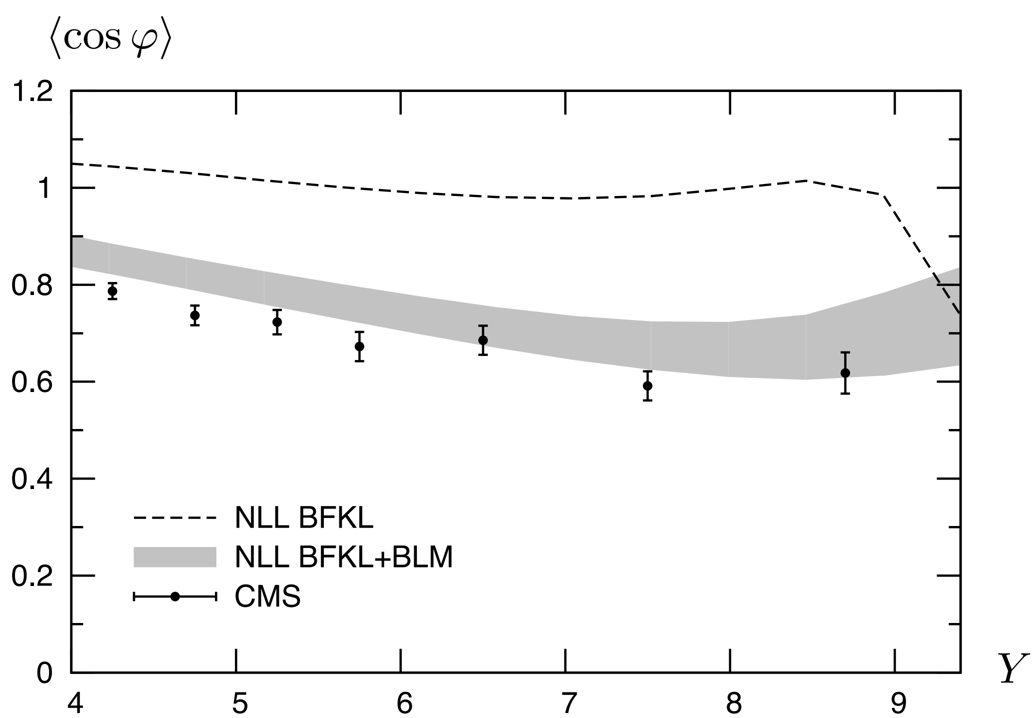

Azimuthal correlation $\langle \cos\varphi \rangle$

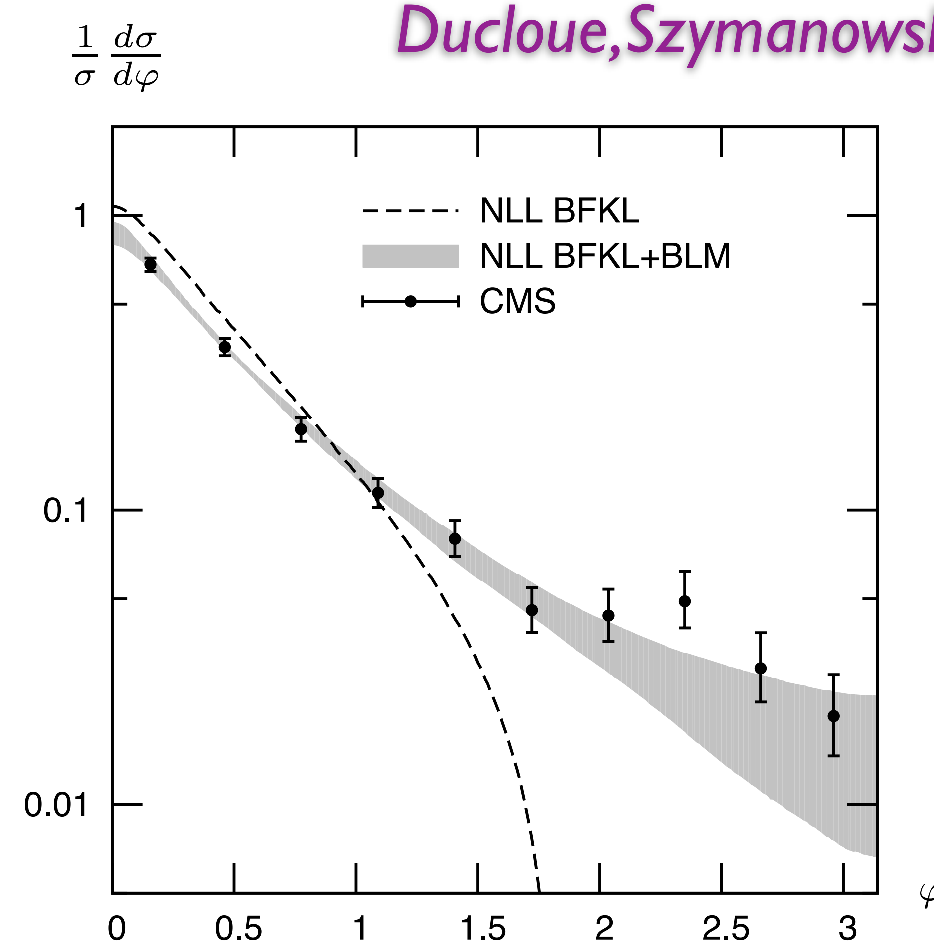

Azimuthal distribution (integrated over $6 < Y < 9.4$)

How about other effects: parton saturation?

At high enough density partons can also merge

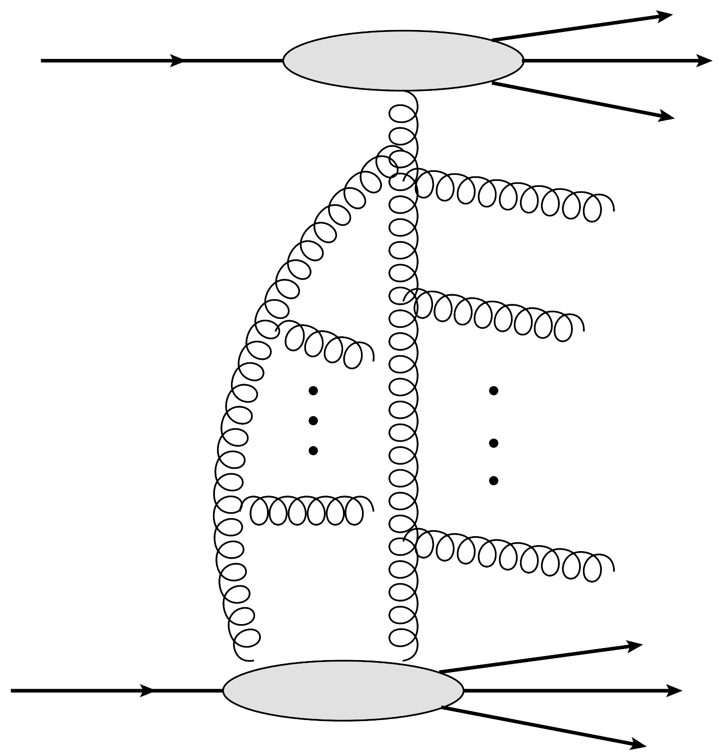

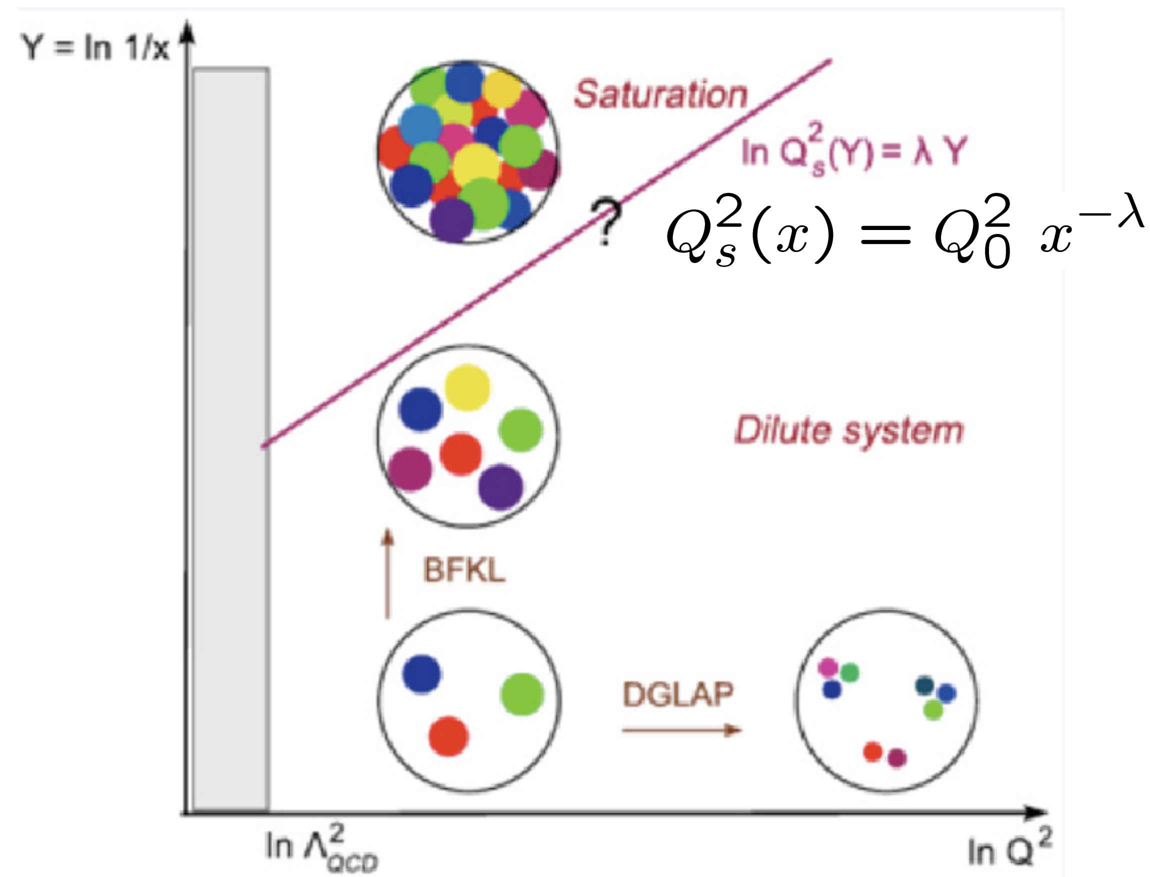

Multiple scatterings/recombination effects essential for the unitarity restoration

- Linear DGLAP evolution works well at HERA.
- Hints of saturation at low Q and low x: deterioration of the global fit in that region.
- Large diffractive component.
- Success of the dipole models in the description of the data.
- The models point at the low value of the saturation scale

Saturation: nonlinear evolution

Parton saturation (recombination or rescattering) corrections lead to the nonlinear (in density) evolution equations.

Various formalisms that include these effects:

- Mueller-Qiu: nonlinear modification to DGLAP
- Gribov-Levin-Ryskin: nonlinear modification to DGLAP
- Bartels: triple Pomeron vertex
- Balitsky: Wilson line operators
- Kovchegov: dipole model
- Jalilian-Marian-Iancu-McLerran-Weigert-Leonidov-Kovner: effective theory for small x, color glass condensate
- ...

Most applications for phenomenology: Balitsky-Kovchegov (BK) equation

BK nonlinear evolution equation

A.H.Mueller

quark-antiquark pair: dipole

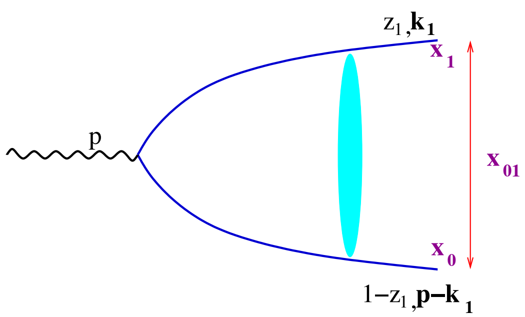

one (soft) gluon emission

dipole splitting

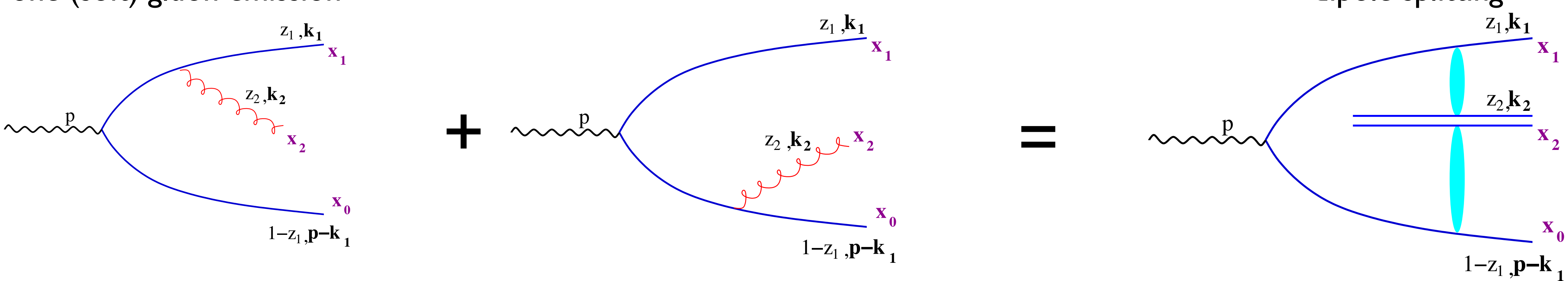

Need to construct the amplitude for scattering of dipoles on target.

One scattering

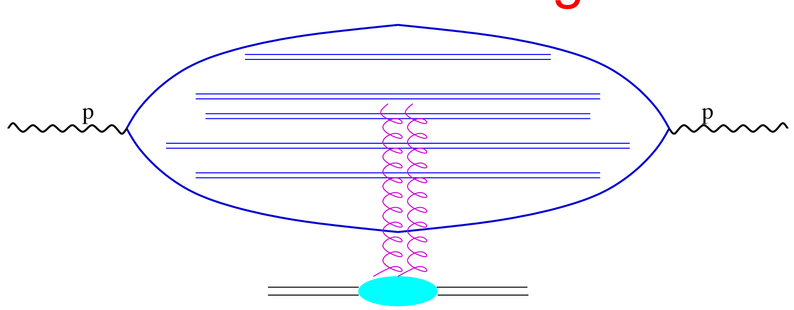

Linear evolution

Multiple scatterings

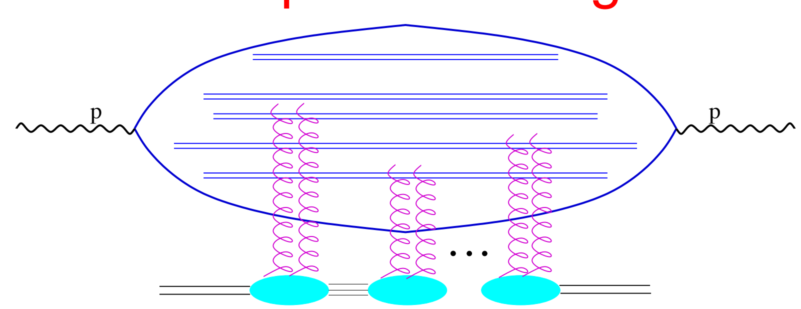

Nonlinear evolution

A.H.Mueller, Y. Kovchegov

BK nonlinear evolution equation

$N(\mathbf{x}_0, \mathbf{x}_1, Y)$ scattering amplitude of a dipole on a target (related to the unintegrated or transverse momentum dependent small x gluon density)

$\mathbf{x}_0, \mathbf{x}_1$ coordinates of the dipole in the transverse space (conjugate to the transverse momentum space)

$Y = \ln \frac{1}{x}$ rapidity difference between the dipole and the target

BK nonlinear evolution at leading logarithmic (in ln1/x) order:

$$\frac{\partial N_{\mathbf{x}_0\mathbf{x}_1}}{\partial Y} = \overline{\alpha}_s \int \frac{d^2\mathbf{x}_2}{2\pi} \frac{(\mathbf{x}_0 - \mathbf{x}_1)^2}{(\mathbf{x}_0 - \mathbf{x}_2)^2(\mathbf{x}_1 - \mathbf{x}_2)^2} [N_{\mathbf{x}_0\mathbf{x}_2} + N_{\mathbf{x}_1\mathbf{x}_2} - N_{\mathbf{x}_0\mathbf{x}_1} - N_{\mathbf{x}_0\mathbf{x}_2} N_{\mathbf{x}_1\mathbf{x}_2}]$$

linear part: equivalent to LLx BFKL

nonlinear part equivalent to the triple Pomeron vertex (in the Moebius representation)

Note that N=1 solves the equation, which is the black disk limit.

I.Balitsky, Y. Kovchegov

BK equation: solution

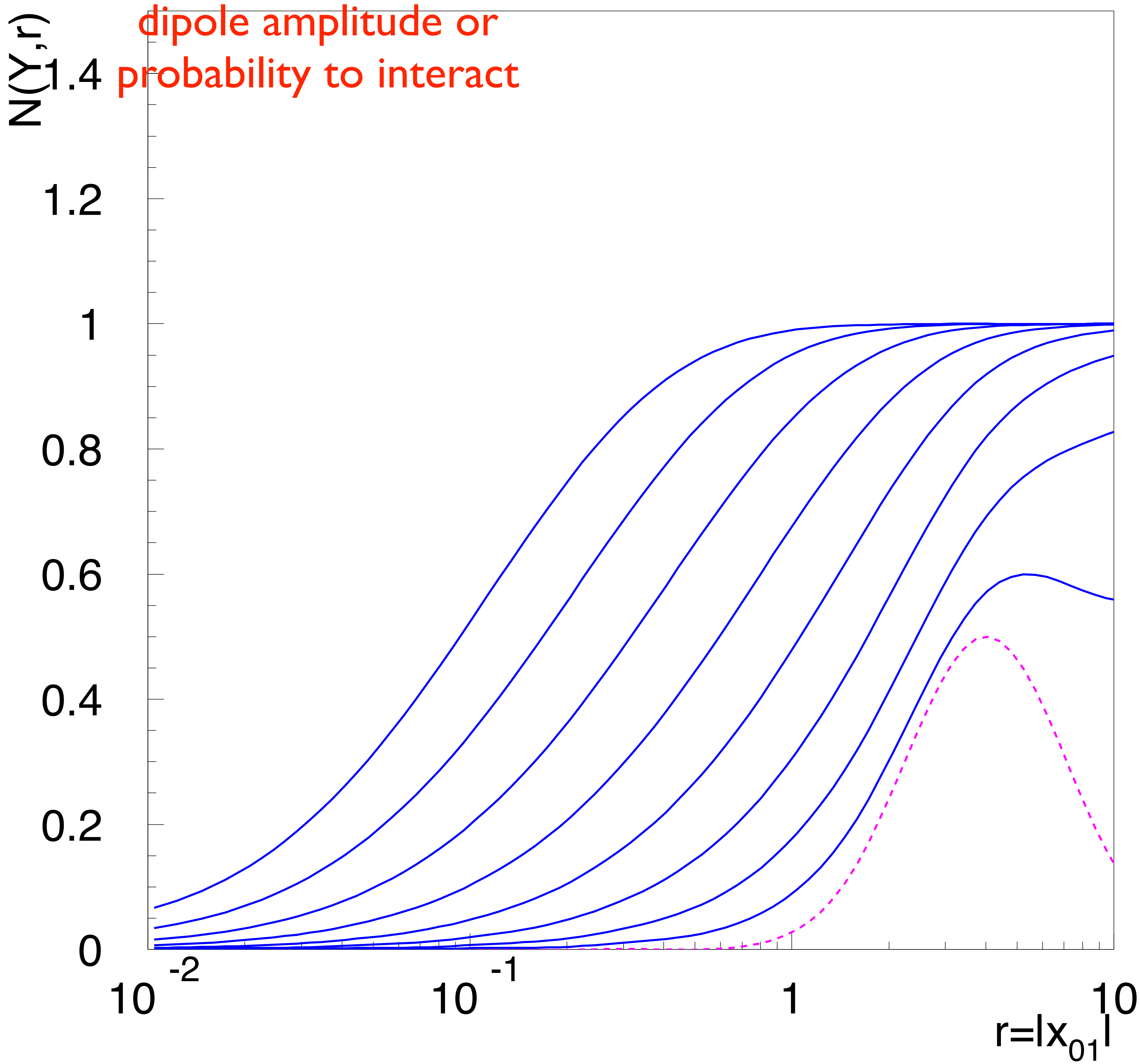

BK equation: solution

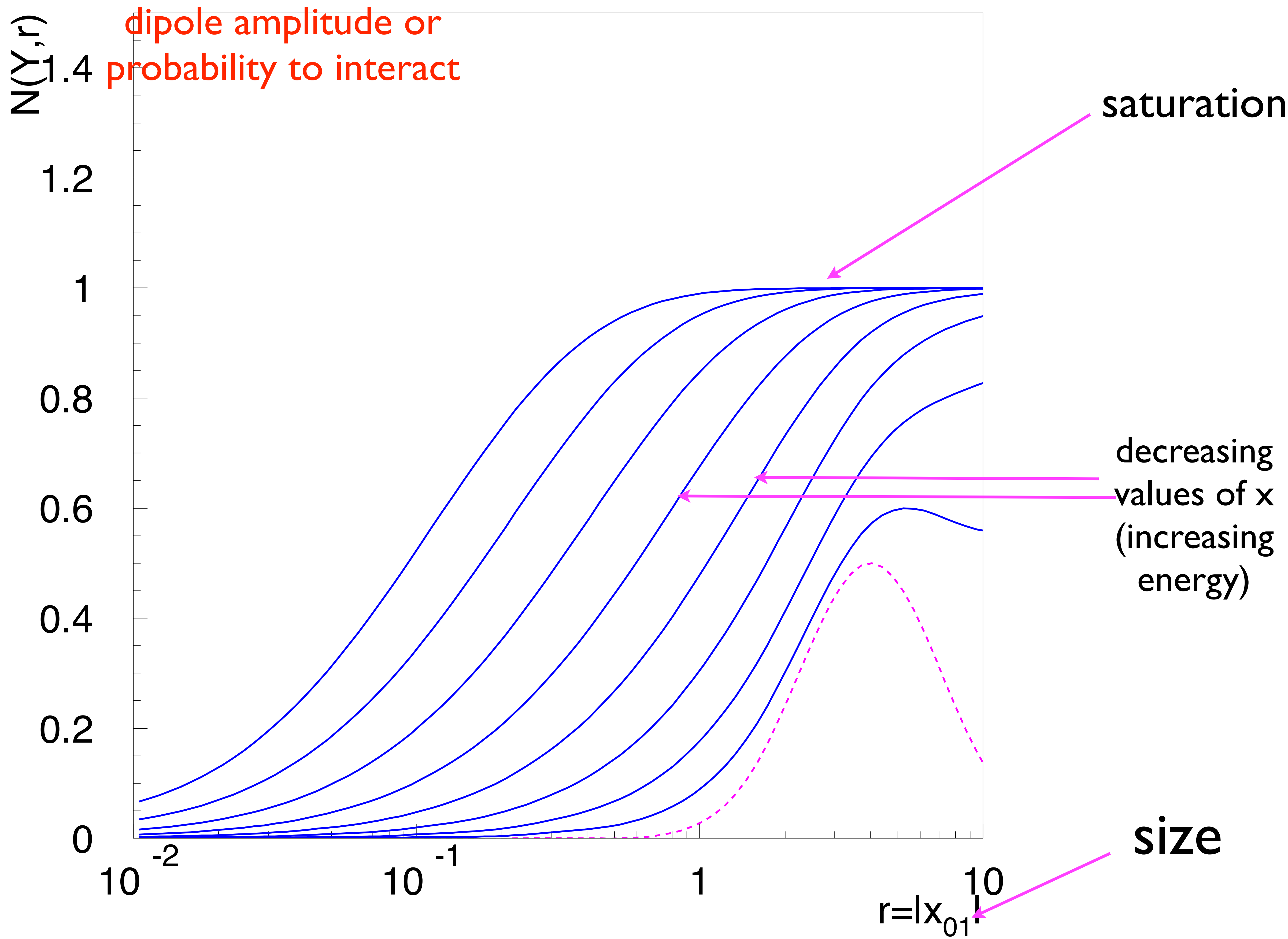

BK equation: solution

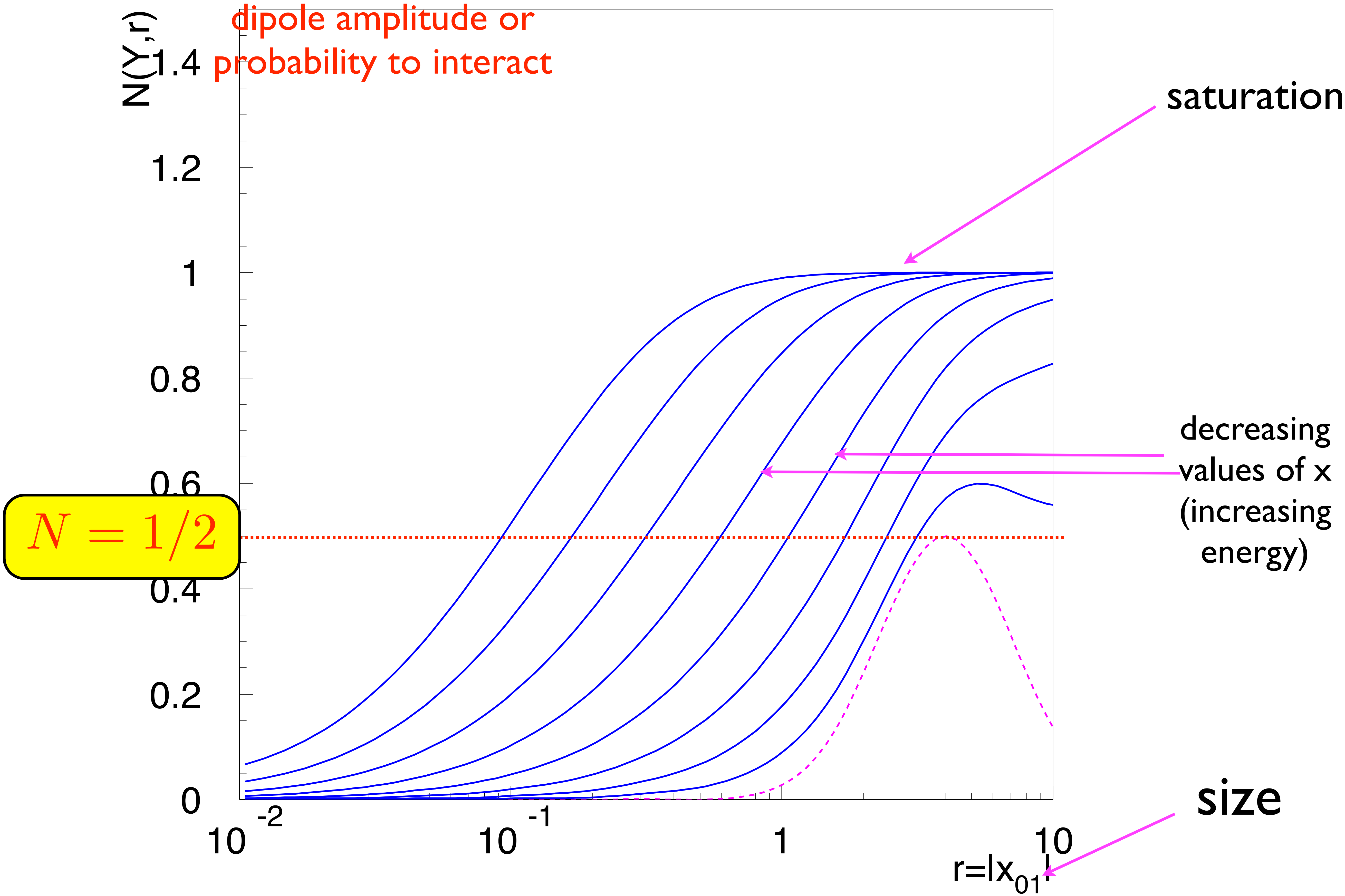

BK equation: solution

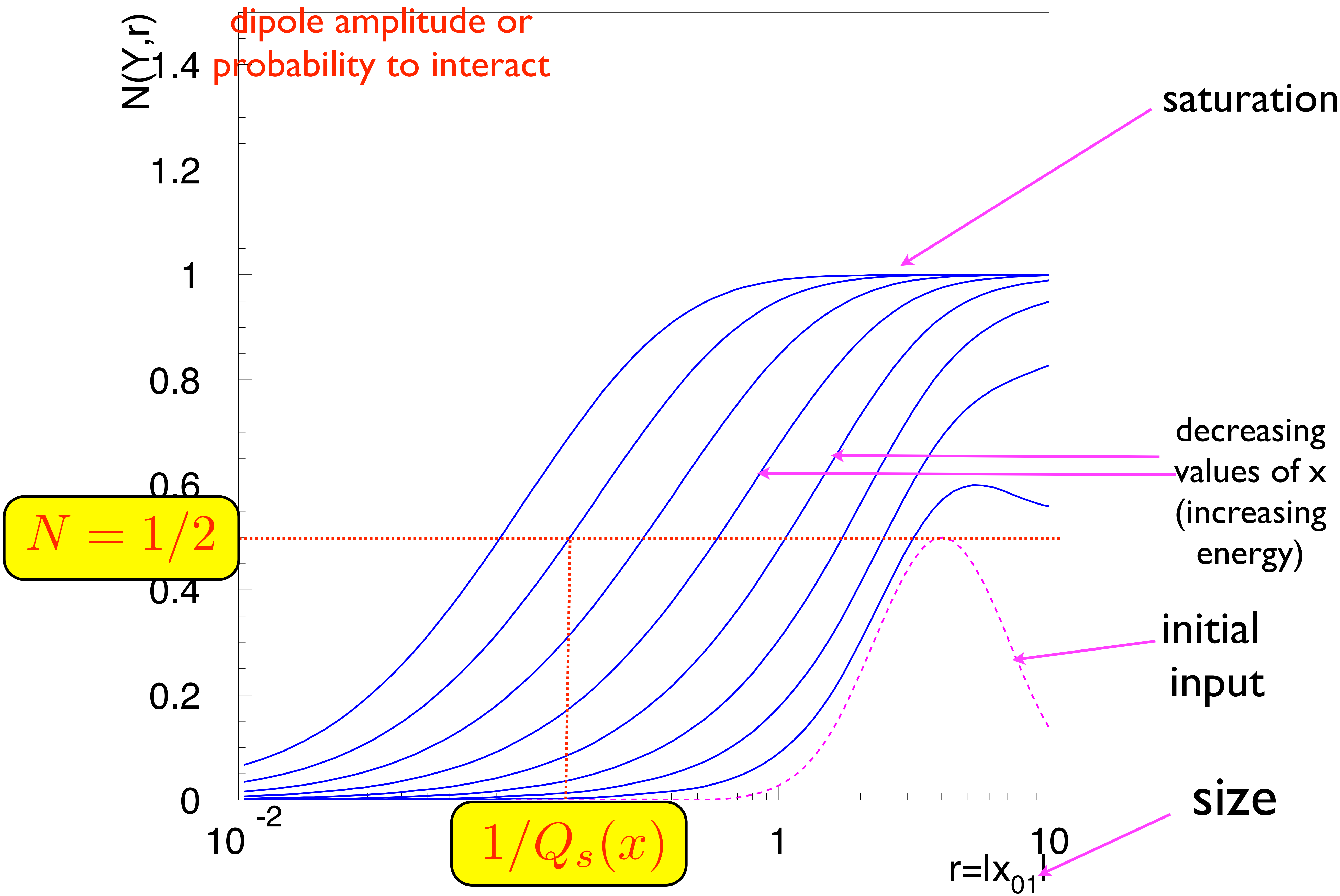

Saturation scale

Solution to nonlinear evolution equation generates the characteristic scale: saturation scale which divides the dense and dilute region.

$$\boxed{Q_s(x)^2 \simeq Q_0^2 x^{-\lambda_s}}$$

λ_s related to (but not exactly equal) to the BFKL Pomeron intercept

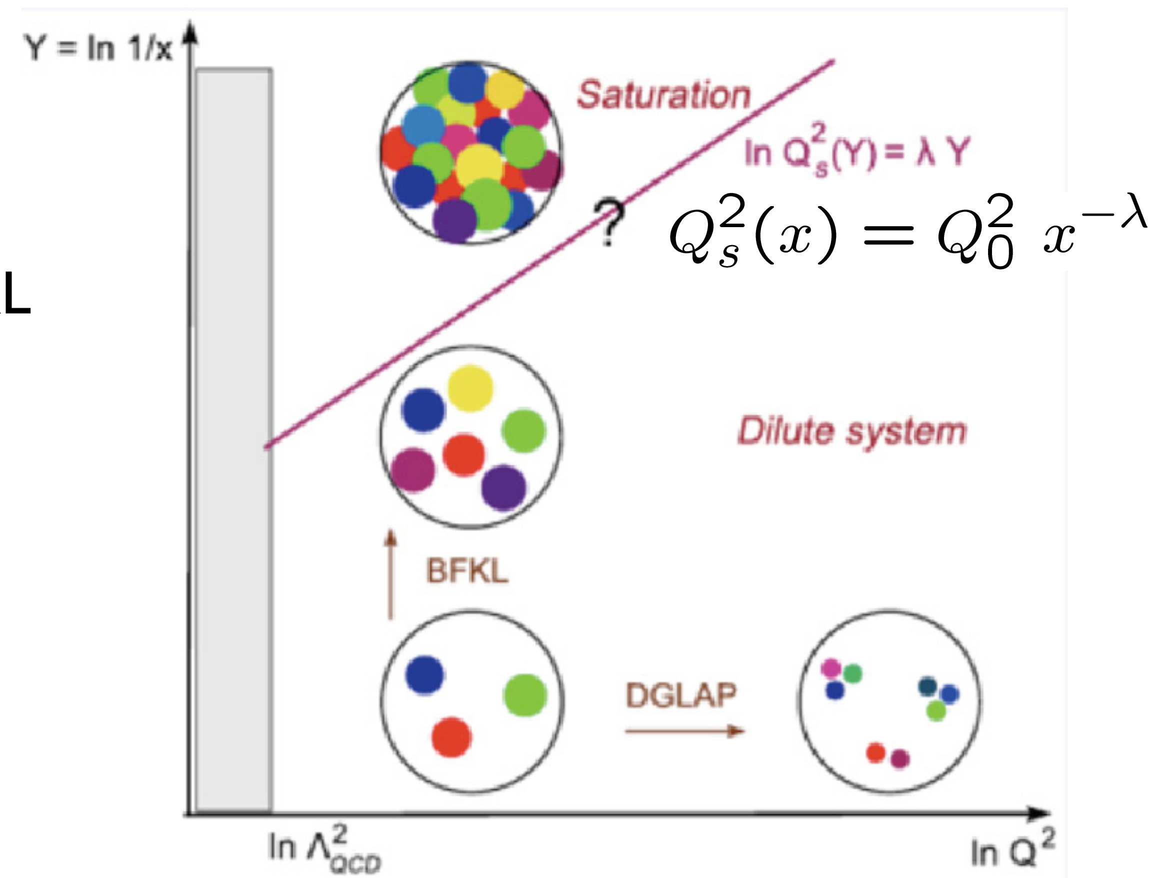

If the target is nucleus, there is additional enhancement due to nuclear number A:

$$\boxed{Q_s(x)^2 \simeq A^{1/3} Q_0^2 x^{-\lambda_s}}$$

The normalization of the saturation scale cannot be computed analytically, it is determined by the initial condition. In practice it is fitted parameter.

NLLx corrections to nonlinear evolution

Balitsky-Chirilli (2007,2010): NLLx computation of the BK equation and photon impact factors for DIS

Kovchegov-Weigert (2007): running coupling calculation for the BK evolution

Kovner-Lublinsky-Mulian (2014): NLLx calculation of the JIMWLK equations

So far most of the phenomenology only includes LLx nonlinear evolution with running coupling (partial NLLx) but not the full NLLx.

NLLx, resummation vs saturation

fixed coupling

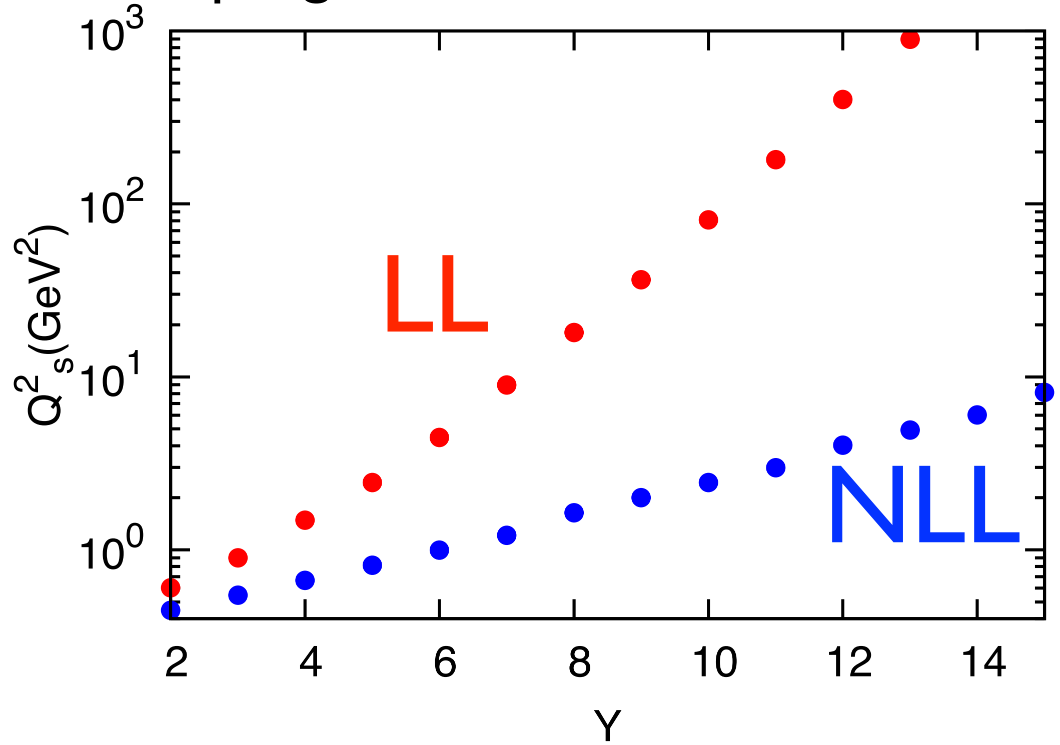

running coupling

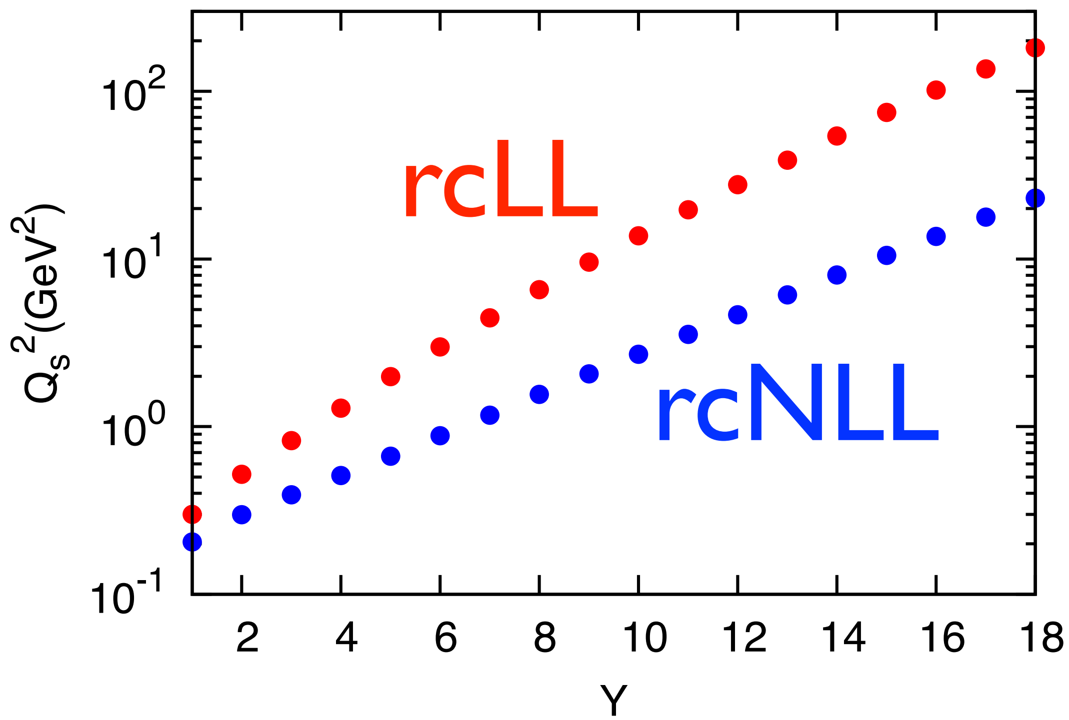

comparing with resummation

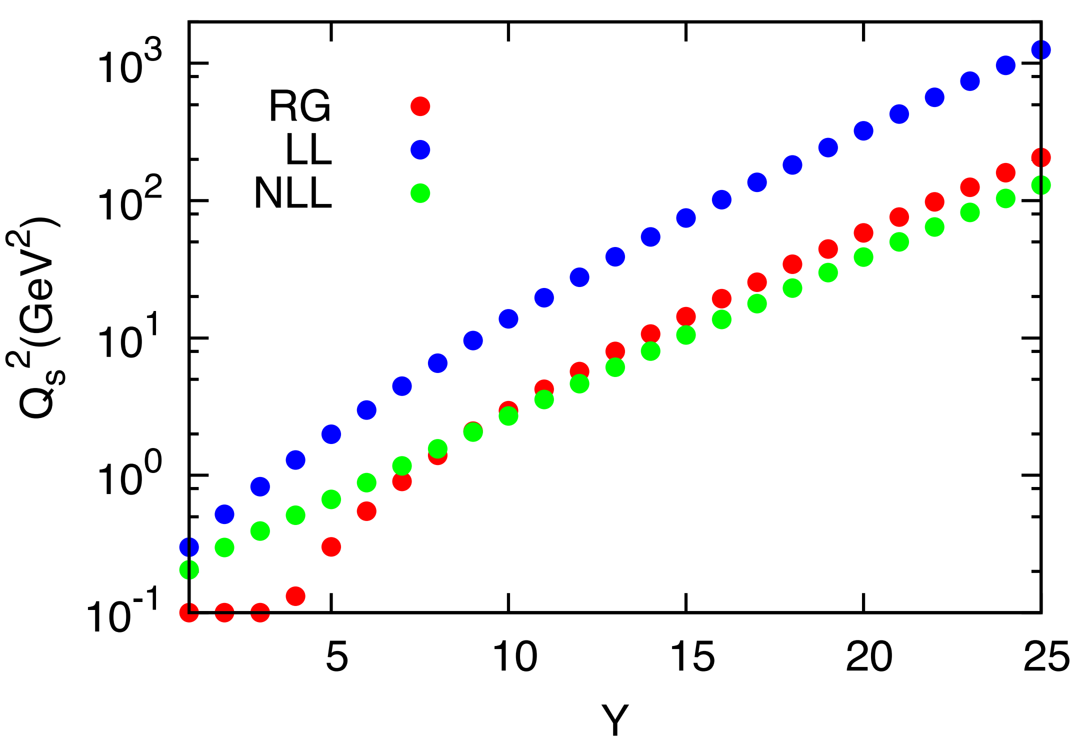

- Saturation scale obtained from the boundary method : solving linear equation with the imposed saturation boundary.
- NLLx should have sizeable effect on saturation scale
- slower energy dependence
- resummation further delays the onset of saturation
- important for precise phenomenology

NLLx, resummation vs saturation

fixed coupling

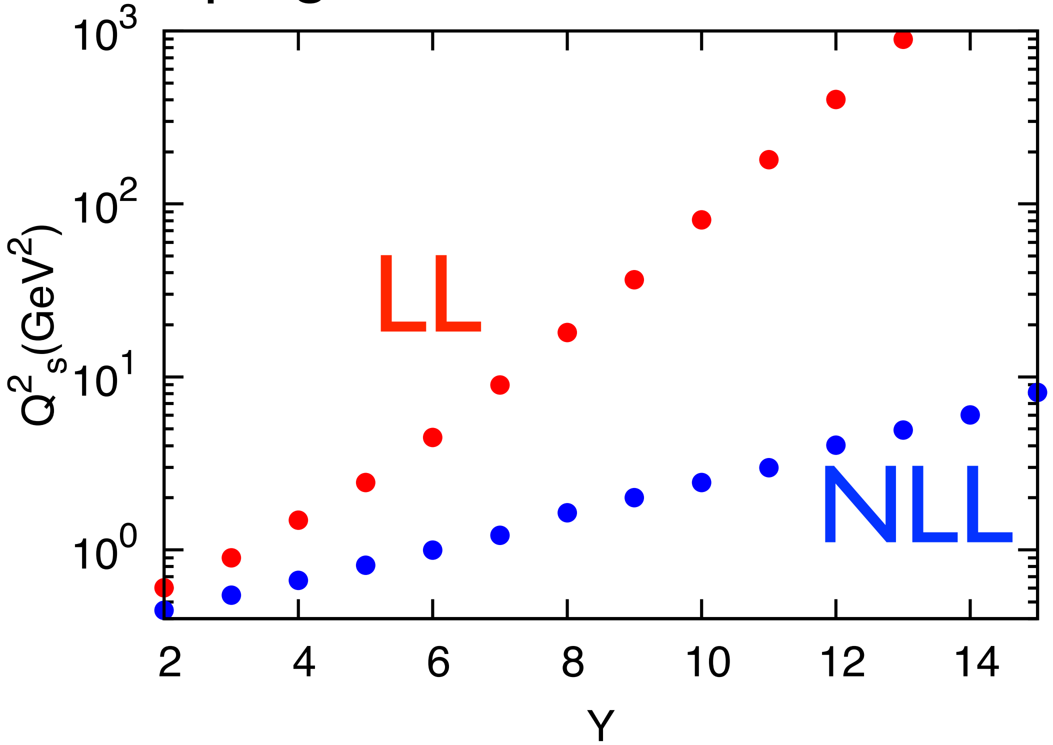

running coupling

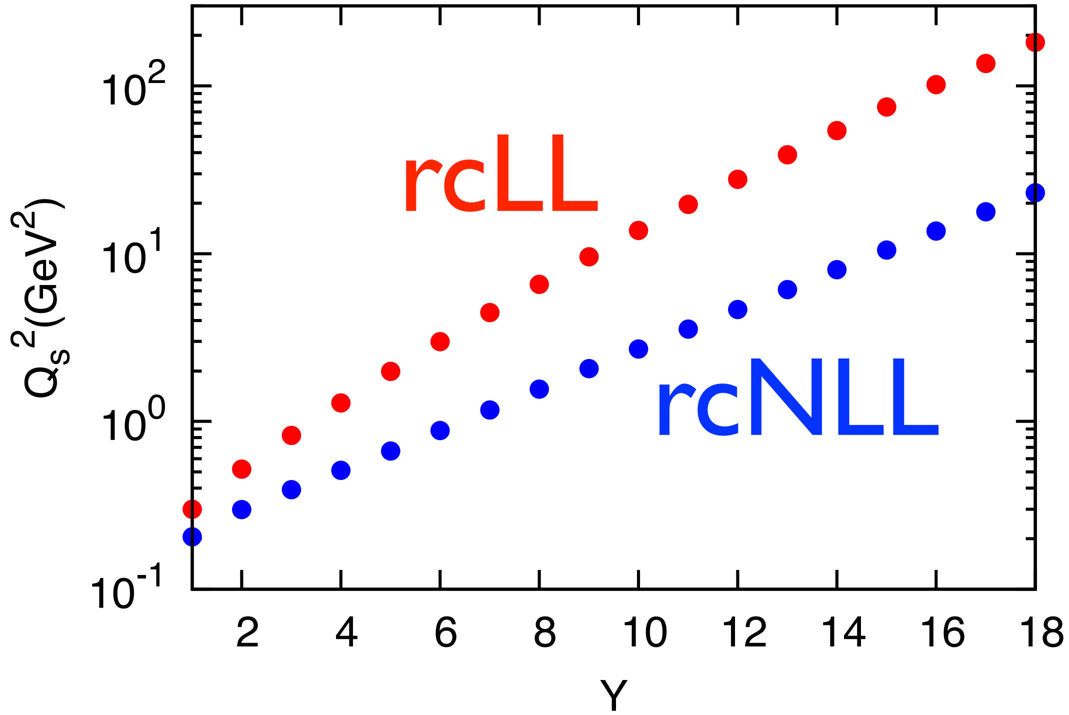

comparing with resummation

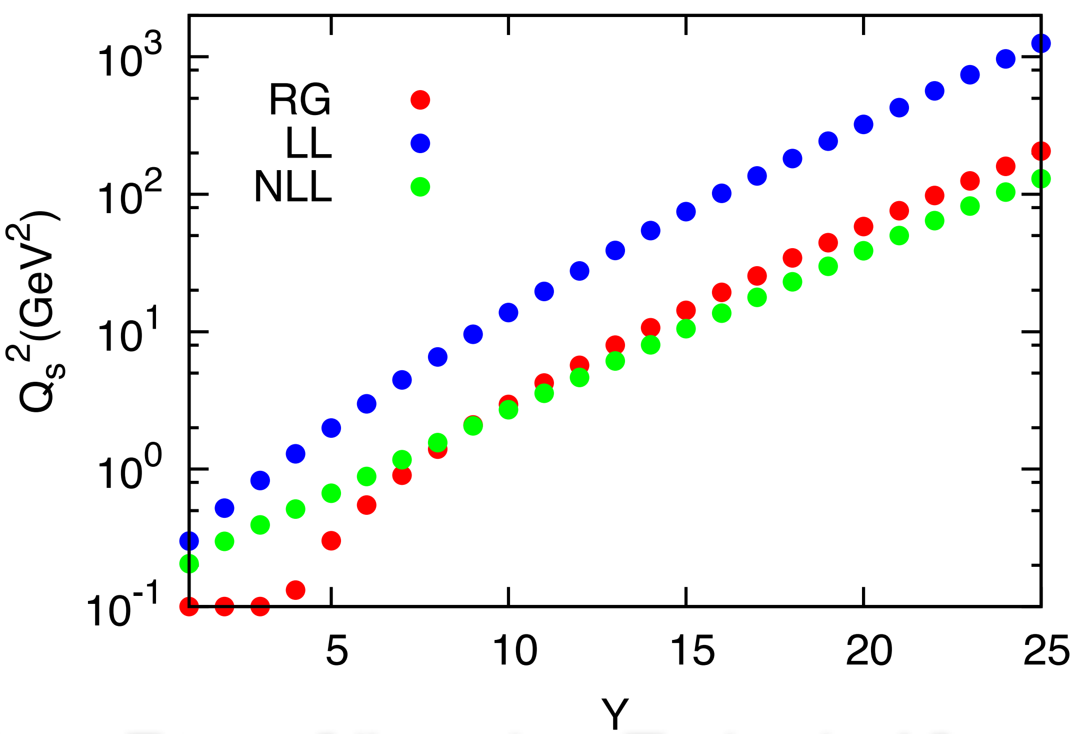

Avsar, Triantafyllopoulous, Zaslavsky, AS

- Saturation scale obtained from the boundary method : solving linear equation with the imposed saturation boundary.
- NLLx should have sizeable effect on saturation scale
- slower energy dependence
- resummation further delays the onset of saturation
- important for precise phenomenology

Neutrino cross sections

$$\frac{d^2\sigma^{CC}}{dxdy} = \frac{2G_F^2 M_N E_\nu}{\pi}\left(\frac{M_W^2}{Q^2+M_W^2}\right)^2 \cdot \left[xq(x,Q^2) + x\bar{q}(x,Q^2)(1-y)^2\right]$$

$xq(x,Q^2)$, $x\bar{q}(x,Q^2)$ are parton densities.
Since $xq(x,Q^2) \sim x^{-\lambda}$ this implies that

$$\sigma(E_\nu) = \int dxdy \frac{d^2\sigma^{CC}}{dxdy} \sim E_\nu^\lambda$$

Need extrapolations of parton densities to very small x

Contribution to the cross section in Q and x plane:

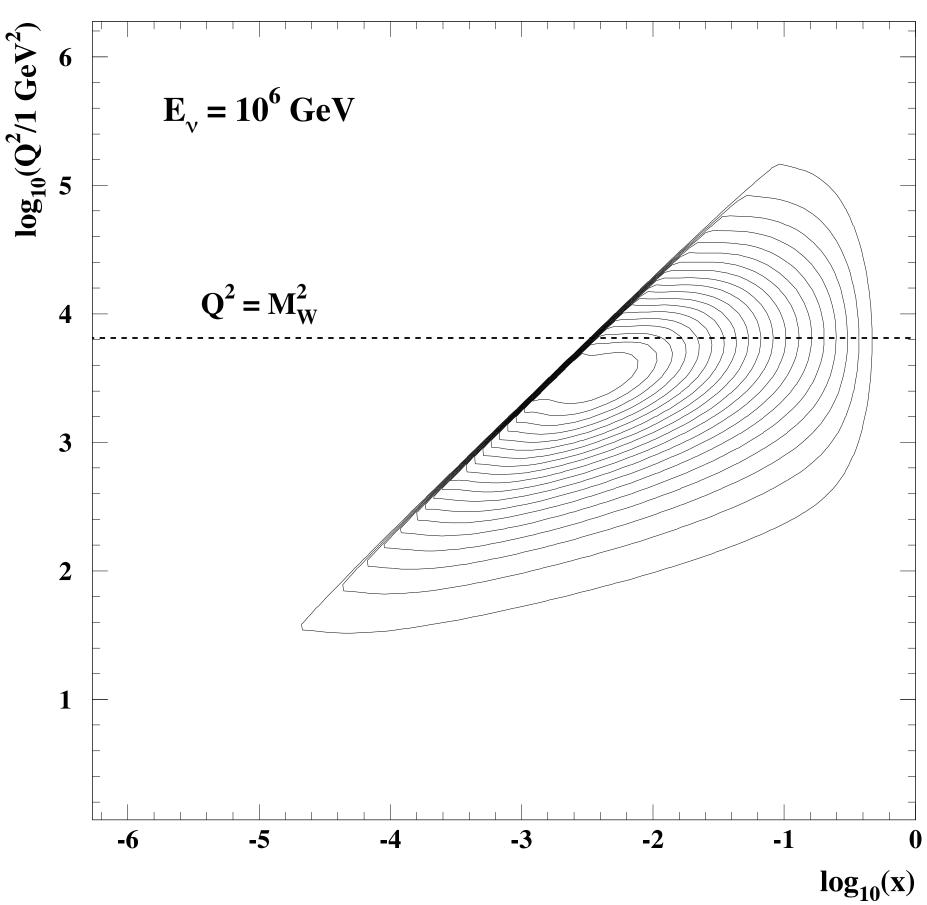

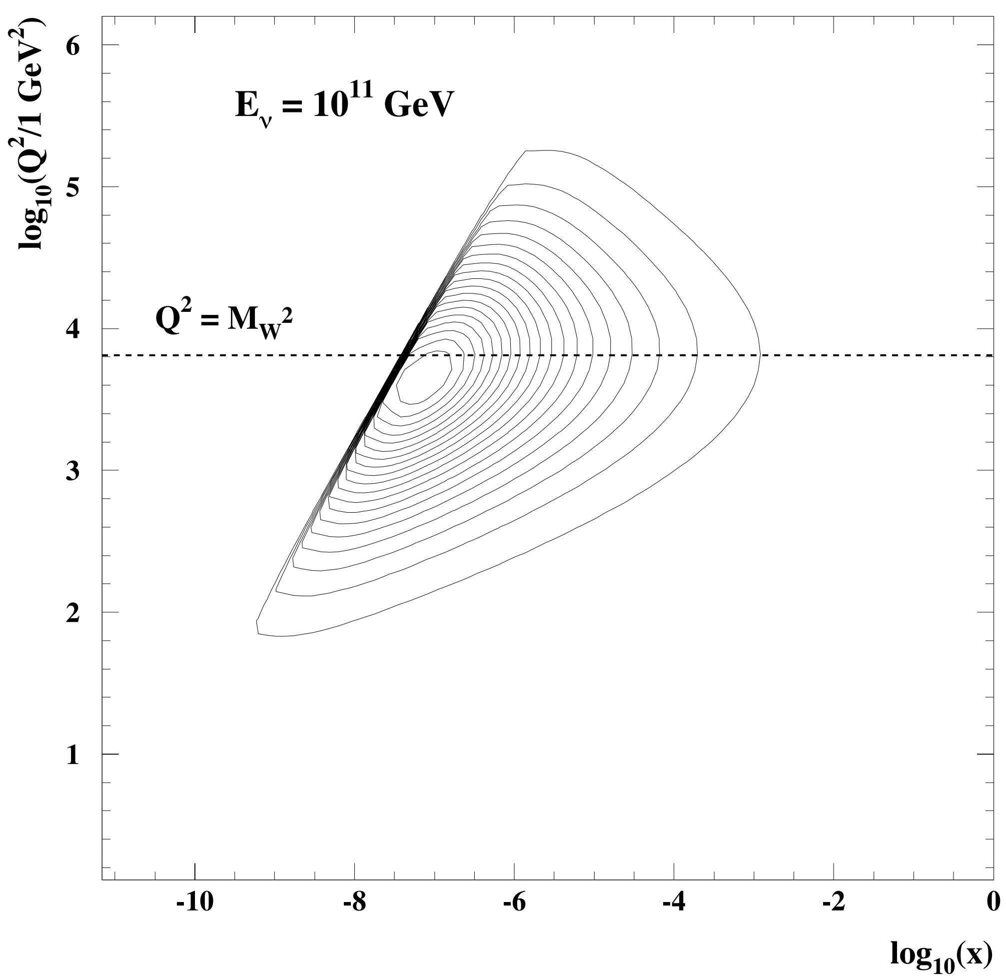

Neutrino cross sections

Calculation of the neutrino cross section using the unified BFKL/DGLAP evolution (includes resummation effects).

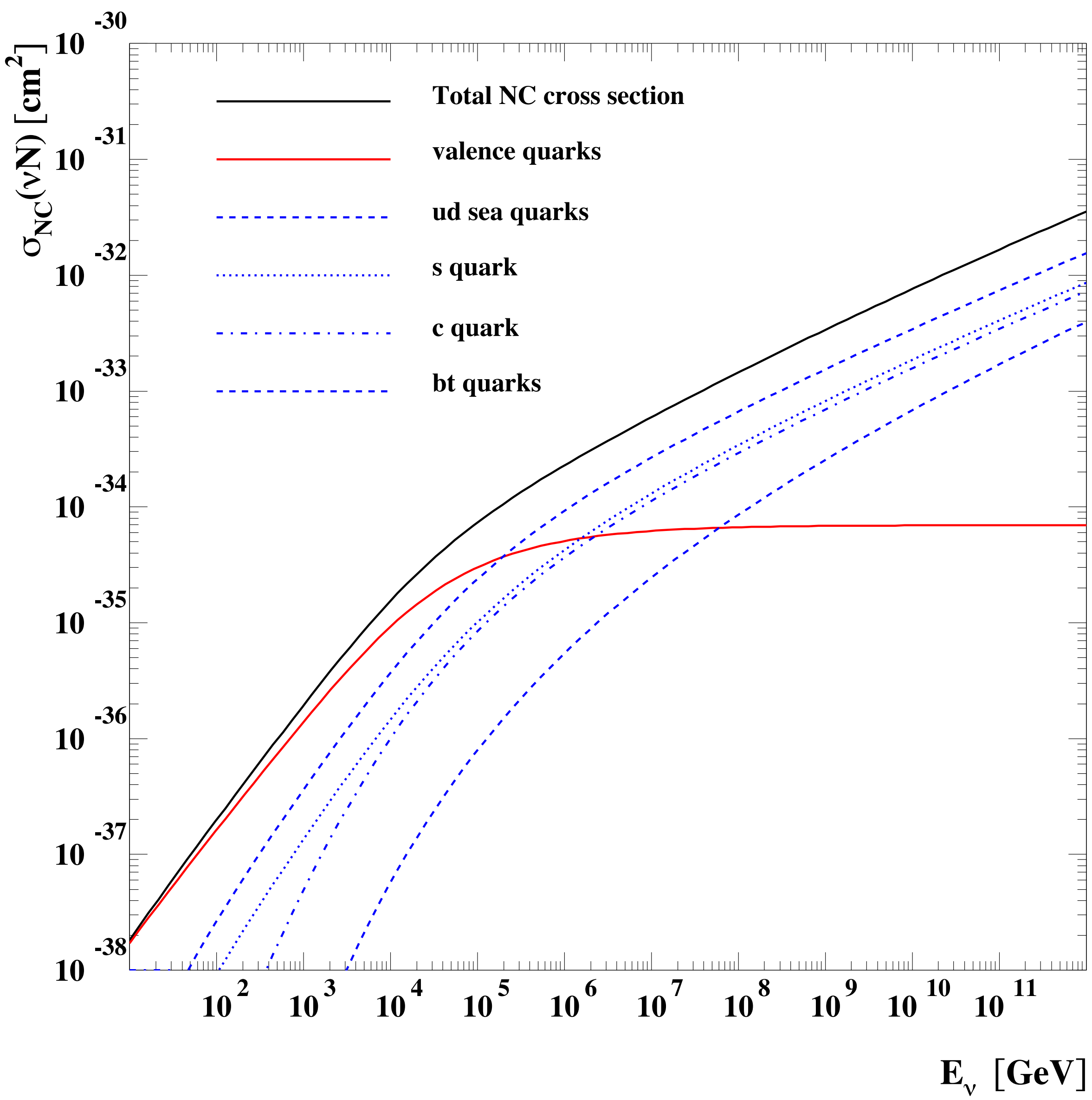

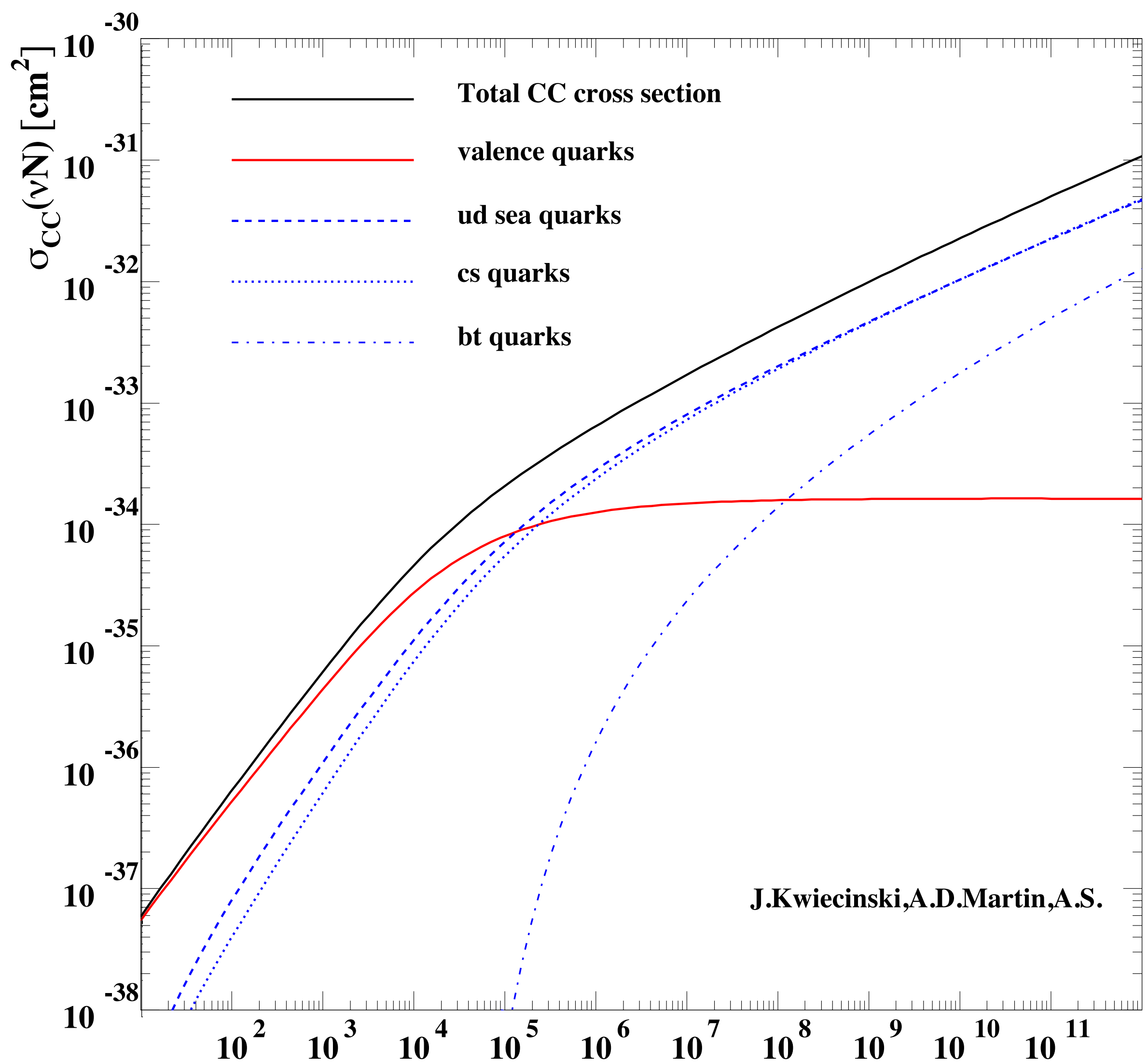

Behavior at high energies controlled dynamically by the resummed evolution equation, rather than the parametrized extrapolation.

Neutrino cross sections

Calculation of the neutrino cross section using the unified BFKL/DGLAP evolution (includes resummation effects).

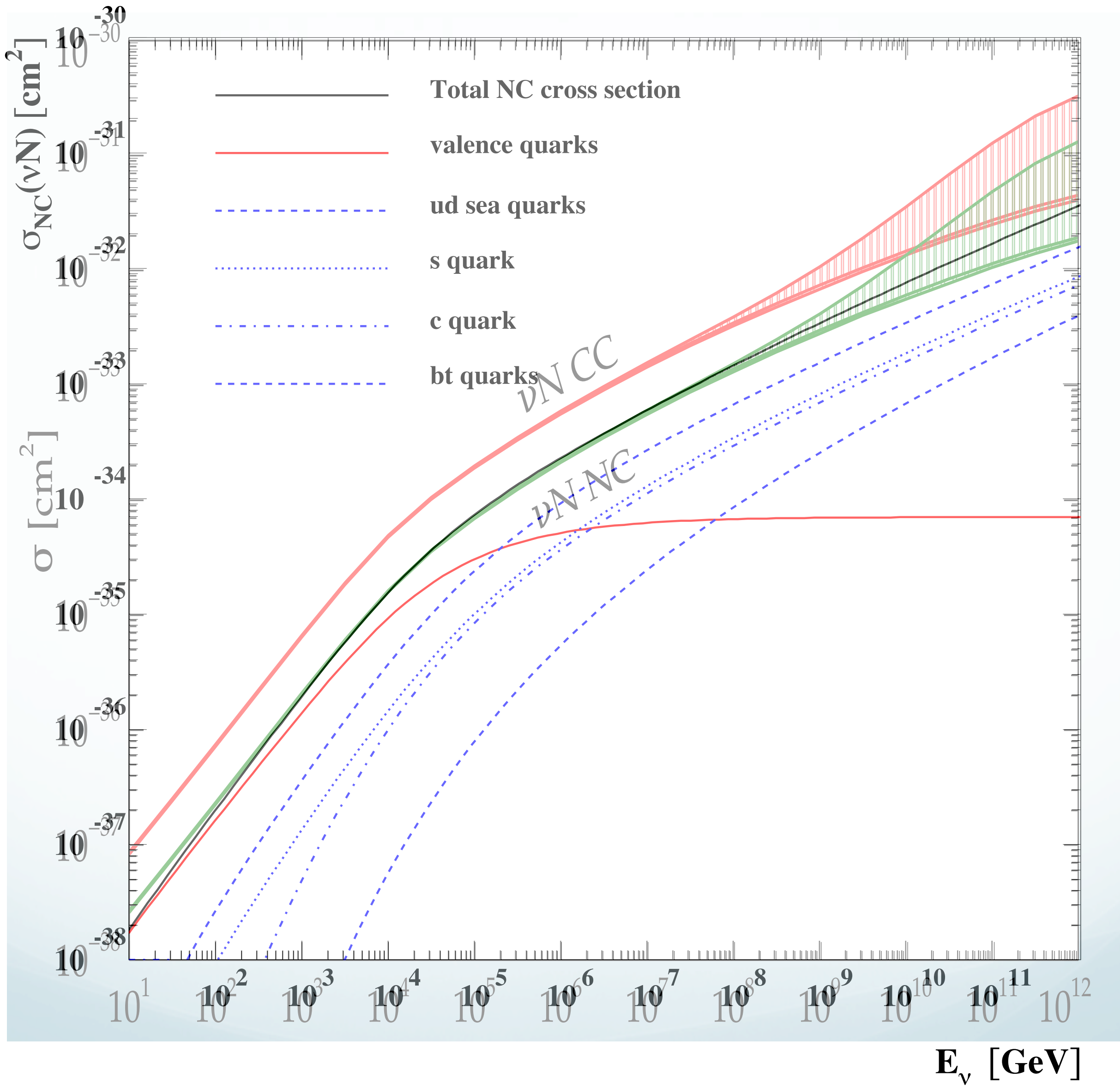

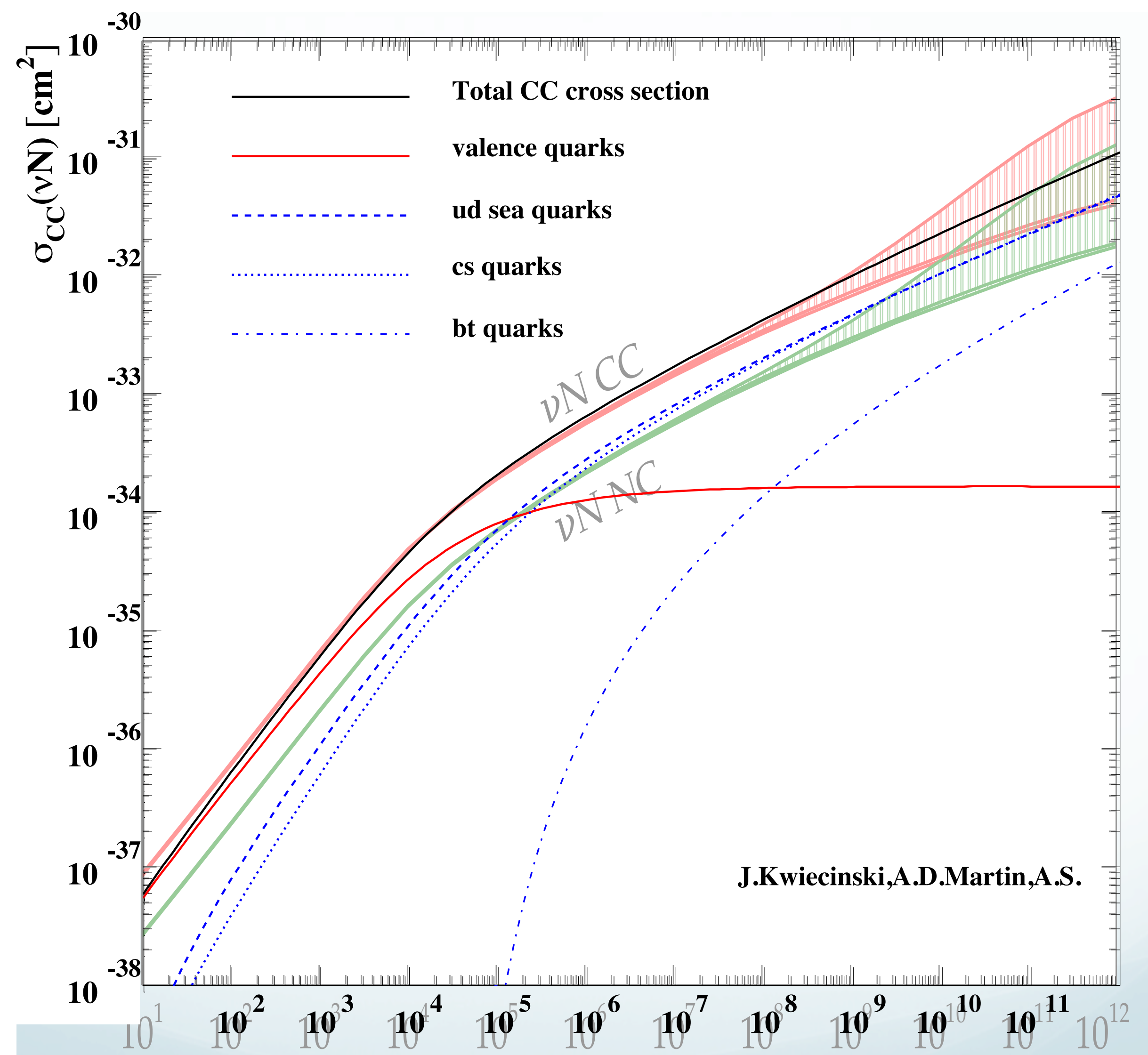

Comparison with latest estimates, see I. Sarcevic talk.
BFKL/DGLAP unified calculation still works well, within the uncertainty bounds for DGLAP
LHC data do not provide (so far) additional strong constraints on PDFs(relevant for this process)

Neutrino cross sections

Does gluon saturation play a role in neutrino interactions?
x is small but the scale rather high, so the dominant contribution above the saturation scale.

Kutak, Kwiecinski

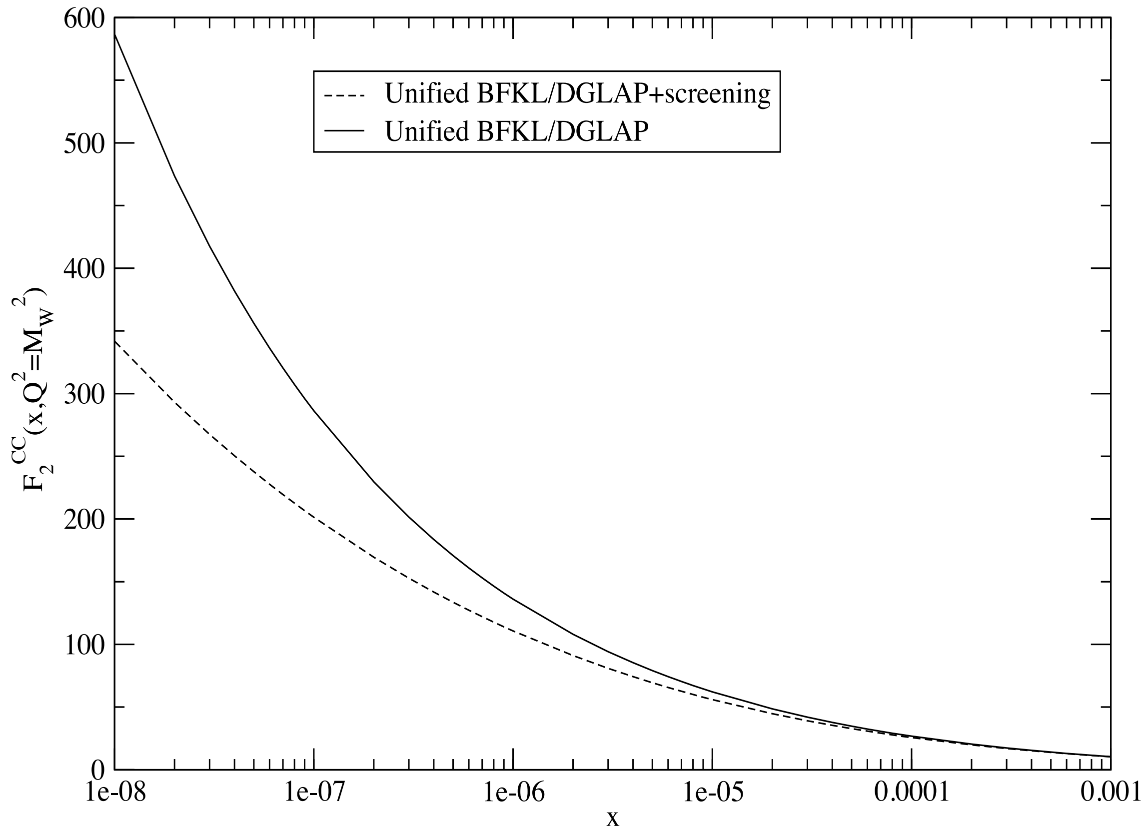

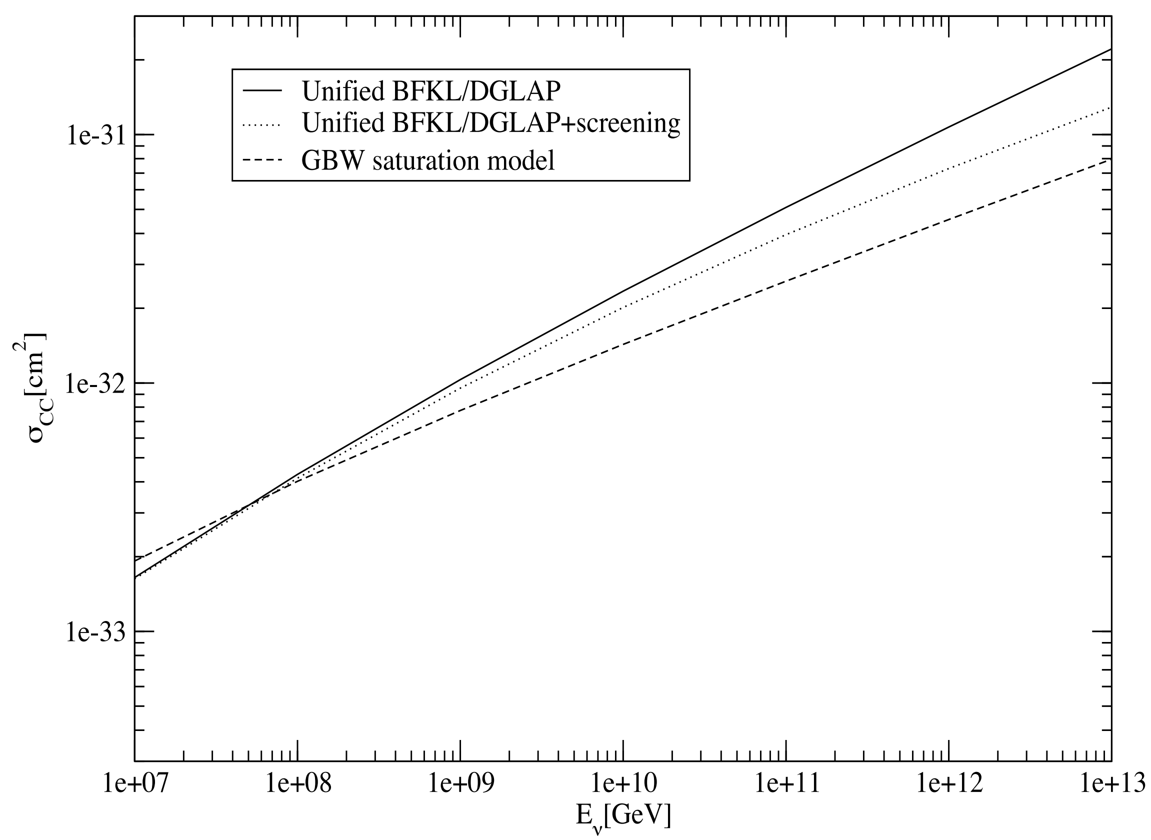

The structure function F_2^{cc} reduced by factor 2 at $x = 10^{-8}, Q^2 = M_W^2$

Small but non-negligible reduction of the cross section for highest energies due to saturation. Within the bounds of the DGLAP extrapolation: DGLAP flexible enough to accommodate BFKL with and without saturation (at least for this process).

Note: GBW model lacks proper Q evolution, this is corrected in the BFKL/DGLAP approach with saturation.

Neutrino cross sections

Does gluon saturation play a role in neutrino interactions?
x is small but the scale rather high, so the dominant contribution
above the saturation scale.

overlay with calculation by Sarcevic et al.

Kutak, Kwiecinski

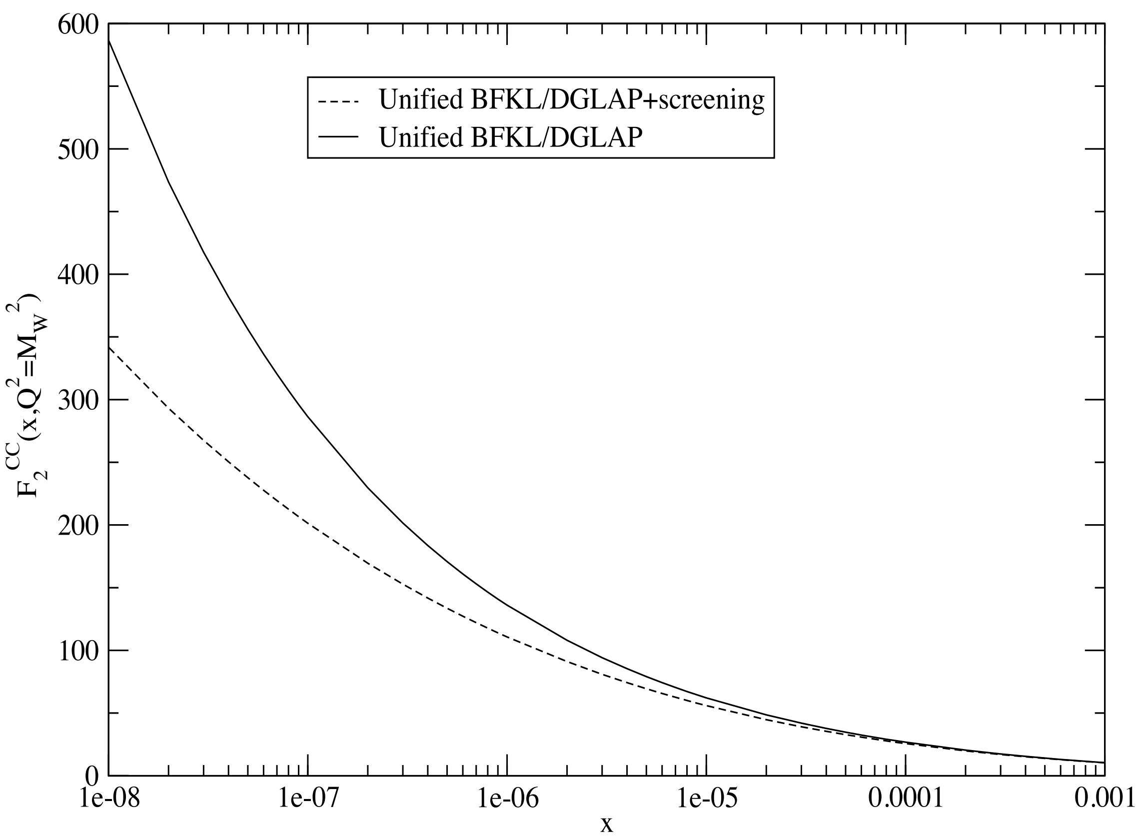

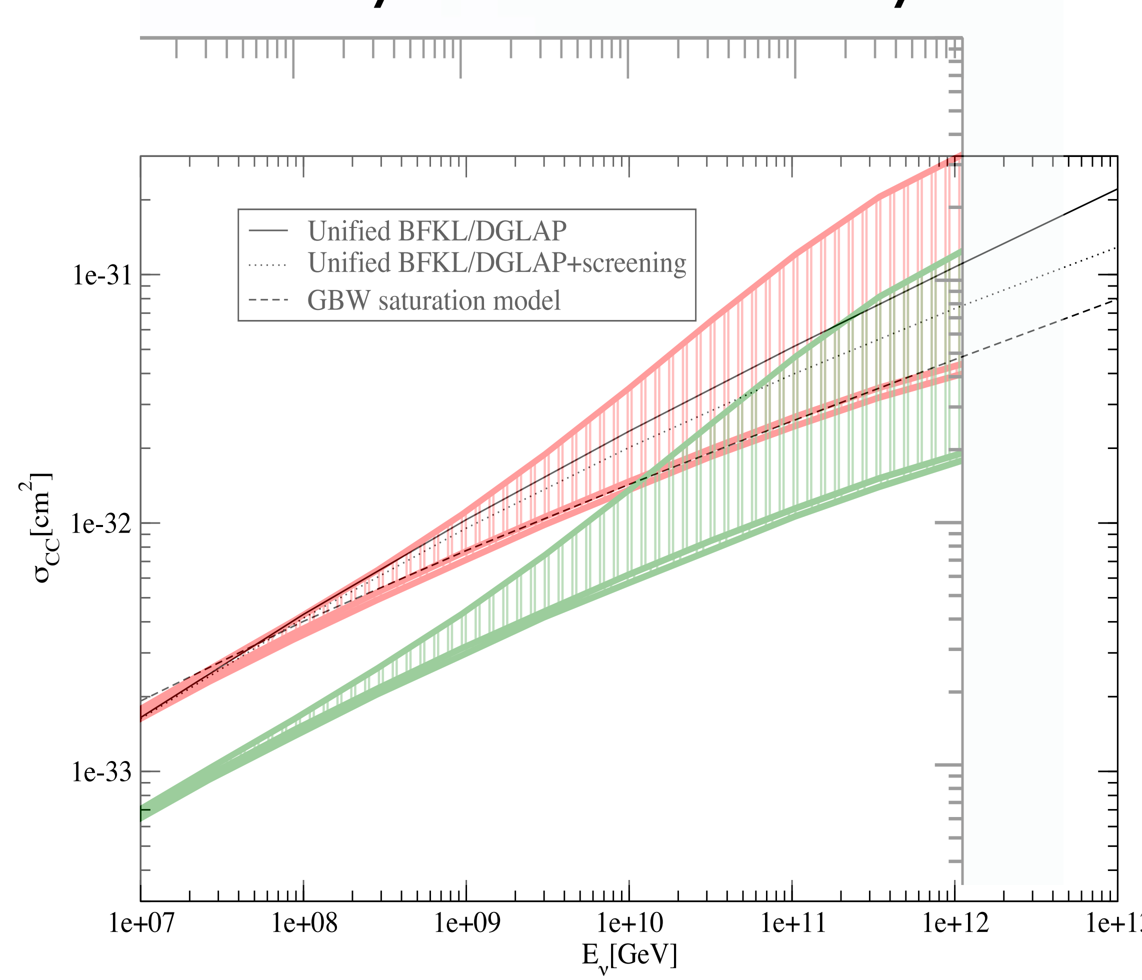

The structure function F_2^{cc} reduced by factor 2 at $x = 10^{-8}, Q^2 = M_W^2$
Small but non-negligible reduction of the cross section for highest energies due to saturation. Within the bounds of the DGLAP extrapolation: DGLAP flexible enough to accommodate BFKL with and without saturation (at least for this process).

Note: GBW model lacks proper Q evolution, this is corrected in the BFKL/DGLAP approach with saturation.

Neutrino cross sections

Saturation on a nuclear target: include A dependence in the nonlinear term.

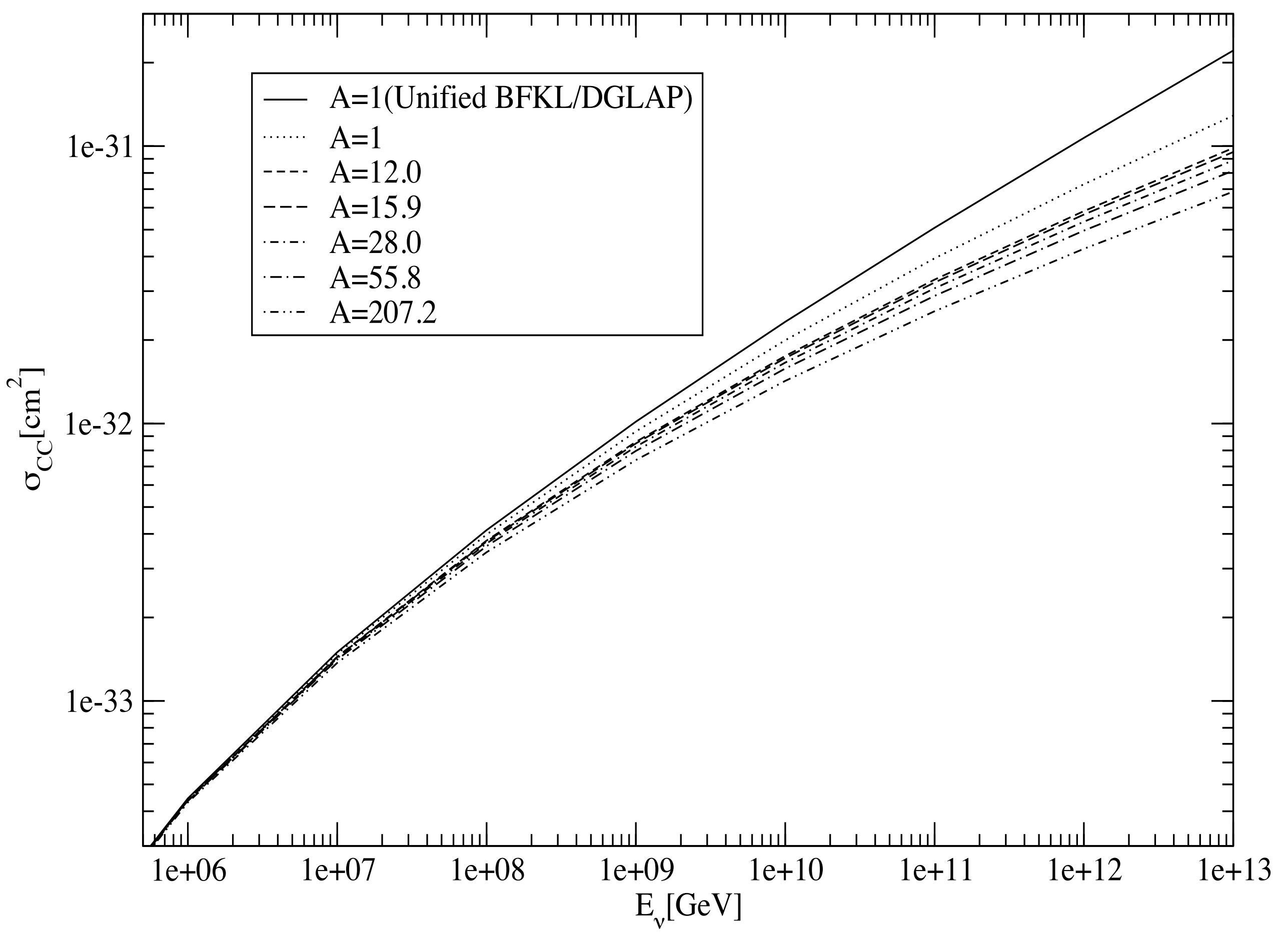

Nuclear effects further reduce the cross section.
Note: this simulation done with simple $A^{1/3}$ enhancement.

Prompt neutrino flux

Calculation of the prompt neutrino flux with saturation. For this case GBW model is fine since the typical value of Q probed is not large.

Z-moment:

$$\int_0^1 dx_F \frac{d\sigma^{pp\to c\bar{c}+X}(E_c)}{dx_F} x^\gamma$$

Primary CR flux:

$$F_{CR}^{(0)}(E) \sim E^{-(\gamma+1)}$$

with $\gamma = 2.02$

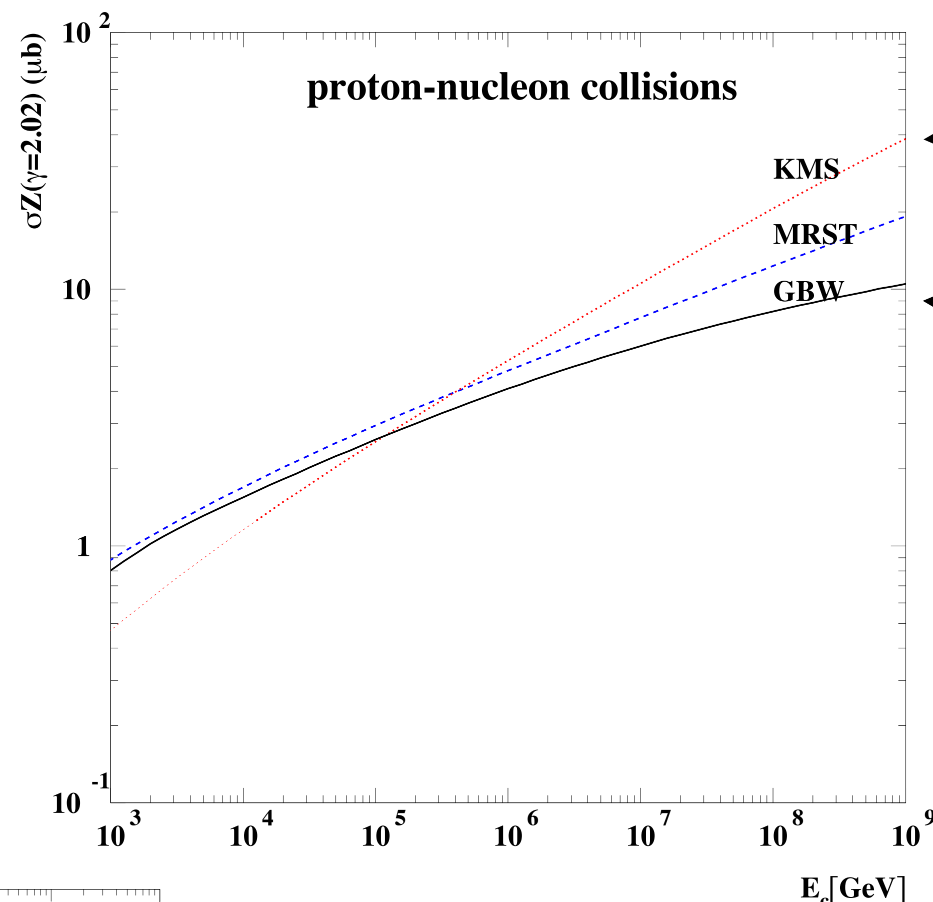

including BFKL effects

including saturation

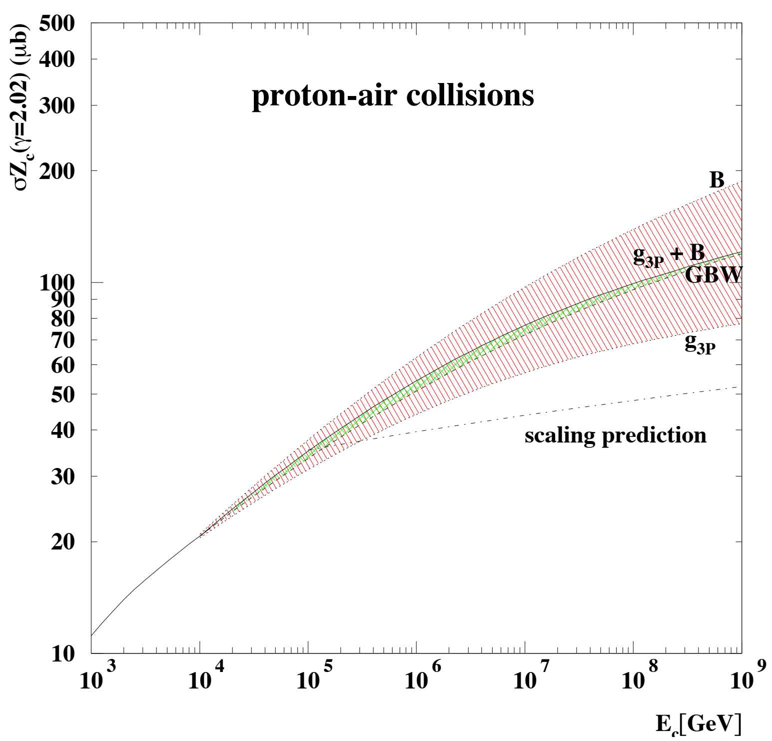

However, uncertainties in the way saturation is treated.

Larger estimate for triple Pomeron vertex
Growth of the proton radius with energy.
Scaling prediction: lower bound on the charm production.

$$\frac{d\sigma(E)}{dx_F} = \frac{d\sigma(E_0)}{dx_F}\frac{\sigma_{\rm inel}(E)}{\sigma_{\rm inel}(E_0)}$$

Prompt neutrino flux

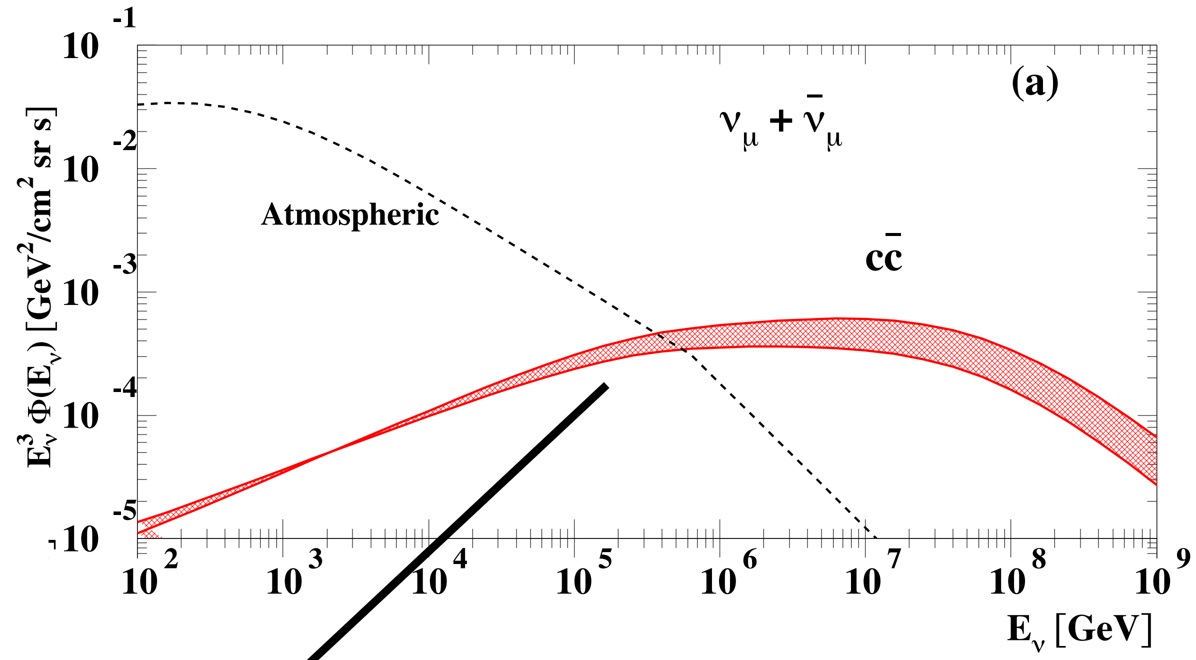

Plot from Enberg,Reno,Sarcevic

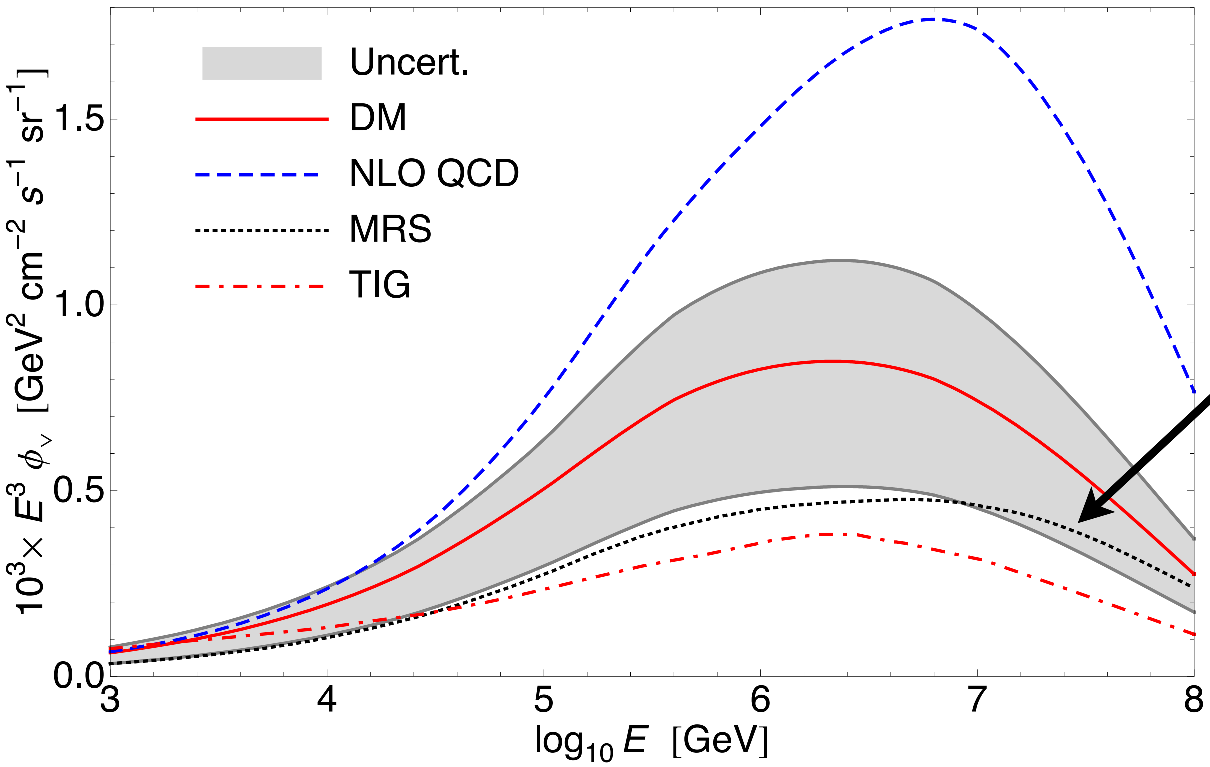

Martin,Ryskin,AS

Differences due to choice of the dipole model and fragmentation functions (more substantial).

What would be the differences in predictions due to pdfs here, and can we get the constrain on low x gluon on low scales from prompt neutrinos?

Prompt tau neutrino from beauty production

- 30 times smaller cross section for $b\bar{b}$ production
- but more decay channels (to τ) are opened: $B^{\pm}, B^0, B_s, \Lambda_b$
- 40% correction at $E = 10^5 \mathrm{GeV}$ and more at higher energies
- small correction to ν_μ, ν_e fluxes

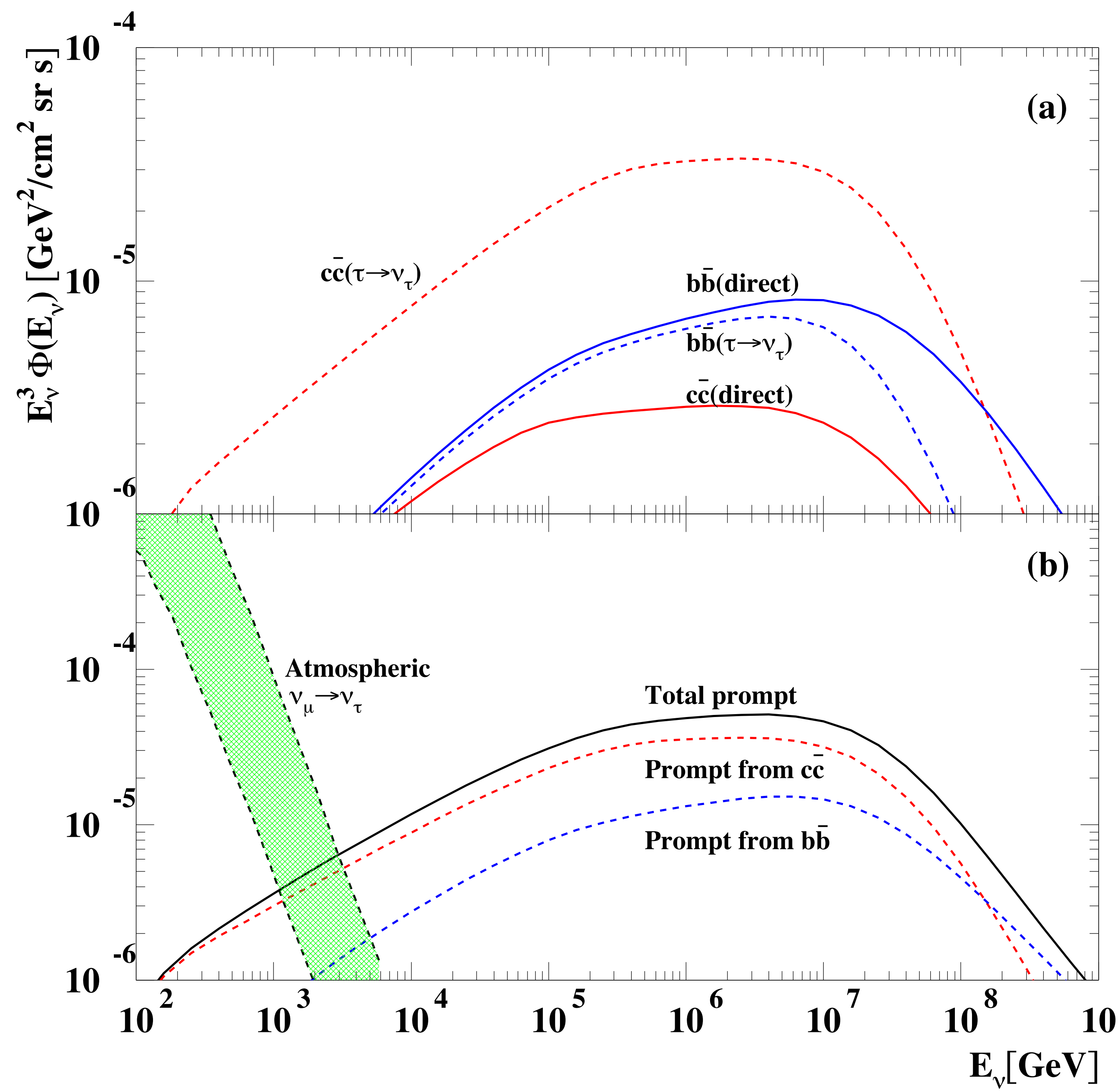

Note: larger fraction from beauty is due to the decreased yield of Ds and the fact that saturation effects are less important for B than D

What about spatial distribution of partons?

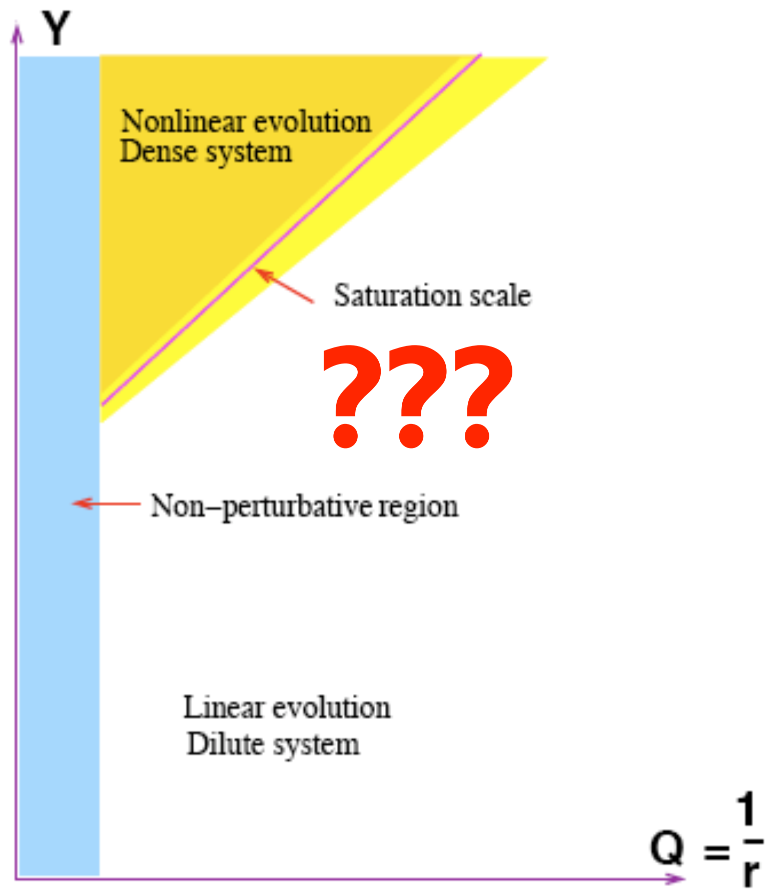

Usual approximation:

$$N(Y; \mathbf{x}_0, \mathbf{x}_1) = N(Y; |\mathbf{x}_0 - \mathbf{x}_1|)$$

- The target has infinite size, no impact parameter.
- Local approximation suggests that the system becomes more perturbative as the energy grows.
- But this cannot be true everywhere (IR in QCD)

What about spatial distribution of partons?

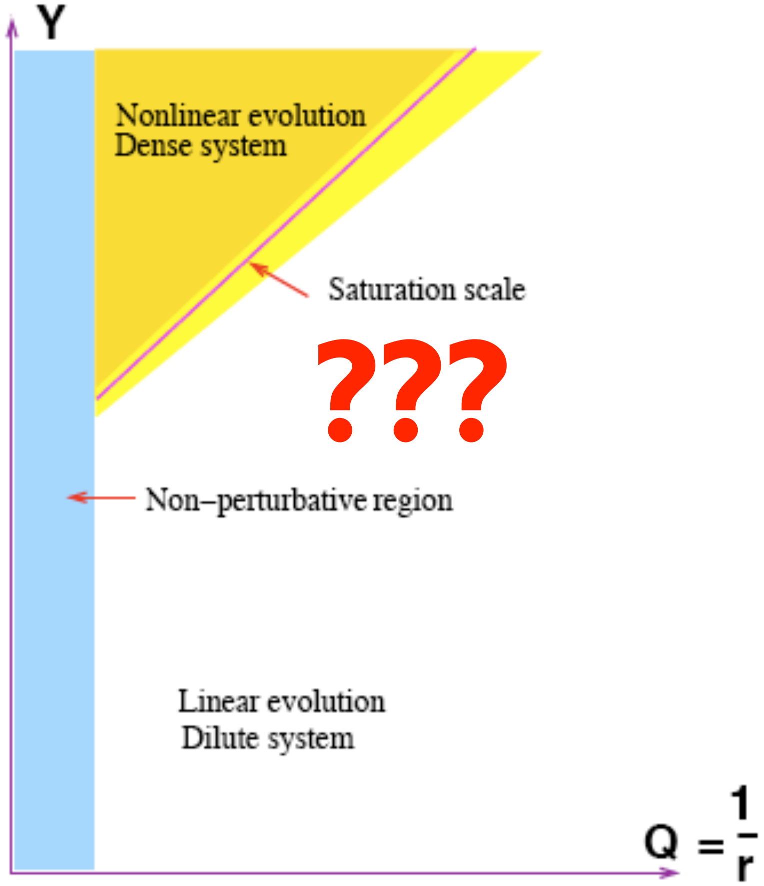

Usual approximation:

$$N(Y; \mathbf{x}_0, \mathbf{x}_1) = N(Y; |\mathbf{x}_0 - \mathbf{x}_1|)$$

- The target has infinite size, no impact parameter.
- Local approximation suggests that the system becomes more perturbative as the energy grows.
- But this cannot be true everywhere (IR in QCD)

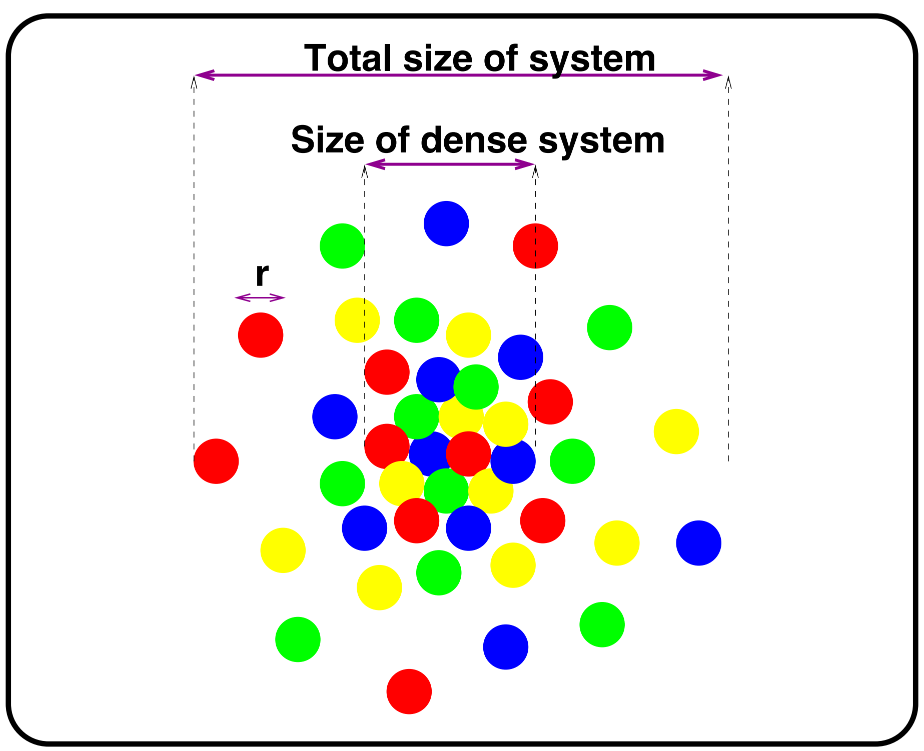

Impact parameter profile

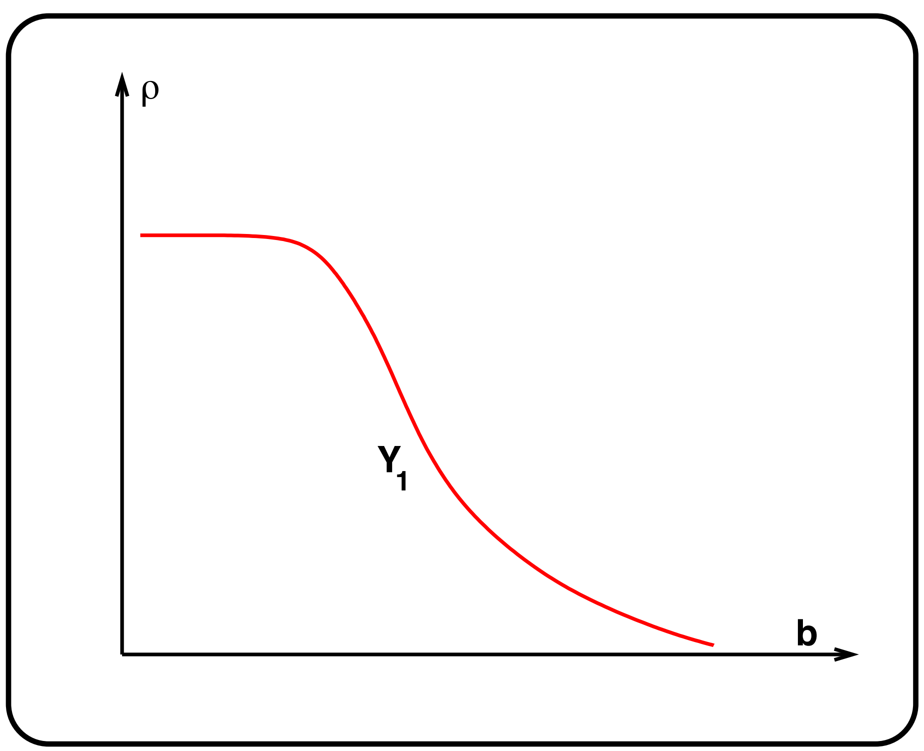

What about spatial distribution of partons?

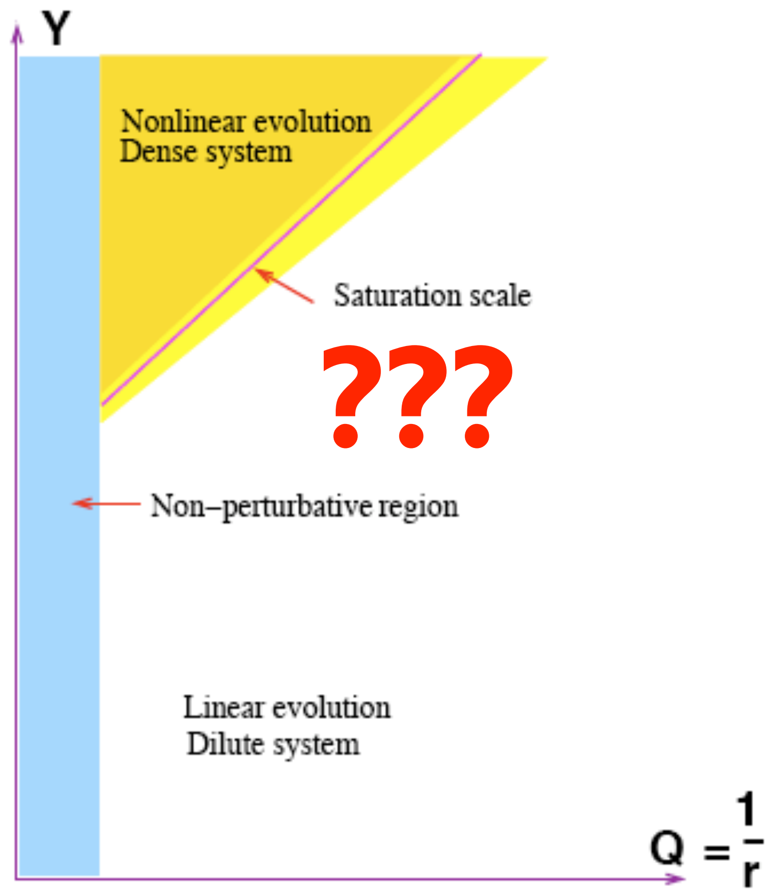

Usual approximation:

$$N(Y;\mathbf{x}_0,\mathbf{x}_1) = N(Y;|\mathbf{x}_0-\mathbf{x}_1|)$$

- The target has infinite size, no impact parameter.
- Local approximation suggests that the system becomes more perturbative as the energy grows.
- But this cannot be true everywhere (IR in QCD)

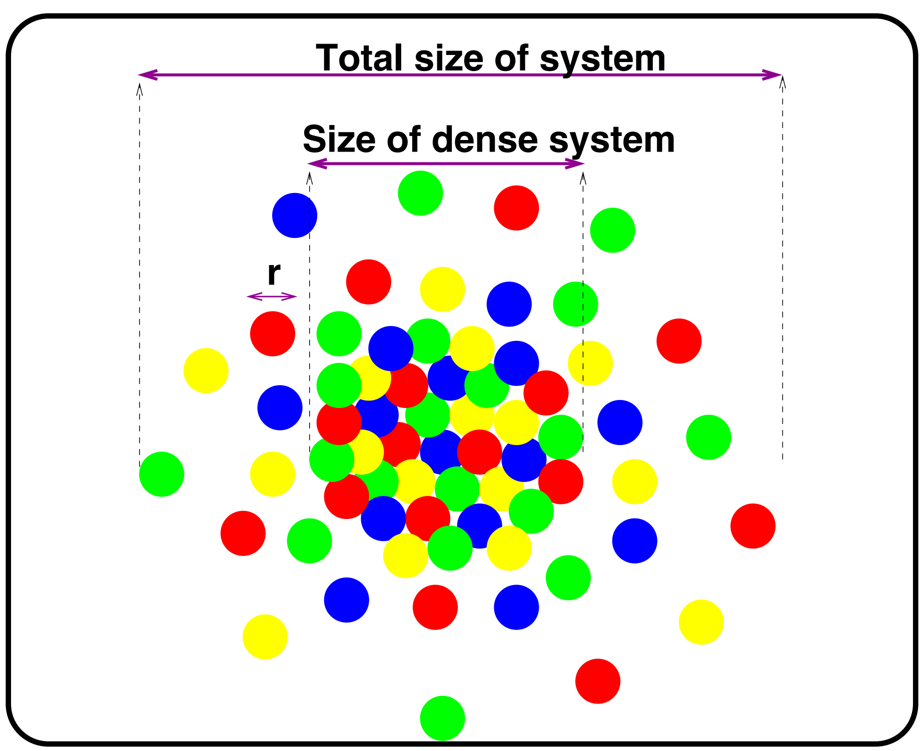

Impact parameter profile

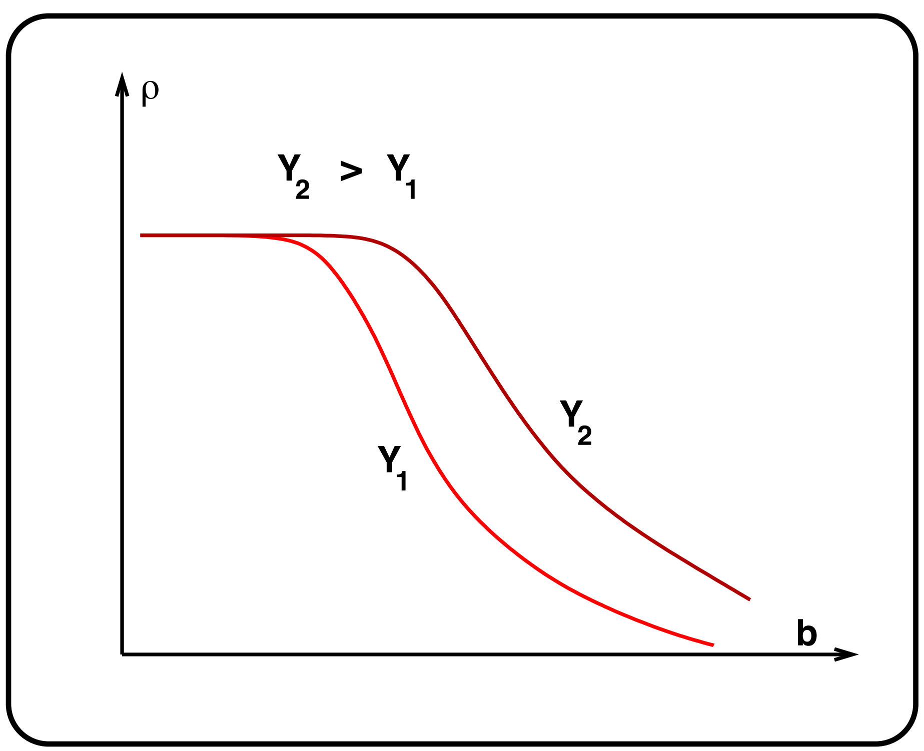

Energy dependent proton radius

Typically parametrizations of the proton profile in impact parameter are energy independent:

Gaussian: $$\rho(r) \propto \exp(-r^2)$$

Double Gaussian: $$\rho(r) \propto (1-\beta)\,\frac{1}{a_1^3}\,\exp\left(-\frac{r^2}{a_1^2}\right) + \beta\,\frac{1}{a_2^3}\,\exp\left(-\frac{r^2}{a_2^2}\right)$$

Energy dependent proton radius modeled in PYTHIA

$$\rho(r,x) \propto \frac{1}{a^3(x)}\,\exp\left(-\frac{r^2}{a^2(x)}\right) \qquad a(x) = a_0\left(1 + a_1 \ln\frac{1}{x}\right)$$

a_0 tuned to diffractive data

a_1 free parameter,

$a_1 \to 0$ single fixed gaussian is recovered

Energy dependent proton radius

Typically parametrizations of the proton profile in impact parameter are energy independent:

Gaussian: $$\rho(r) \propto \exp(-r^2)$$

Double Gaussian: $$\rho(r) \propto (1-\beta)\,\frac{1}{a_1^3}\,\exp\left(-\frac{r^2}{a_1^2}\right) + \beta\,\frac{1}{a_2^3}\,\exp\left(-\frac{r^2}{a_2^2}\right)$$

Corke,Sjostrand Energy dependent proton radius modeled in PYTHIA

$$\rho(r,x) \propto \frac{1}{a^3(x)}\,\exp\left(-\frac{r^2}{a^2(x)}\right) \qquad a(x) = a_0\left(1 + a_1 \ln\frac{1}{x}\right)$$

a_0 tuned to diffractive data

a_1 free parameter,

$a_1 \to 0$ single fixed gaussian is recovered

Energy dependent impact parameter profile

Gribov diffusion idea:

High energy behavior of cross sections related to small x partons. Parton evolution in x, produces random walk in transverse momenta, thus leading to the diffusion of partons in transverse momentum space. As a result the spatial distribution changes with decreasing x.

Energy dependent impact parameter profile

Gribov diffusion idea:

High energy behavior of cross sections related to small x partons. Parton evolution in x, produces random walk in transverse momenta, thus leading to the diffusion of partons in transverse momentum space. As a result the spatial distribution changes with decreasing x.

Simulating dipole(gluon) small x evolution:

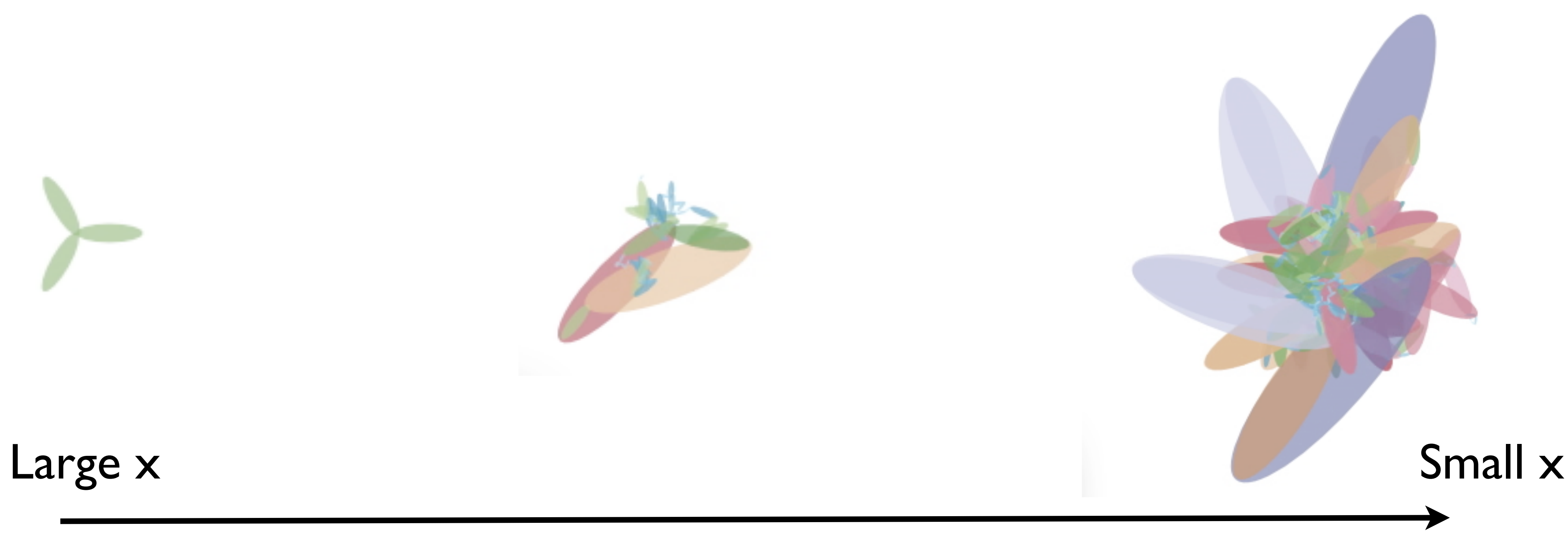

Impact parameter profile from BK/BFKL evolution

Qualitatively BFKL and BK gives the diffusion, the growth in radius is however too strong due to lack of confinement.

Impact parameter profile generated from BK evolution with impact parameter dependence

Expanding black disk with increasing energy

Power-like tail due to lack of non-perturbative effects

Violates Froissart bound: power like increase of cross section with energy.

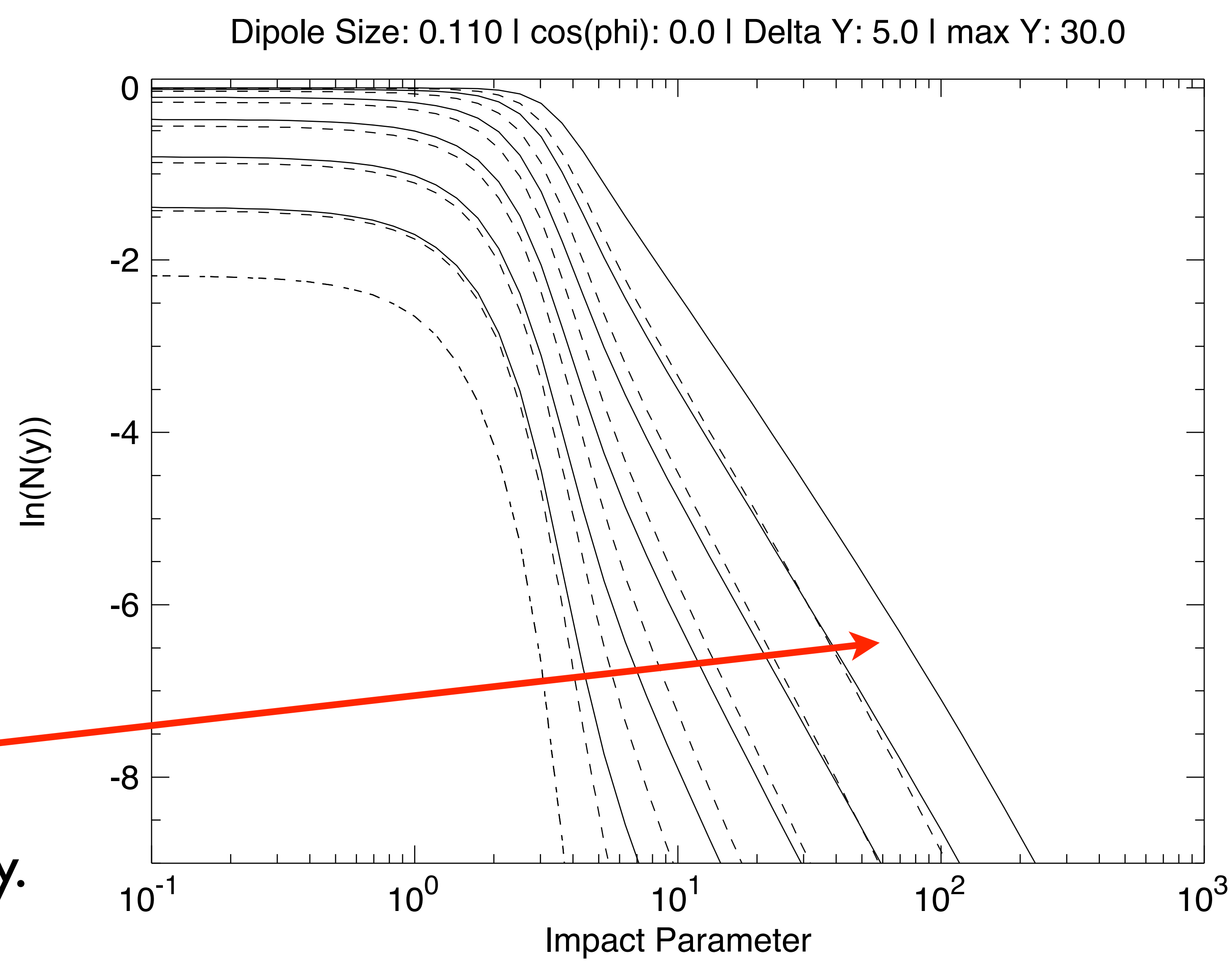

Impact parameter profile from BK/BFKL evolution

Qualitatively BFKL and BK gives the diffusion, the growth in radius is however too strong due to lack of confinement.

Berger,AS

Impact parameter profile generated from BK evolution with impact parameter dependence

Expanding black disk with increasing energy

Power-like tail due to lack of non-perturbative effects

Violates Froissart bound: power like increase of cross section with energy.

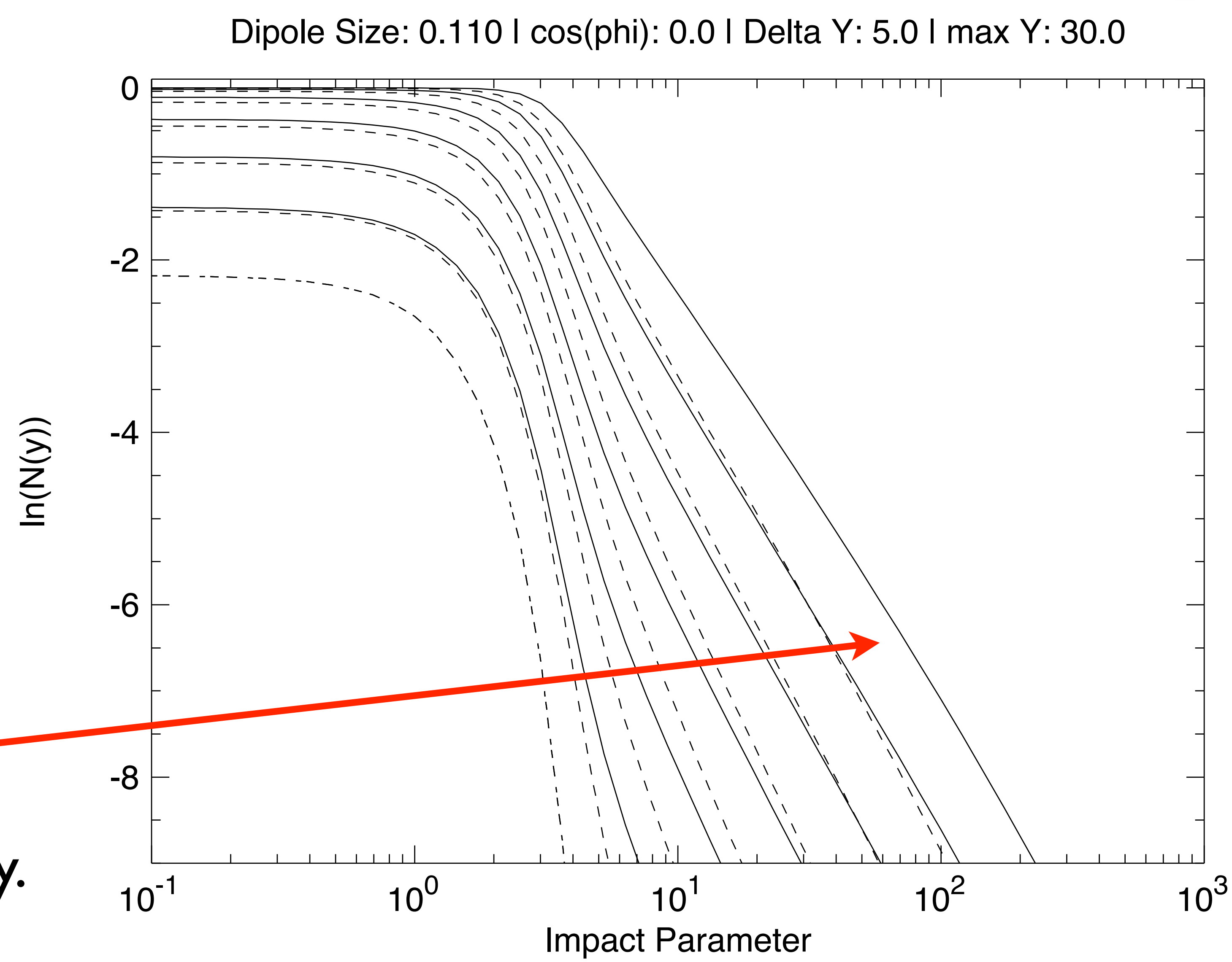

Impact parameter profile: modeling confinement

Need to regulate in the IR region in the small x evolution.
Non-perturbative problem, introduce phenomenological mass (cutoff) parameter.
which regulates large dipole sizes

$$1/r_{\mathrm{max}} \simeq m \simeq 350\ \mathrm{MeV}$$

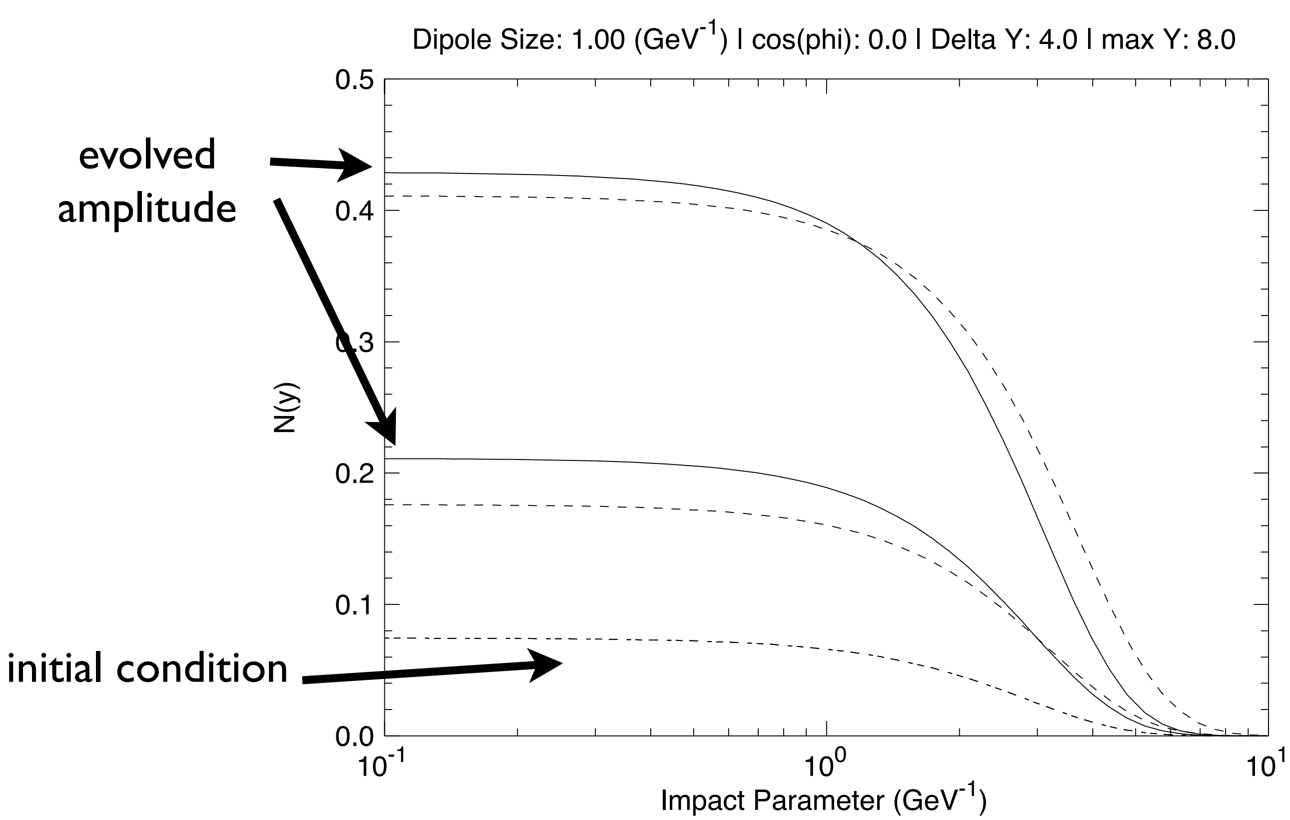

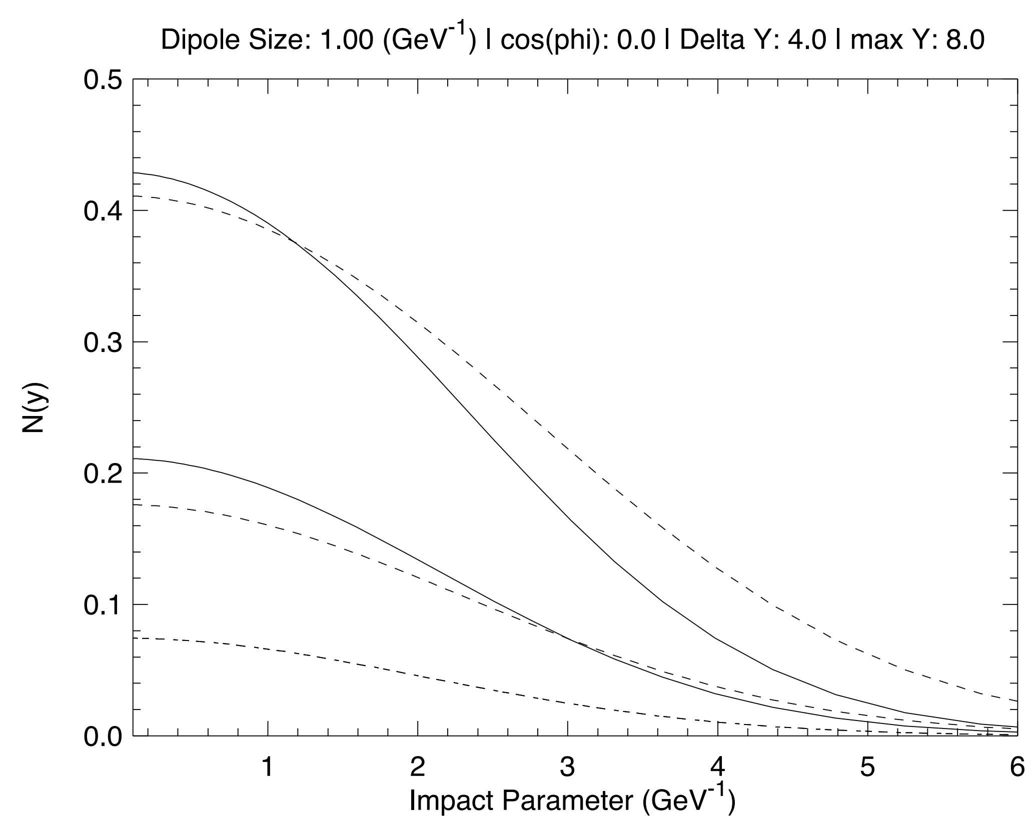

Impact parameter profile: modeling confinement

Need to regulate in the IR region in the small x evolution.
Non-perturbative problem, introduce phenomenological mass (cutoff) parameter.
which regulates large dipole sizes

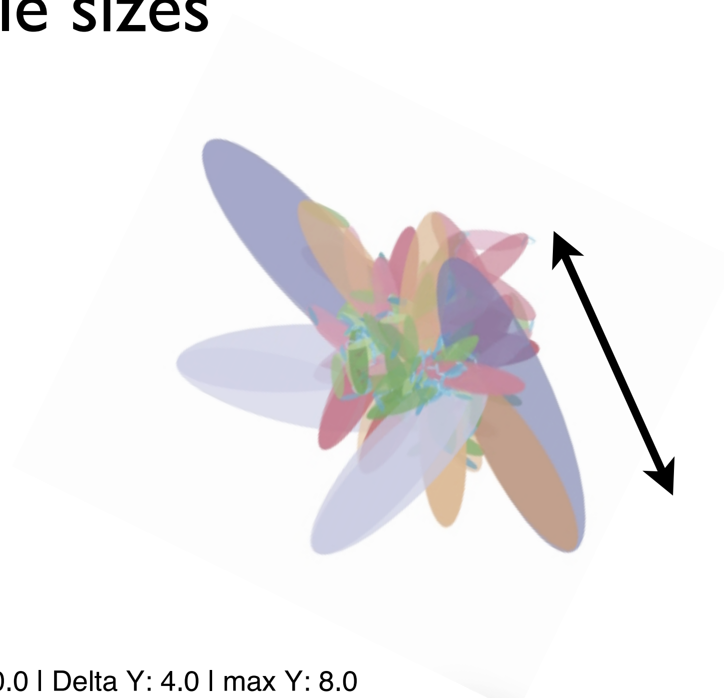

$$1/r_{\text{max}} \simeq m \simeq 350 \text{ MeV}$$

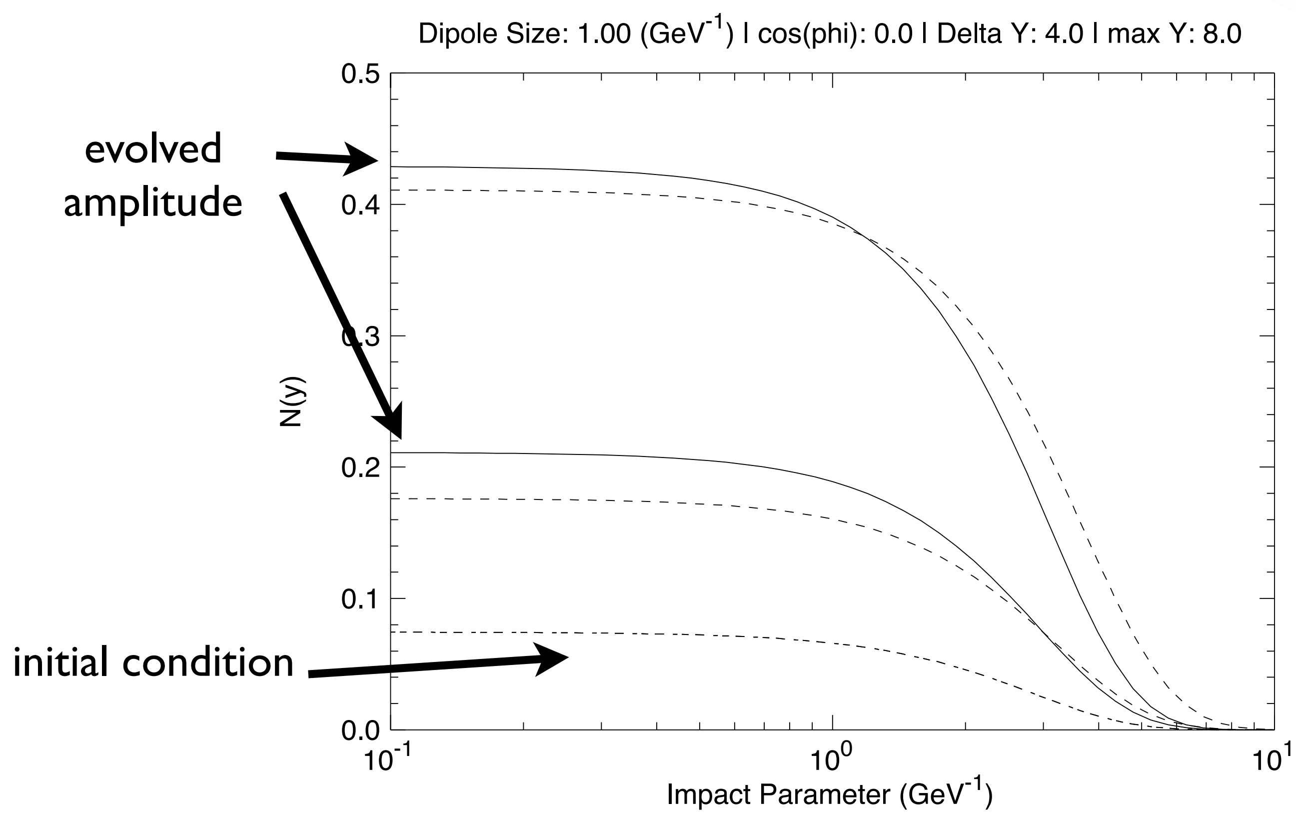

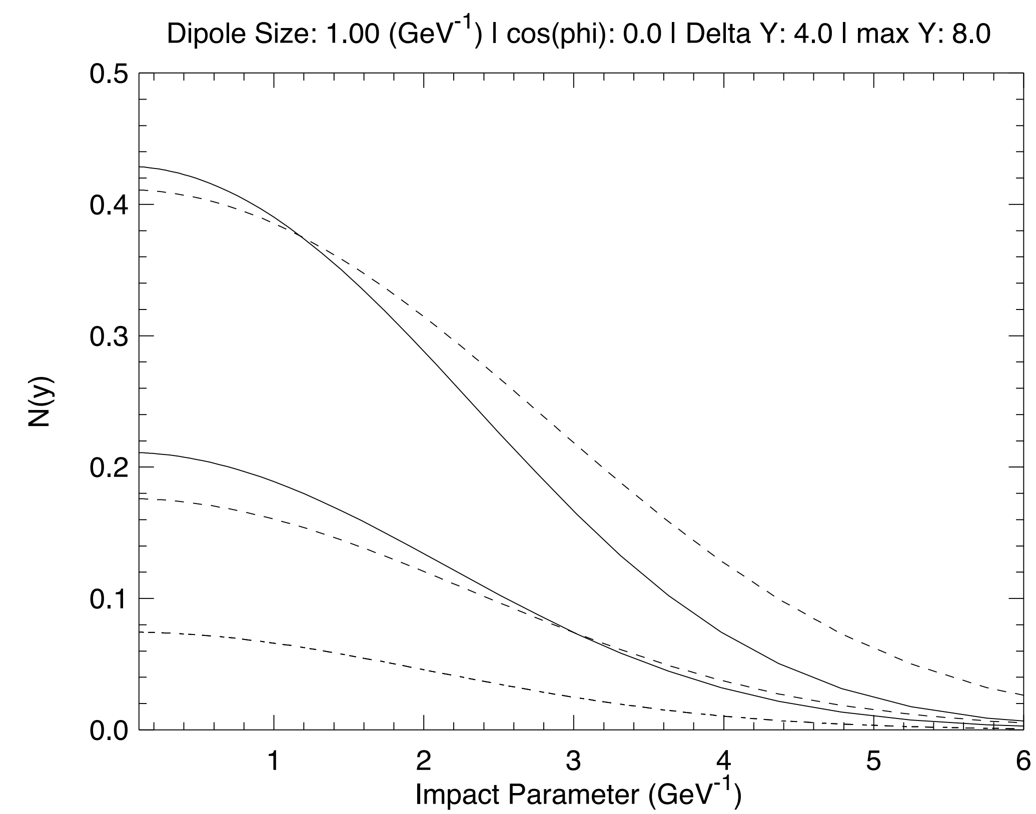

Testing the small x evolution with impact parameter

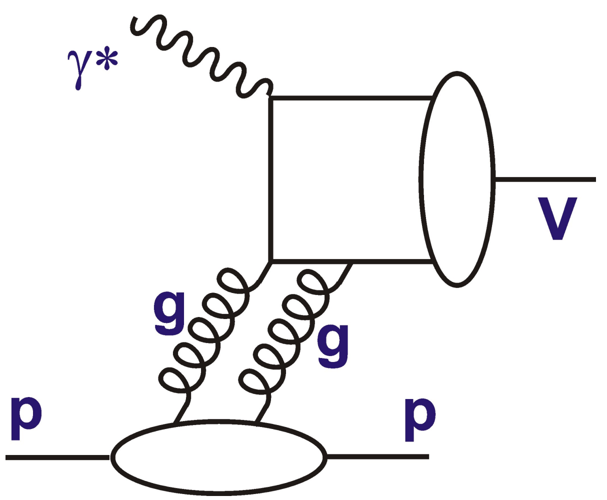

- Testing the small x evolution with diffractive vector meson production
- Exclusive diffractive production of VM in DIS is an excellent process for extracting the dipole amplitude
- Suitable process for estimating the 'blackness' of the interaction.
- t-dependence provides an information about the impact parameter profile of the amplitude.

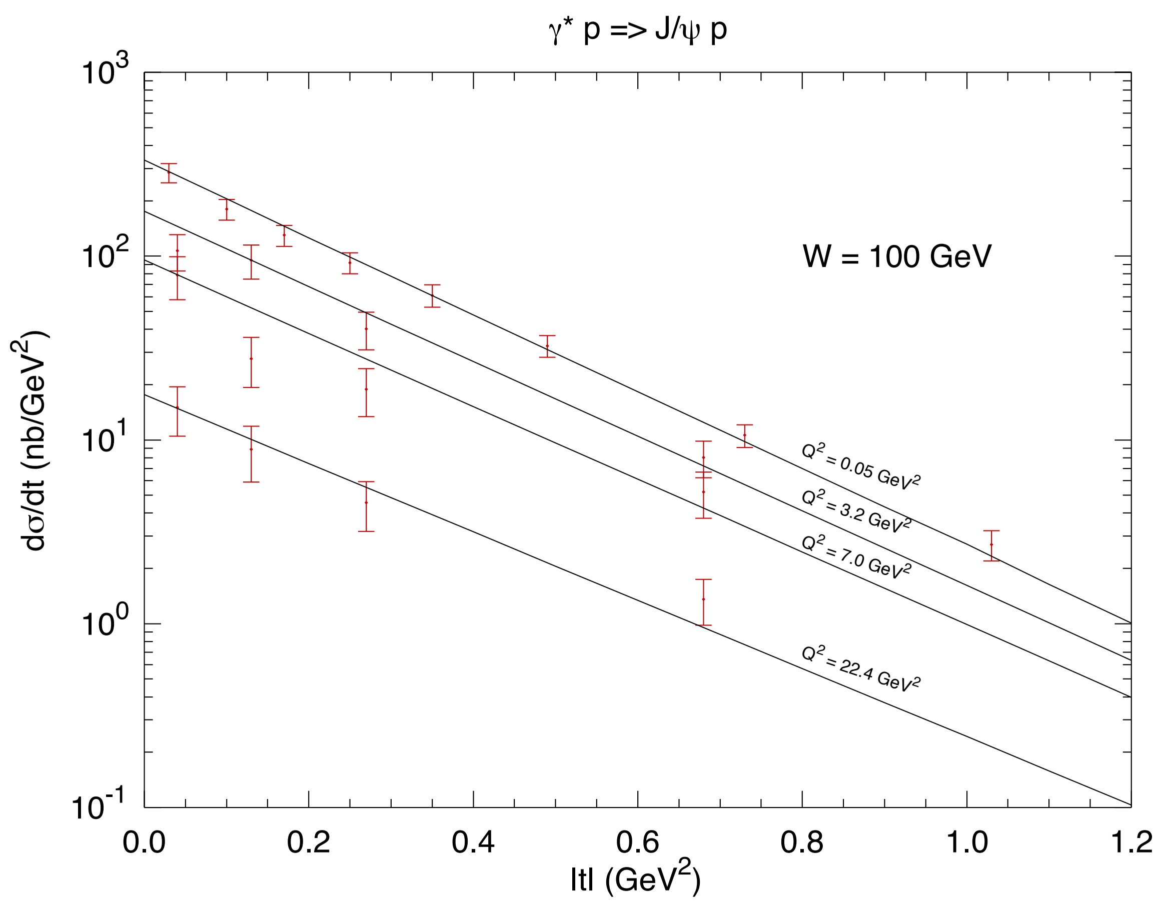

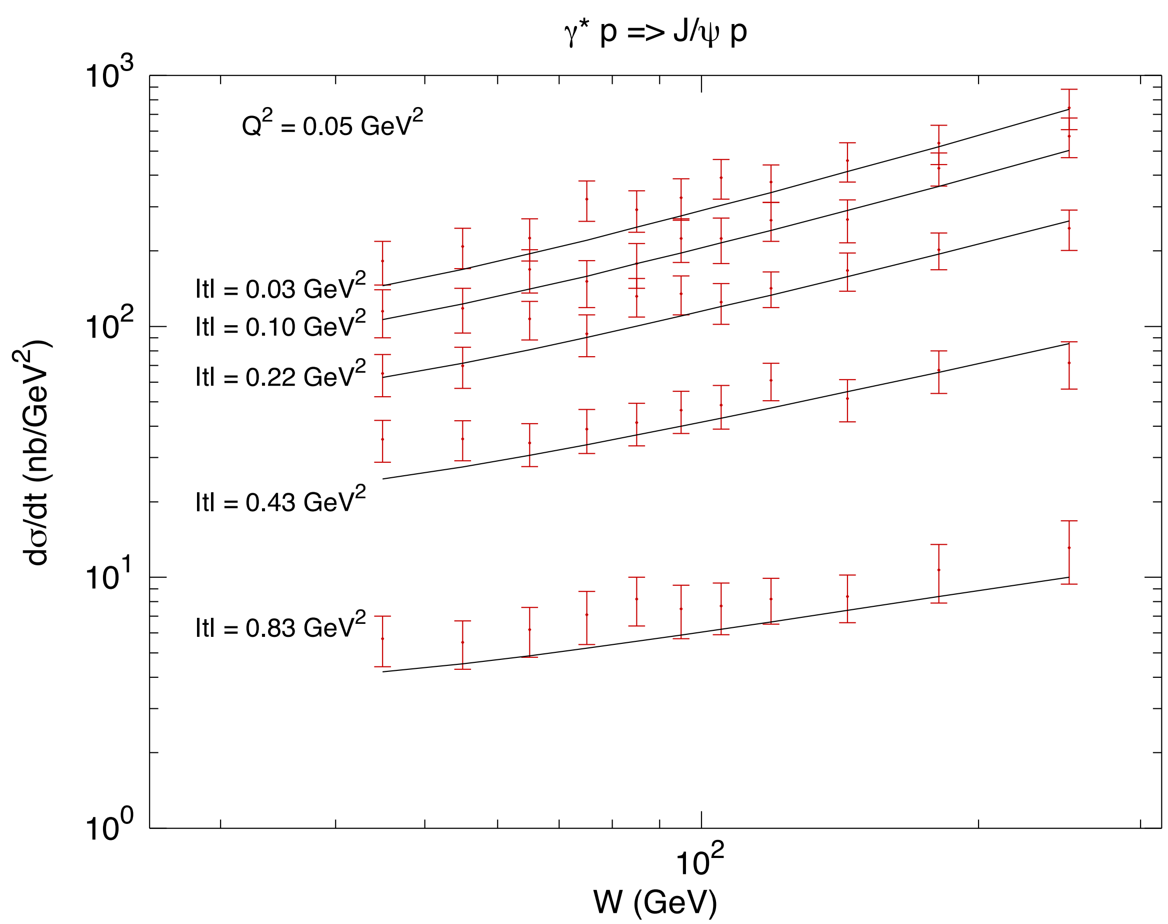

t-slope for VM production vs energy

$$\frac{d\sigma}{dt} \sim e^{-B_D|t|}$$

Intercept controlled by the initial profile in b, slope controlled by the mass regulator in the kernel.

Increasing trend of the data reproduced by the small x evolution with impact parameter dependence.

t-slope for VM production vs energy

$$\frac{d\sigma}{dt} \sim e^{-B_D|t|}$$

Intercept controlled by the initial profile in b, slope controlled by the mass regulator in the kernel.

Increasing trend of the data reproduced by the small x evolution with impact parameter dependence.

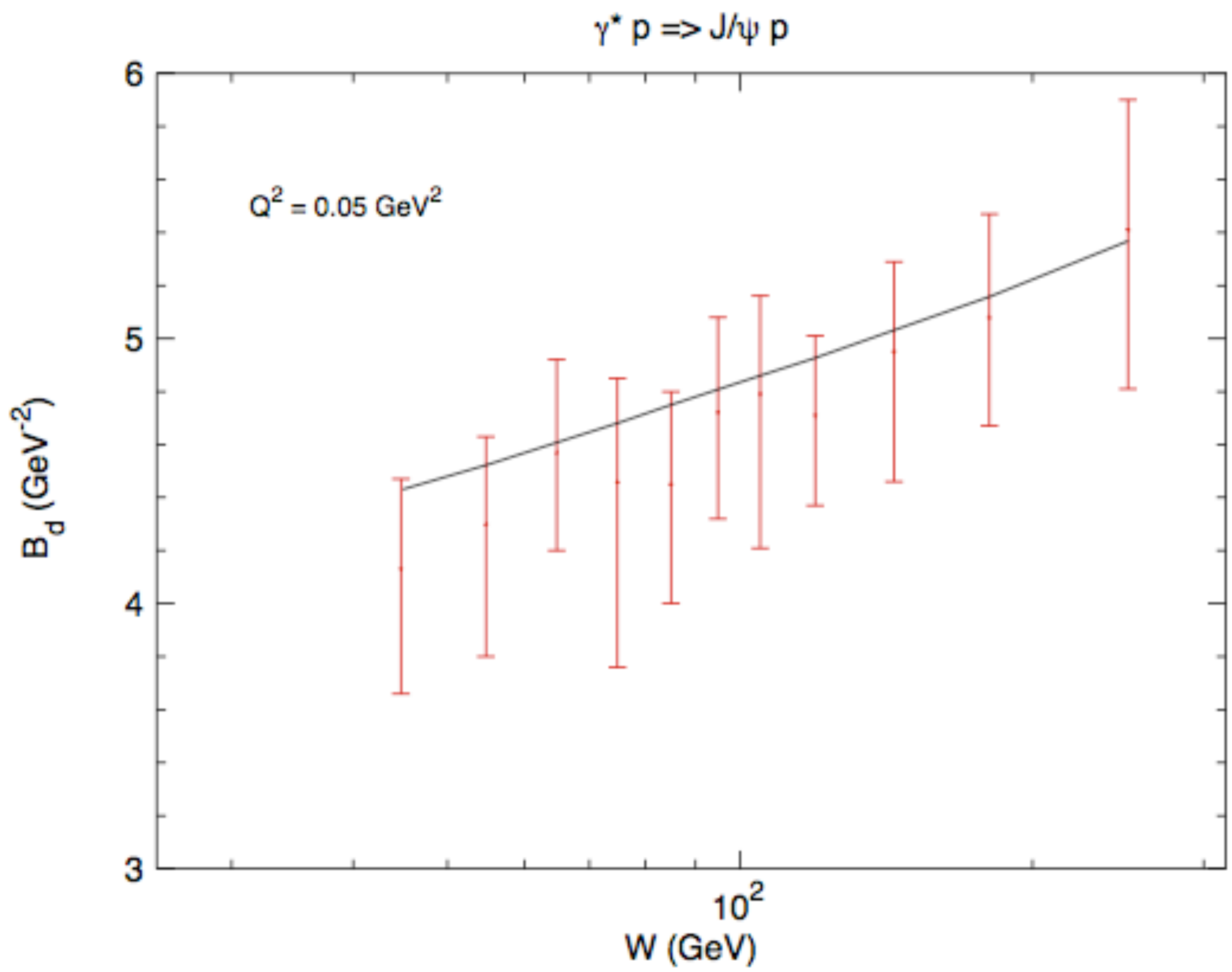

t-slope for VM production vs energy

$$\frac{d\sigma}{dt} \sim e^{-B_D|t|}$$

Intercept controlled by the initial profile in b, slope controlled by the mass regulator in the kernel.

Increasing trend of the data reproduced by the small x evolution with impact parameter dependence.

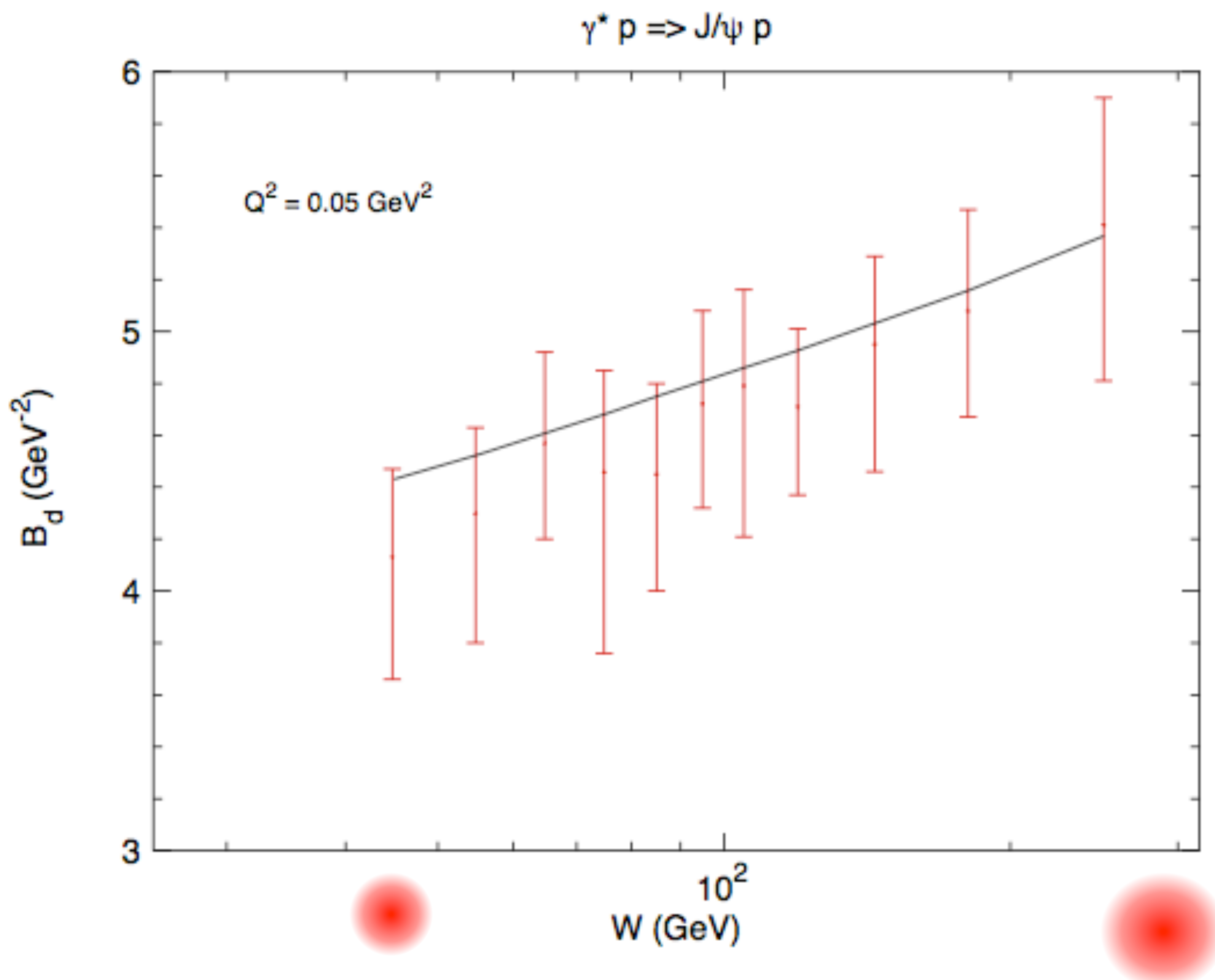

t-slope for VM production vs energy

$$\frac{d\sigma}{dt} \sim e^{-B_D|t|}$$

Intercept controlled by the initial profile in b, slope controlled by the mass regulator in the kernel.

Increasing trend of the data reproduced by the small x evolution with impact parameter dependence.

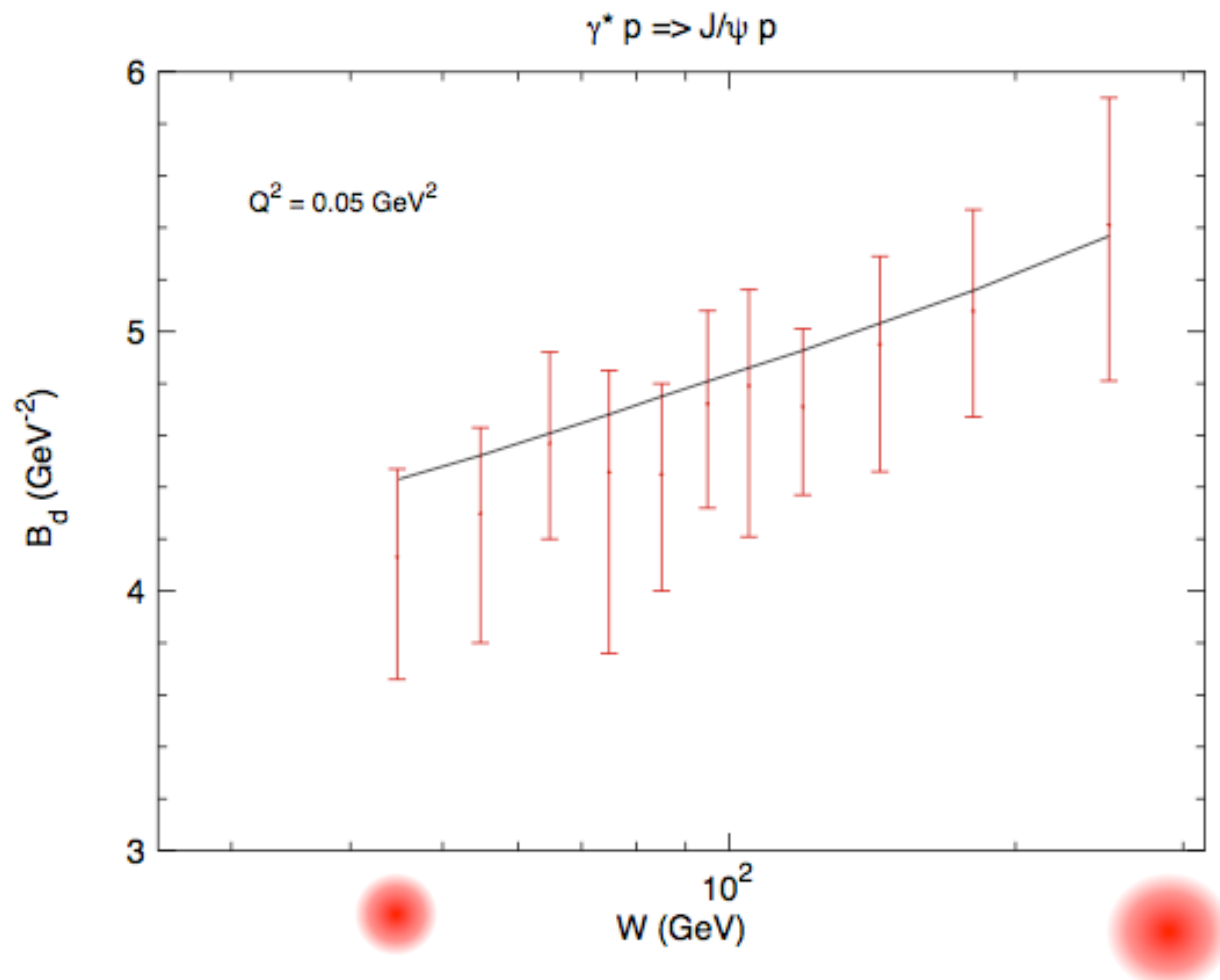

Size in the energy range of HERA ep collider:

$$0.6 - 0.66 \text{ fm}$$

Extrapolation for LHCb energy range:

$$0.7 - 0.75 \text{ fm}$$

compare with electromagnetic radius of the proton

$$0.87 \text{ fm}$$

Signature for parton saturation?

Armesto-Rezaeian

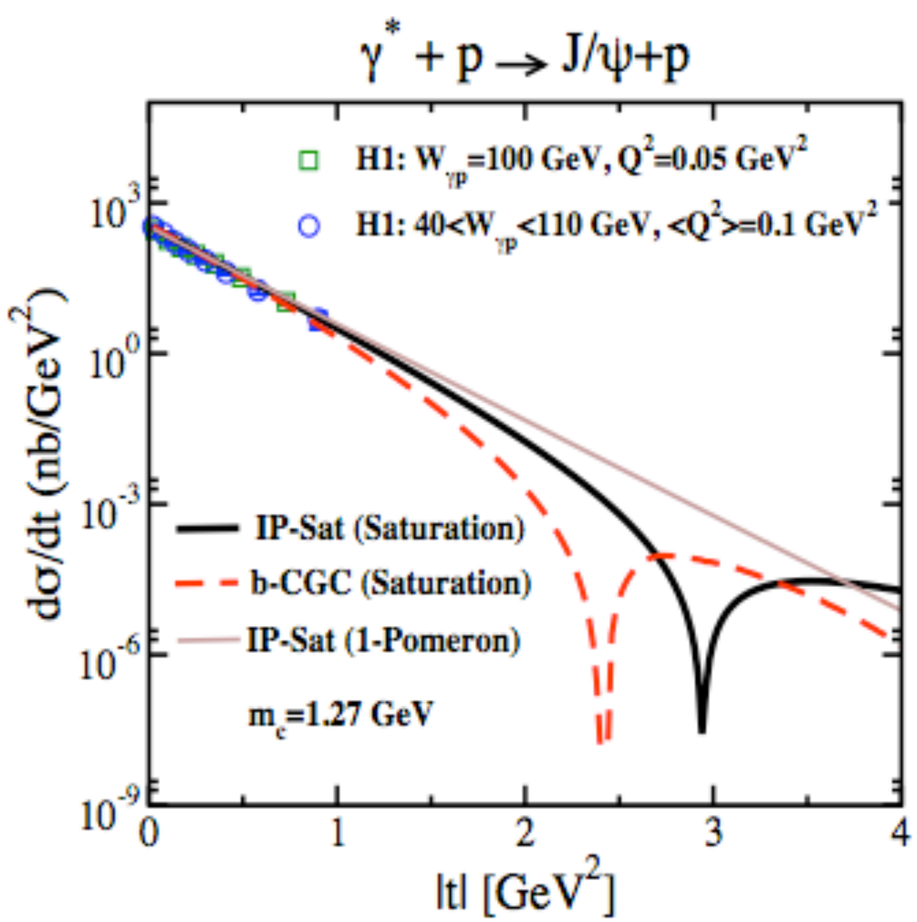

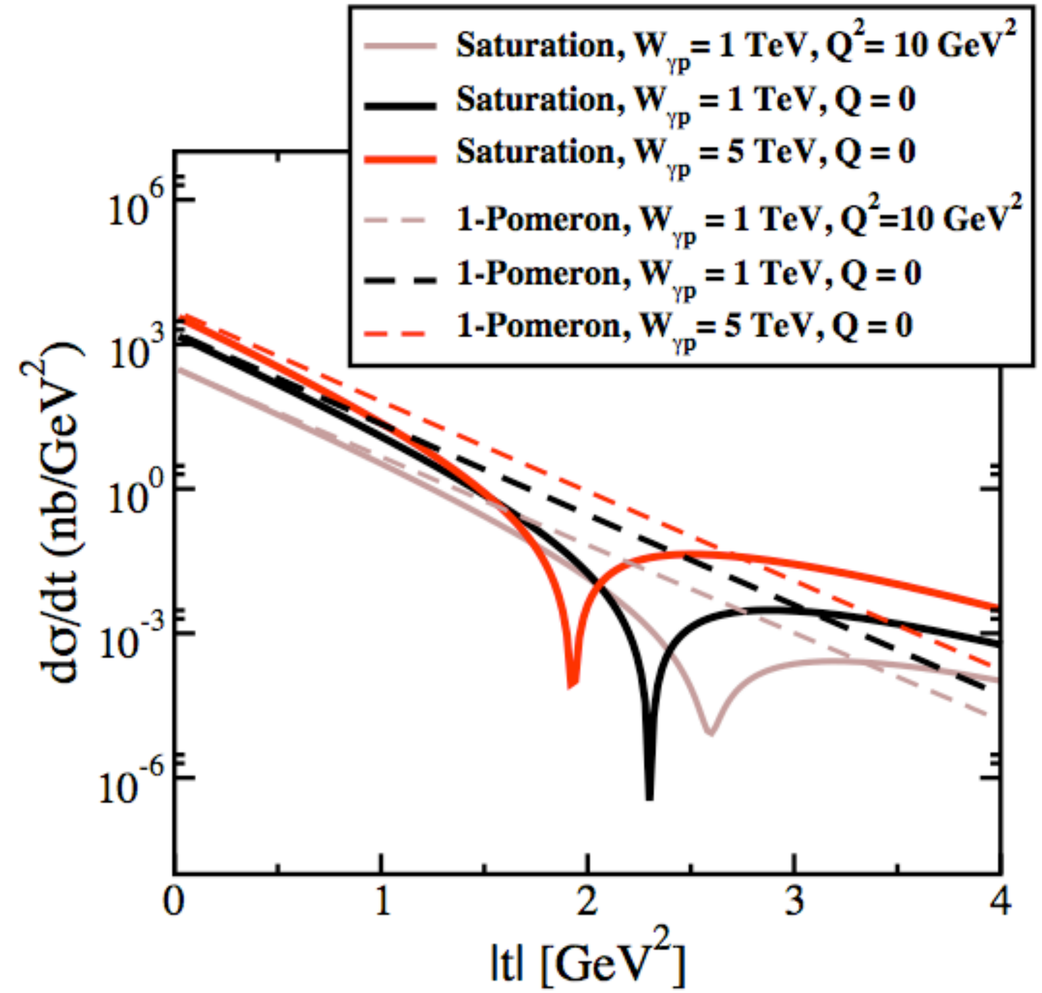

- t-profile is a Fourier transform of the impact parameter profile
- characteristic dips as a feature of saturation
- position of dips depends on energy and scale
- within the LHC range or future electron-hadron collider like LHeC

Signature for parton saturation?

Armesto-Rezaeian

talk at ISVHECRI by E.Radicioni

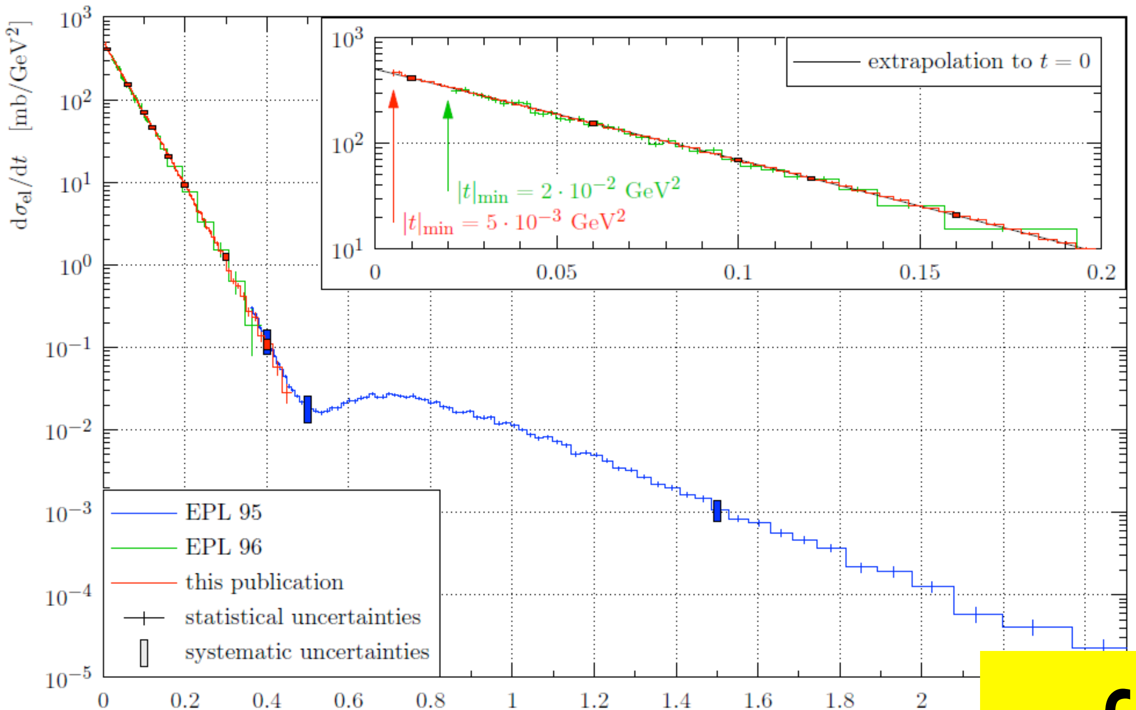

soft

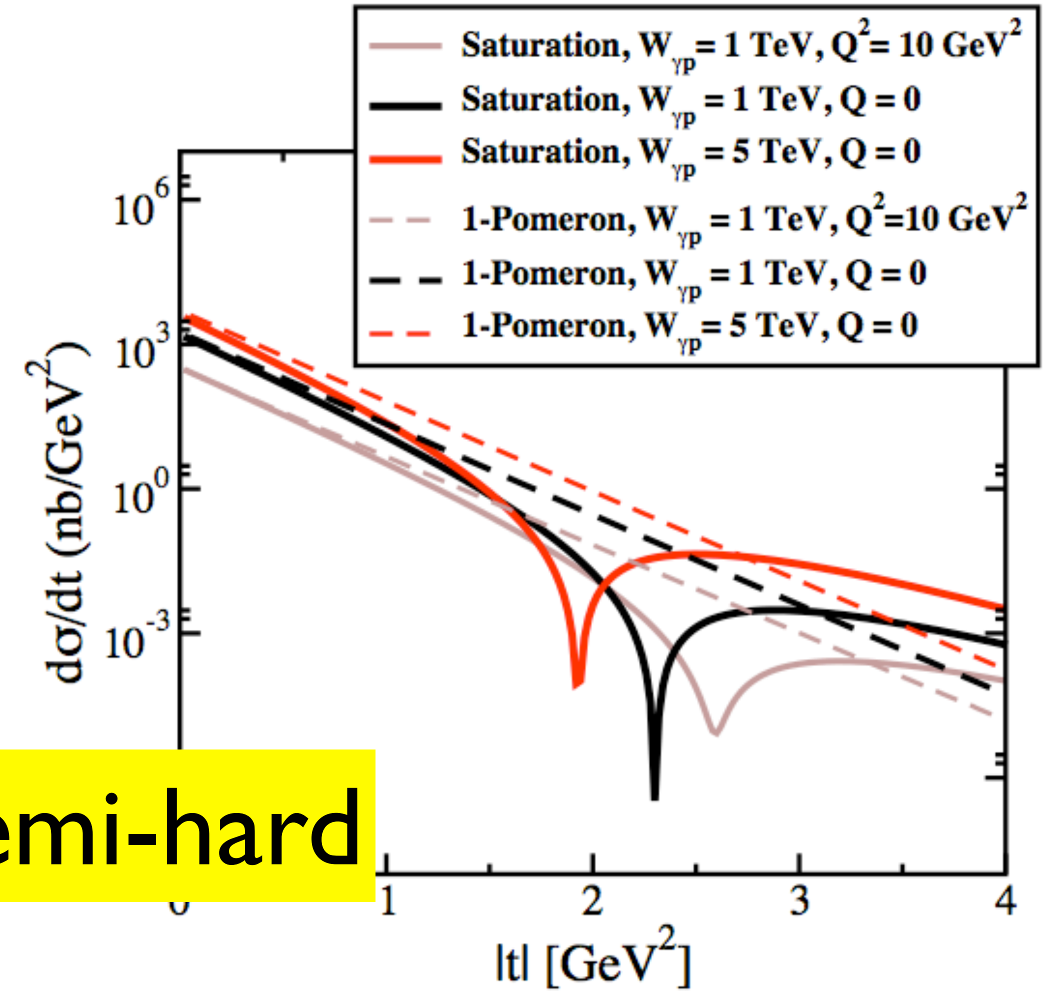

semi-hard

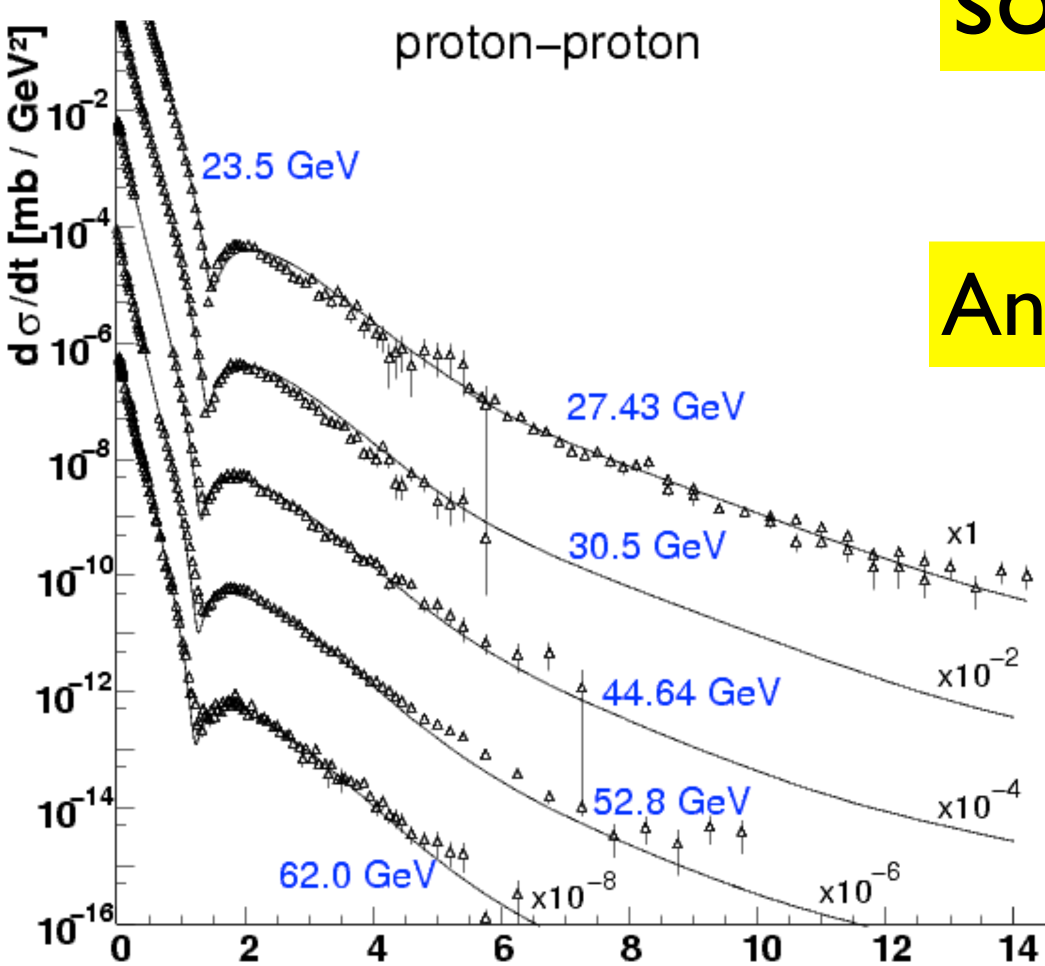

Analogous to what happens in proton-proton

- t-profile is a Fourier transform of the impact parameter profile
- characteristic dips as a feature of saturation
- position of dips depends on energy and scale
- within the LHC range or future electron-hadron collider like LHeC

Summary

- Cosmic ray and neutrino interactions open a new regime where small x effects are important. However, BFKL formalism has large higher order corrections.

- Resummation schemes for linear evolution have been developed which can very well compare with the existing experimental data

- Saturation formalism at next to leading order accuracy recently derived, needs more thorough phenomenological studies. Resummation with saturation…

- Unified BFKL/DGLAP cross sections for neutrinos consistent with the latest DGLAP analysis within the error bands of uncertainty. Power behavior at high energies. Saturation effects small, but not entirely negligible. Could be more important in the differential distributions. Flexibility of DGLAP parametrization can still account for the BFKL power and/or saturation...

- Saturation could be sizeable for prompt production from charm. Importance of beauty decays for tau neutrinos.

Summary ctd.

- The impact parameter profile of the hadron at high energy is reproduced by the small x evolution. Proton size varying with energy should be taken into account.

- t-slope in diffractive production of VM as a signature of saturation?

- Topic not covered: forward production in pA vs pp. Leading order saturation formalism successfully describes the data from RHIC and LHC. But, recently computed NLO corrections to forward production are quite large, some theoretical problems there which need to be understood. Also, LHCf data on pion production in pA very intriguing but low scales provide challenge for saturation models.

Backup slides

Problems at low x

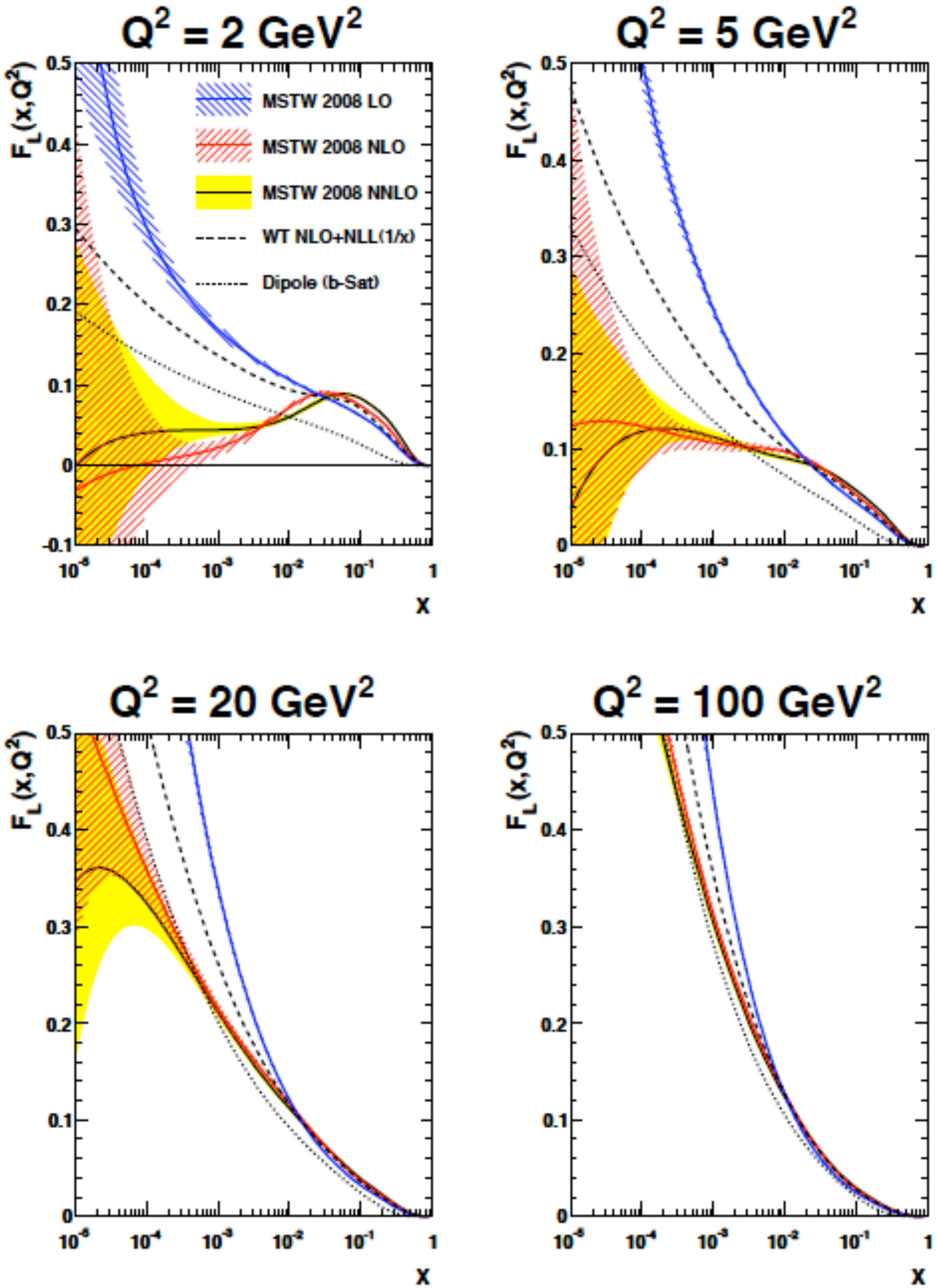

Problems at low x

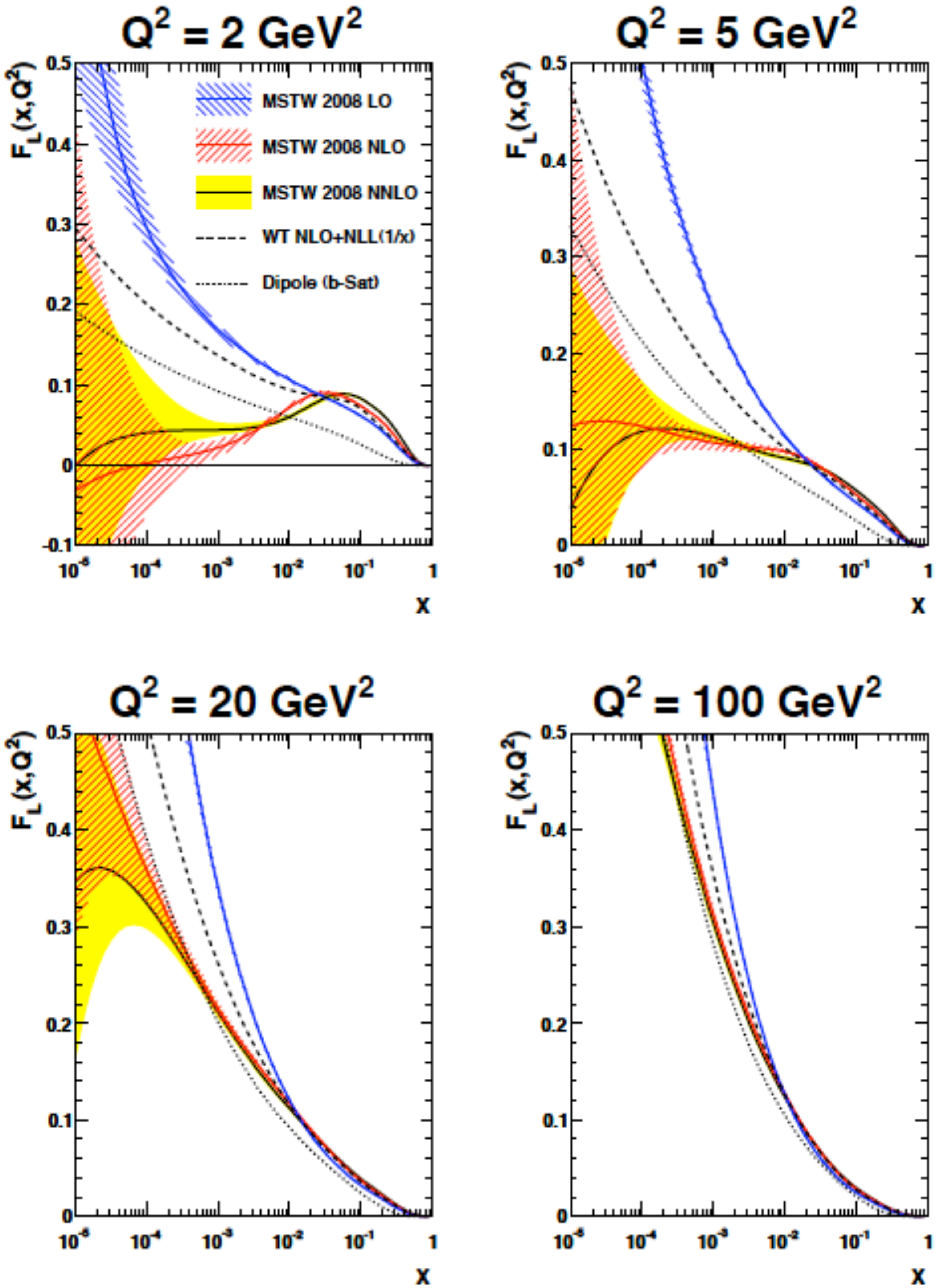

- Uncertainties of the gluon distribution translate into the observable FL.

Problems at low x

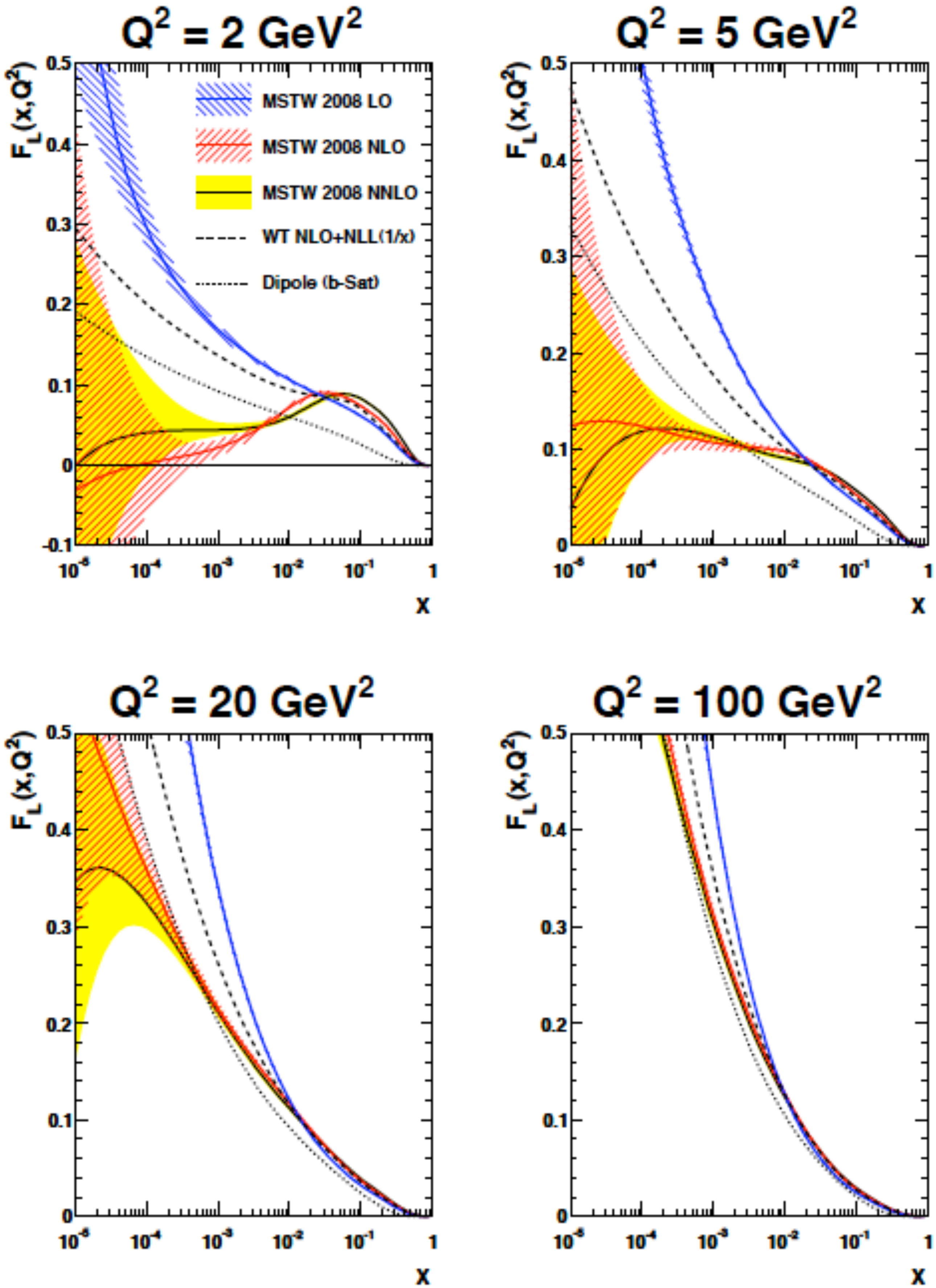

- Uncertainties of the gluon distribution translate into the observable FL.
- NLO,NNLO predictions allow for the negative structure function.

Problems at low x

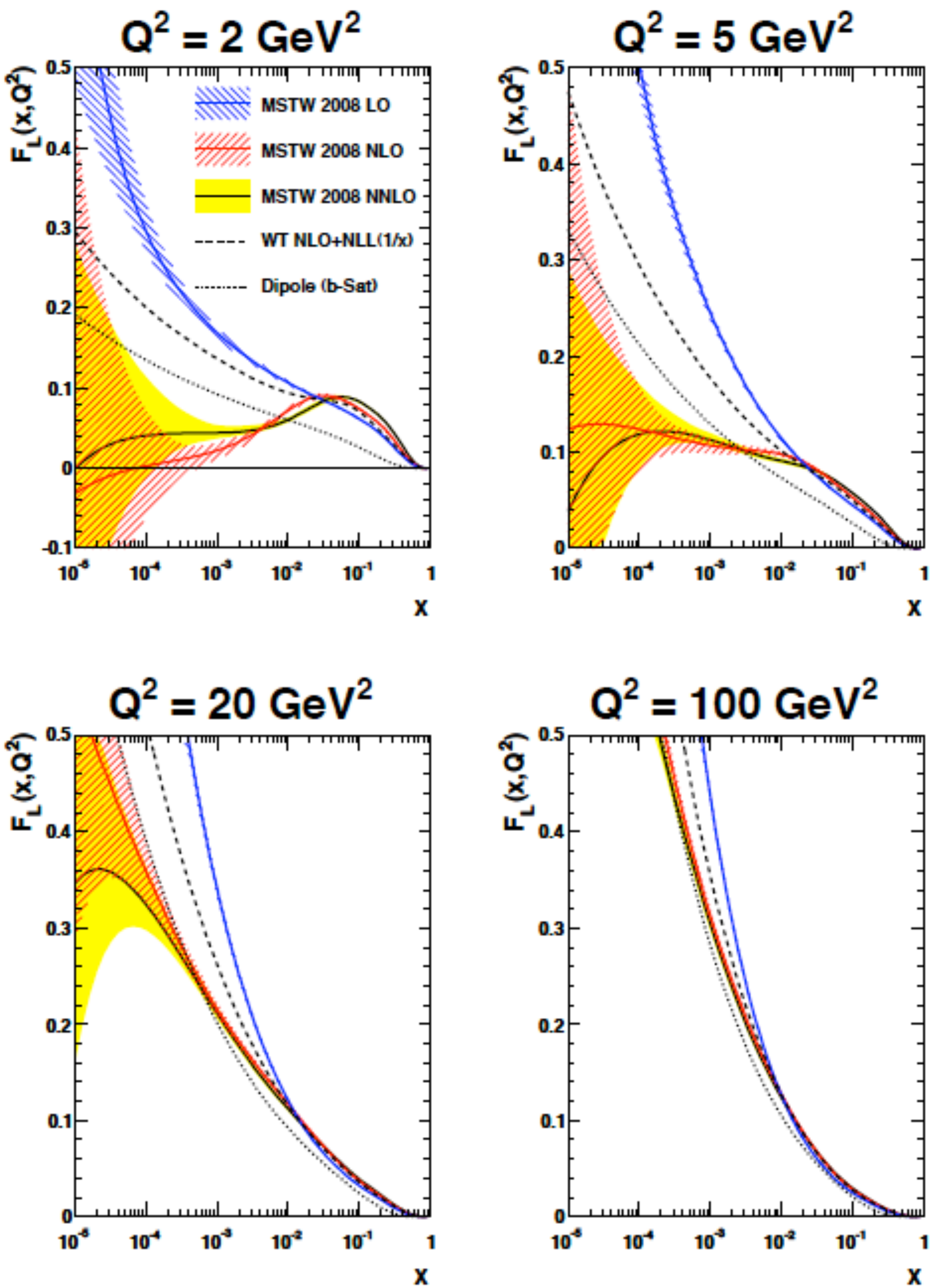

- Uncertainties of the gluon distribution translate into the observable FL.
- NLO,NNLO predictions allow for the negative structure function.
- Note that the problem remains even for larger values of Q, it is though pushed towards lower values of x.

NLLx, resummation vs saturation

Attempt to quantify the size of the NLLx vs saturation. Solve the NLLx and resummed linear equations in the presence of absorptive boundary which mimics saturation.

Start from linear equation:

$$\frac{df_g(x,k_T)}{d\ln 1/x} = \frac{\alpha_s N_c}{\pi}\int d^2k'_T \mathcal{K}(k_T,k'_T)\, f_g(x,k'_T)$$

Define the critical value: $$f(x,k_c(x)) = c$$

Satisfy given boundary condition for:

$$\rho \le \rho_c - \Delta, \quad \rho_c = \ln(k_c^2(x)/k_0^2), \rho = \ln(k^2/k_0^2)$$

Δ, c numerical parameters

Boundary condition:

cutoff: $$f(x,\rho) = 0 \qquad \rho \le \rho_c - \Delta$$

freeze: $$f(x,\rho) = f(x,\rho_c - \Delta)$$

Dips in t-profile for VM production

Photoproduction of $J/\psi, \phi, \rho$

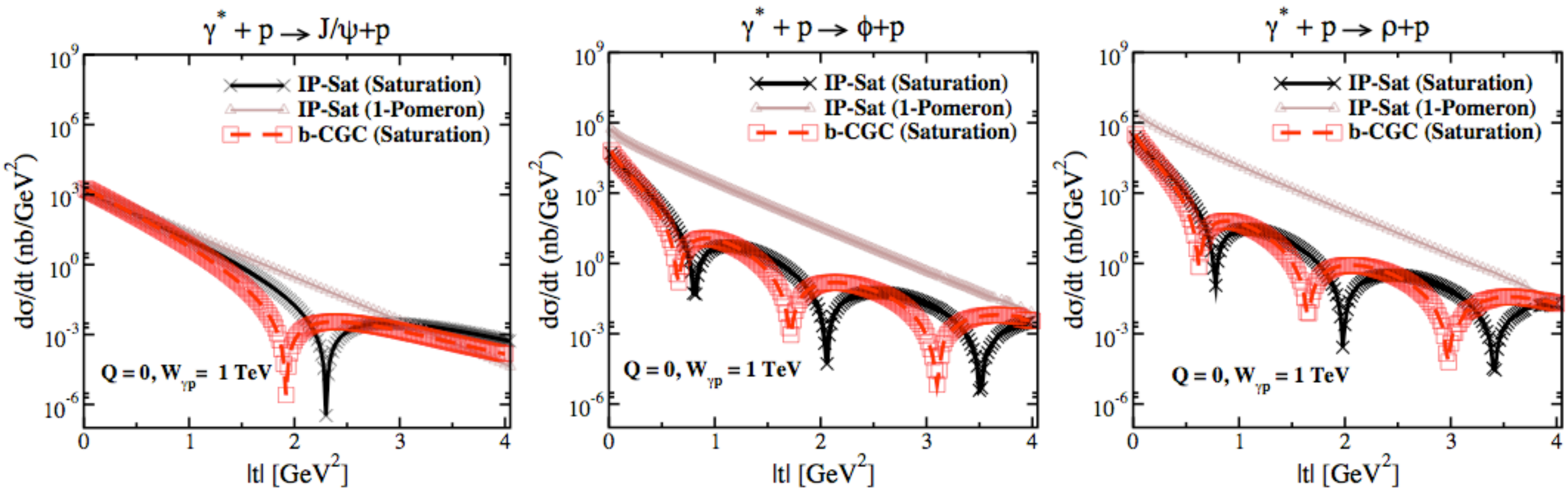

Dips in t move to lower values for lighter vector mesons

This feature could be very helpful in confirming parton saturation